MITOCHONDRIA ORCHESTRATE THE SURVIVAL OF MELANOMA CELLS AND CHRONICALLY DEPOLARIZED SYMPATHETIC NEURONS

by

ALI ABDULLAH A. ALSHAMRANI

(Under the Direction of James L. Franklin)

ABSTRACT

The work presented herein illustrates the multifaceted role of mitochondria in the survival of different *in vitro* disease and developmental models, including melanoma cancer cells and developing sympathetic neurons, respectively. In the first study, we sought to investigate the use of mitochondria-targeted therapeutics as an approach to disrupt metabolic reprogramming in poorly targeted melanoma tumor cells with wild-type BRAF. Interestingly, disrupting mitochondrial bioenergetics with the mitochondria-targeted lipophilic cation mitoquinone (MitoQ) induces significant cytotoxic effects, surpassing other investigative and conventional therapeutics. Here, we demonstrate for the first time that divergent targeting of glycolysis and mitochondrial oxidative phosphorylation result in an additive cytotoxic effect in melanoma cells with different genetic backgrounds. Our data suggest that inhibiting glycolysis forces these cells to rely more heavily on mitochondrial oxidative phosphorylation to survive, which makes them more vulnerable to the effects of the lipophilic cation MitoQ. In addition to the role of mitochondria in regulating cellular bioenergetics, cellular redox homeostasis is another crucial function. The mitochondria-derived reactive species (RS) is a central mediator of physiological and pathological apoptotic death of neurons. Many neurons generated during the embryogenesis of the vertebrate nervous system undergo apoptotic death before birth or soon thereafter. Among them are the sympathetic neurons not obtaining sufficient amounts of the nerve growth factor (NGF). Chronic depolarization of the plasma membranes of these neurons promotes their survival in the absence of NGF by an unknown mechanism. In this study, we aimed to identify the mechanism by which chronically depolarized neurons resist apoptotic death following NGF withdrawal. Previous evidence showed that the activation of the intrinsic apoptosis pathway and the Bax-dependent increase of mitochondrial-derived RS are critical events in the death of these cells. Our novel findings demonstrate that chronically depolarized neurons prevent developing pro-oxidant status and therefore resist cell death by upregulating the critical antioxidant glutathione (GSH). These findings strengthen the ever-growing association of mitochondria-derived RS with apoptotic death in neurons. Furthermore, our study will expand our knowledge about the critical players in the development and progression of some neurodegenerative diseases in which electrical activity is profoundly disturbed.

INDEX WORDS: Mitochondria, Melanoma, BRAF, MitoQ, Targeted therapy, Cytotoxicity, Reactive species, Sympathetic neurons, Nerve growth factor, Elevated Potassium ($[K^+]_E$), Chronic depolarization, Neuronal Survival, Apoptosis, BH3-only proteins, Cytochrome *c*.

MITOCHONDRIA ORCHESTRATE THE SURVIVAL OF MELANOMA CELLS AND CHRONICALLY DEPOLARIZED SYMPATHETIC NEURONS

by

ALI ABDULLAH A. ALSHAMRANI

B.S., College of Pharmacy, King Saud University, Riyadh, Saudi Arabia, 2010

A Dissertation Submitted to the Graduate Faculty of The University of Georgia in Partial Fulfillment of the Requirements for the Degree

DOCTOR OF PHILOSOPHY

ATHENS, GEORGIA

2018

MITOCHONDRIA ORCHESTRATE THE SURVIVAL OF MELANOMA CELLS

AND CHRONICALLY DEPOLARIZED SYMPATHETIC NEURONS

by

ALI ABDULLAH A. ALSHAMRANI

Major Professor:	James L. Franklin
Committee:	Brian S. Cummings
	Shelley Hooks
	John J. Wagner

Electronic Version Approved:

Suzanne Barbour
Dean of the Graduate School
The University of Georgia
December 2018

DEDICATION

I dedicate this dissertation to my whole family, whose love and belief in me made this possible.

To the best parents one could ask for: my father, Abdullah A. Alshamrani, and my mother, Zinah S. Alshkleeah, for their unconditional love and endless encouragement and support throughout my life. None of what I have achieved today would have been possible without your patience, your guidance, and your motivation since my first day of school.

To my lovely wife, Zinah A. Alshkleeah, who has been a constant source of motivation and support during the challenges of graduate school and life. I could not have earned this degree without having you in my life. You sacrificed so much for me to achieve my goal. You always put a smile on my face in the darkest moments, and I owe you enormously.

To my kindest siblings: Kholoud, Khaled, Abdulmajeed, Ragad, and my little angel Dala, you have always believed in me and supported me throughout the years. Thank you for everything.

To my teachers throughout my academic life, everything you ever taught me helped to shape the man I am today. I absolutely cannot thank you enough!

ACKNOWLEDGEMENTS

First and foremost, all praise, thanks, and gratitude go to the Almighty Allah (God), the One and Only, for His countless blessings and immeasurable bounties throughout my life.

Many people have earned my gratitude for their contribution to my journey toward earning this degree. First, I cannot express enough how grateful I am to the best and the kindest advisor one could have, Dr. James L. Franklin. In the past few years, Dr. Franklin has been the light that disperses darkness, the hope whenever I felt hopeless, and the guide that kept me on track when I thought I was lost. Thank you for your patience, support, mentoring, and your scientific wisdom that helped me to become an independent researcher. I would be remiss not to mention that this work would not have succeeded without Rebecca Kirkland, who taught me how to dissect and culture sympathetic neurons.

Thanks are also due to my previous and current committee members, Dr. Shelley Hooks, Dr. Brian Cummings, Dr. Han-Rong Weng, and Dr. John Wagner, for their insightful comments and advice that helped me finish this project.

I would also like to extend my gratefulness and appreciations to all my fellow colleagues at the Department of Pharmaceutical & Biomedical Sciences, especially Kun Qian, Liza Ngo, Sary Alsanea, Mohammed Alqinyah, Omar Alsaidan, Faris Almutairi and my current lab mates Melissa Young and Mital Patel for their help and endless support to complete my research. To my other friends, Mohammed Alasmari, Mohammed Aljutaily, Mazen Shawoosh, and Ibrahim Assiri, thank you for supporting me, encouraging me, and, most importantly, believing in me. Many thanks to the wonderful UGA animal facility staff member Robin Johnston for her never-ending cooperation. Finally, I would like to thank the funding agencies, especially my sponsor, King Saud University, and my employer, the University of Georgia, for providing the financial support necessary to earn this degree.

TABLE OF CONTENTS

LIST OF TABLES

Page

LIST OF FIGURES

Page

CHAPTER 1

LITERATURE REVIEW ON HOW MITOCHONDRIA CONTRIBUTE TO CELL DEATH AND SURVIVAL IN DIFFERENT MODELS: NEURODEGENERATIVE DISEASES Vs. CANCER

Mitochondria are unique cellular micro-organelles that play central and diverse roles in eukaryotic cells that ultimately determine the fate of the host cell. Since the first observation of these cellular organelles, previously known as "bioblasts," in the 1840s, extensive evidence has demonstrated their crucial role in meeting the cellular demands of energy and metabolites (Ernster & Schatz, 1981). Mitochondria are double-membrane organelle, with a porous outer membrane that freely allows the exchange of ions and small, uncharged molecules with the cytoplasm without the need for translocases, and a highly selective, almost impermeable inner membrane whose permeability is tightly controlled by electrochemical membrane potential (Kuhlbrandt, 2015). The human mitochondrial DNA (mtDNA) is a small, circular multicopy genome, approximately 16 kilobases, that contains the genetic coding information of two mitochondrial-ribosome coding RNAs, 22 transfer RNAs, and 13 different proteins. Among them are the subunits of oxidative phosphorylation enzyme complexes embedded in the inner mitochondrial membrane (IMM) (Friedman & Nunnari, 2014; Taanman, 1999). The cornerstone of mitochondrial significance is the production of most of the cellular adenosine triphosphate (ATP) through a process called oxidative phosphorylation (OXPHOS). ATP synthesis requires coordinated communications between the tricarboxylic acid cycle

(TCA) or Krebs cycle and the electron transport chain (ETC) protein complexes I-V. Enzymes of the TCA cycle utilize pyruvate from cytoplasmic glycolysis to produce Acetyl-Coenzyme A (AcCoA) and the reduced forms of nicotinamide adenine dinucleotides (NAD+) and flavin adenine dinucleotides (FAD+). The reduced forms, NADH and FADH2, then transfer electrons to the ETC via complex I (NADH ubiquinone oxidoreductase) and complex II (succinate dehydrogenase), respectively. The mobile carrier ubiquinone (coenzyme Q) shuttles electrons to complex III (ubiquinol cytochrome *c* oxidoreductase), where they are taken one at a time to complex IV (cytochrome *c* oxidase) by cytochrome *c*. The energy resulting from electron transfer between the respiratory complexes in the IMM and is used to transfer protons from the mitochondrial matrix into the intermembrane space, thereby establishing an electrochemical proton gradient across the IMM. ATP is produced from ADP when these protons cross the IMM back into the matrix, via the negative force of the mitochondrial membrane potential $\Delta\psi m$, through the F_1F_o–ATP synthase (respiratory complex V) (Kann & Kovacs, 2007). In addition to functioning as ATP reservoirs, mitochondria serve other equally crucial functions including intracellular Ca^{2+} buffering, biosynthesis of lipids and steroids, production of reactive species, and controlling different forms of programmed cell death (W. L. Miller, 2013; Nunnari & Suomalainen, 2012). Unlike other types of cells, neurons are entirely dependent upon the OXPHOS and aerobic metabolism for ATP synthesis, as their ability to switch to cytosolic glycolysis is limited in case of mitochondrial bioenergetic failure (Knott, Perkins, Schwarzenbacher, & Bossy-Wetzel, 2008). Mounting evidence has associated mitochondrial dysfunction as a central cause of the development of several pathologies, including neurodegenerative disorders and many types of cancers (Wallace, 2005). In the first section of this chapter, I will briefly discuss how defects in mitochondrial bioenergetics (specifically, respiratory chain complexes) and oxidative stress contribute to neuronal death in neurodegenerative disorders. In the second section of this chapter, I will review the significance of mitochondrial bioenergetics in the survival of cancer cells (melanoma cells in particular), and then use this framework to discuss how targeting mitochondrial bioenergetics could serve as a viable therapeutic approach by making these cancer cells more vulnerable to other cytotoxic agents.

Mitochondrial Bioenergetic Failure and Oxidative Stress in Neurodegenerative Diseases

Neurodegenerative disorders are a set of chronic, delayed-onset, predominantly age-associated diseases resulting from an irreversible death (degeneration) in specific neuronal populations in the brain. Among the most common, well-investigated neurodegenerative disorders are Parkinson's disease (PD), Alzheimer's disease (AD), and Huntington's disease. The regions of the brain affected and the intensity of neuronal loss determine the magnitude and characterization of manifested symptoms. For example, the muscle rigidity, bradykinesia (slowness of movement) and tremors seen in patients with PD are due to neuronal loss in the substantia nigra (melanin-containing dopaminergic neurons), which leads to striatal dopamine deficiency (Poewe et al., 2017). Impairments in cognitive functions (learning and memory) are symptomatic manifestations of Alzheimer's disease patients, in whom cortical and hippocampal neurons are damaged (Masters et al., 2015). Despite the physiological, environmental, and genetic factors that contribute to the development of such debilitating neurologic disorders, the role of mitochondrial bioenergetics dysfunction and consequent oxidative stress have been shown to be central in these neuronal pathologies.

During the process of generating ATP by mitochondrial OXPHOS, several ETC enzymes are capable of transferring a single electron to the diatomic oxygen (O_2) to form the superoxide radical anion ($O_2^{\cdot -}$) and other reactive species that can oxidize critical cellular components, including nucleic acids, proteins, and lipids (Ray, Huang, & Tsuji, 2012). Oxidative stress is a term used to describe a state of cellular stress caused when the rate of reactive species production exceeds the rate of clearance (detoxification by antioxidants). Reactive species are a family of molecules that contain both reactive oxygen (ROS) and nitrogen species (RNS). Superoxide ($O_2^{\cdot -}$), hydroxyl radicals ($OH^{\cdot}$), peroxyl radicals ($RO_2^{\cdot}$), and alkoxyl radicals ($RO^{\cdot}$) belong to the free-radical ROS that are formed by partial O_2 reduction and have at least one unpaired electron, making them highly reactive with cellular components. Mitochondrial superoxide dismutase (SOD) enzyme rapidly dismutates $O_2^{\cdot -}$ to form a reactive, non-free radical ROS, hydrogen peroxide (H_2O_2). Glutathione peroxidase enzyme (Gp_x) then catalyzes the conversion of most H_2O_2 to H_2O by oxidizing the tripeptide glutathione (GSH). A state of oxidative stress occurs when one or more complexes of the ETC (complexes I-III) are functionally impaired or genetically misassembled, which results in electron leakage forming $O_2^{\cdot -}$ or accumulation of H_2O_2 as a result of GSH deficiency or other enzymes involved in the detoxification process (Liu, Fiskum, & Schubert, 2002; Ray et al., 2012). Mitochondrial dysfunction and oxidative stress have emerged as central players in all common aging-associated neuronal pathologies.

Parkinson's Disease

Mounting lines of evidence strongly associate mitochondrial dysfunction and oxidative stress with the development and progression of PD (Chaturvedi & Flint Beal, 2013; Kawamata & Manfredi, 2017; M. T. Lin & Beal, 2006). Dysfunctional complex I of the mitochondrial respiratory chain has been suggested as the cornerstone of the pathogenesis of PD, reviewed here (Greenamyre, Sherer, Betarbet, & Panov, 2001). Since the first observation of PD-like symptoms in drug abusers who accidentally injected themselves with complex I selective inhibitor MPTP (1-methyl 4-phenyl-1,2,3,6-tetrahydropyridine) (Nicklas, Vyas, & Heikkila, 1985), an overwhelming number of studies have successfully demonstrated a similar correlation between complex I defect and Parkinsonian-like hallmarks and symptoms. For example, neuropathological features of parkinsonism including the nigrostriatal dopaminergic degeneration and accumulating cytoplasmic inclusions positively immunostained for ubiquitin and α-synuclein were successfully recapitulated after chronic infusion of complex I inhibitors, rotenone (Betarbet et al., 2000) and MPTP (Fornai et al., 2005), in rats and mice, respectively. More clinically relevant evidence for the role of mitochondrial dysfunction in PD pathogenesis comes from examining the brains of idiopathic PD patients. A significant decrease in the activity of complex I and functional and structural impairments of complex I subunits have been reported in the substantia nigra and frontal cortex of postmortem PD patients (Hattori, Tanaka, Ozawa, & Mizuno, 1991; Janetzky et al., 1994; Mizuno et al., 1989; Parker, Parks, & Swerdlow, 2008; Schapira et al., 1990). James P.B. Jr. et al. reported that brain mitochondria from postmortem PD patients showed misassembled, functionally impaired, and oxidatively damaged complex-I subunits (Keeney, Xie, Capaldi, & Bennett, 2006).

Under physiological conditions, the majority of ROS are produced by mitochondrial electron transport chain complexes (I-III) (M. T. Lin & Beal, 2006). A compromised or deficient complex I results in electron leakage and superoxide $O_2^{\cdot -}$ production by the one-electron reduction of O_2 (Andreyev, Kushnareva, & Starkov, 2005; Liu et al., 2002). Todd B.S. *et al*. demonstrated that oxidative damage was necessary for rotenone-induced cell death in three different models of PD *in vitro* and *in vivo* (Sherer et al., 2003). In addition to complex I deficiency, impairment in the cellular antioxidant defenses, primarily glutathione (GSH), is linked to PD symptoms. Several lines of evidence have shown that levels of the reduced form of GSH were significantly lower in the substantia nigra of PD patients compared to controls, even at early stages of the disease (Perry, Godin, & Hansen, 1982; Sian et al., 1994; Sofic, Lange, Jellinger, & Riederer, 1992). These studies strongly suggest the involvement of defective mitochondrial bioenergetics and subsequent oxidative stress in PD pathogenesis.

Alzheimer's Disease

Mechanistically, the cornerstone of the more common sporadic AD pathology is the augmented sequential proteolytic cleavage of the β- and γ-secretases of the amyloid-β (Aβ) precursor protein (APP), resulting in the accumulation and aggregation of the most toxic oligomer, $A\beta_{1-42}$. In addition to the pathological hallmarks of AD, including accumulation of extracellular senile plaques composed primarily of amyloid-β peptide (Aβ) and intracellular tau neurofibrillary tangles (NFT) (aggregates of hyperphosphorylated tau), an overwhelming number of studies demonstrate that dysfunctional mitochondria energetics and the accumulation of oxidative damage precede signs of AD pathogenesis in the brains of transgenic animal models and patients, as reviewed in (Cadonic, Sabbir, & Albensi, 2016; Chaturvedi & Flint Beal, 2013; M. T. Lin & Beal, 2006). Whether a defect of mitochondrial bioenergetics—and thus excessive generation of ROS—or the accumulation of Aβ or hyperphosphorylated tau initiate the cascade of events in AD is still controversial (the mitochondrial vs. amyloid cascade hypotheses) (Hardy & Higgins, 1992; Swerdlow, Burns, & Khan, 2014). On the one hand, oxidative stress may serve as a prerequisite for Aβ formation and accumulation. For example, findings reported by Ohyagi, Y. *et al*. suggested that a mitochondria-induced oxidative damage was necessary for increased intracellular Aβ levels and subsequent neuronal death after treatment with H_2O_2 (Ohyagi et al., 2000). In a transgenic β-amyloid precursor protein (APP)-mutant mouse, partial knockout of the mitochondrial antioxidant enzyme, manganese superoxide dismutase (MnSOD), markedly increased brain Aβ levels and plaque deposition (Li et al., 2004). A similar elevation in the levels and activity Aβ, in addition to the β-secretase levels (β-site amyloid precursor protein cleaving enzyme; BACE1), was reported when cellular energetics were perturbed using different pharmacological agents including insulin, 2-deoxyglucose, 3-nitropropionic acid and kainic acid (Velliquette, O'Connor, & Vassar, 2005). Numerous studies have also reported similar increases in the expression and activity of BACE1 by oxidants, followed by accumulation of Aβ and morphological changes associated with apoptotic cell death (Kao, Krichevsky, Kosik, & Tsai, 2004; Tamagno et al., 2002; Tamagno et al., 2003; Tamagno et al., 2005; Tong et al., 2005).

This increase in BACE1 activity and expression was regulated by an oxidative stress-induced proteolytic enzyme, γ-secretase *in vitro* and *in vivo* (Tamagno et al., 2008). Moreover, brain tissues from patients with sporadic AD showed a tight correlation between BACE1 activity and oxidative markers (Borghi et al., 2007). These data suggest that perturbed mitochondrial bioenergetics and subsequent oxidative stress could contribute to the pathogenesis of the common, sporadic, late-onset form of AD by altering the production and accumulation of Aβ.

On the other hand, mitochondrial dysfunction and oxidative stress have been reported by others as a consequence of the production and aggregation of many of the proteins implicated in AD pathogenesis. For instance, several studies using cultured cells and transgenic animal models demonstrated that both APP and Aβ oligomers can translocate and interact with mitochondria, thereby causing ETC complex dysfunction, impairing aerobic metabolism, and increasing ROS generation (Anandatheerthavarada, Biswas, Robin, & Avadhani, 2003; Casley, Canevari, Land, Clark, & Sharpe, 2002; Crouch et al., 2005; Devi, Prabhu, Galati, Avadhani, & Anandatheerthavarada, 2006; Manczak et al., 2006; Ronnback et al., 2016). Moreover, a tau and an Aβ-dependent decrease in protein levels of complexes I and IV, respectively, and a significant reduction in mitochondrial membrane potential and ATP levels have also been reported in double and triple AD transgenic mice (Eckert et al., 2008; Rhein et al., 2009). Injection of cortical and hippocampal neurons with Aβ resulted in intracellular Ca^{2+} overload, depletion of endogenous GSH, overproduction of ROS, overexpression of mitochondrial permeability transition pore (MPTP)-associated genes, and eventually triggered apoptotic cell death (Ferreiro, Oliveira, & Pereira, 2008; Ren, Zhang, Li, Wu, & Li, 2011). In conclusion, the mechanism(s) by which these disastrous cascades of cellular events are initiated remain elusive and controversial. The above studies indicate that the synaptic loss and cognitive decline seen in AD patients are net results of years of coordinated, highly dynamic interplay between mitochondria, oxidative stress, and AD-associated proteinopathies.

Mitochondria-driven Tumorigenesis

Tumorigenesis is a continuously active process that requires flexible adaptations to cellular and environmental alterations as well as exogenous insults, including cancer treatments. Over the years, in addition to their function as biosynthetic and bioenergetic factories, mitochondria have been shown to play critical roles in regulating innate immunity, redox homeostasis, oncogenic signaling, and survival of cancer cells. In the early 1950s, the biochemist Otto Warburg observed that, unlike normal cells, cancer cells primarily ferment glucose to lactate in the presence of oxygen (aerobic glycolysis) as opposed to aerobic oxidation of glucose to fuel mitochondrial respiration, and proposed that mitochondrial dysfunction is behind this metabolic shift (Warburg, 1956a, 1956b). Advances in cancer research have revealed that not all types of cancer displaying aerobic glycolysis have dysfunctional mitochondria. In this section, I will discuss the multifaceted functions of mitochondria beyond energy production and how mitochondria execute other functions to promote the progression of several types of cancer, particularly melanoma. In addition, I will outline the rationale behind my attempts to target mitochondrial metabolism to slow the growth of and kill human skin cancer cells.

Role of Mitochondria in Metabolic Reprogramming

In order to meet the bioenergetic and macromolecule demands of proliferating cells and to ensure survival in the harsh tumor microenvironment, cancer cells have shown unprecedented ability to reprogram their metabolism, processes in which mitochondria play direct or indirect roles (Pavlova & Thompson, 2016). For example, the vast majority of tumors rely on cytosolic glycolysis and divert their byproducts and intermediates from mitochondrial oxidation to fuel other anabolic pathways involved in cell growth and proliferation including serine/glycine biosynthesis, lipid biosynthesis, glycerol synthesis, pyrimidine biosynthesis, and the pentose phosphate pathway. To ensure sufficient cytosolic accumulation of these intermediates for maintaining the above processes, mitochondria tend to limit the uptake and consumption (oxidation) of the last product of the glycolytic pathway, pyruvate. Pyruvate kinase (PKM) catalyzes the conversion of phosphoenolpyruvate (PEP) to pyruvate, the final step in glycolysis. Numerous lines of evidence have shown that many cancers either overexpress the low-affinity, less-active isoform (PKM2) or downregulate the mitochondrial pyruvate carriers (MPC1 and MPC2). Such an approach allows the accumulation of cytosolic glycolysis intermediates needed for proliferation and growth (Christofk et al., 2008; Schell et al., 2014). In certain situations, for instance, hypoxic conditions, functional mitochondria can promote survival and support bioenergetic homeostasis by limiting pyruvate consumption (Ward & Thompson, 2012).

Pyruvate dehydrogenase (PDH) converts pyruvate to acetyl-CoA, one of the essential components of TCA cycle. Cancer cells phosphorylate and deactivate PDH by overexpressing PDH kinase (PDK1), rerouting the metabolism to cytosolic glycolysis (J.

W. Kim, Tchernyshyov, Semenza, & Dang, 2006; McFate et al., 2008; Sradhanjali, Tripathy, Rath, Mittal, & Reddy, 2017). A recent study suggested that PDK1 is essential for the outgrowth of some subtypes of melanoma *in vivo* (Kaplon et al., 2013). In many cancers, melanoma included, the scarcity of mitochondrial pyruvate for oxidation can lead to upregulation of other mitochondrial compensatory pathways to maintain mitochondrial metabolism, including glutaminolysis.

Glutamine is one of the most abundant and crucial nutrients for cell proliferation in human circulation (0.4-0.7 mM). Once uptaken by mitochondria, the enzyme glutaminase (GLS) converts glutamine to glutamate, which then enters the TCA cycle as an α-ketoglutarate by alanine or aspartate-induced transamination, or glutamate dehydrogenase (GDH) enzyme-mediated deamination (De Vitto, Perez-Valencia, & Radosevich, 2016). Glutamine provides crucial building blocks for macromolecule biosynthesis. It is not surprising, then, that different types of cancer, melanoma included, are critically dependent on glutamine (Filipp et al., 2012). While the proliferation of cancer cells benefits from glutamine as a nitrogen donor for the biosynthesis of nucleic acids (purines, pyrimidines, and NAD) and amino acids (asparagine and glucosamine), their viability depends on glutamine as a carbon source for mitochondrial metabolism (oxidative metabolism, glutathione and lipid biosynthesis) (Zong, Rabinowitz, & White, 2016). *C*-myc, a proto-oncogene that is frequently upregulated in different types of human tumors (D. M. Miller, Thomas, Islam, Muench, & Sedoris, 2012), including melanoma (X. Lin et al., 2017; Mannava et al., 2008; Zhuang et al., 2008), has been shown to promote mitochondrial uptake and metabolism of glutamine by upregulating glutamine transporters and GLS enzymes, respectively (Gao et al., 2009; Nicklin et al., 2009).

Upregulation of lipid biosynthesis to provide building blocks for membranes during proliferation is postulated to be a common feature across most tumors, including melanomas (Beloribi-Djefaflia, Vasseur, & Guillaumond, 2016). Acetyl-coenzyme A (acetyl-CoA), a necessary precursor for *de novo* biosynthesis of fatty acids and cholesterol, is synthesized in the mitochondria and indirectly exported to the cytoplasm. In cancer cells with functional mitochondria, acetyl-CoA is first condensed with glutaminolysis-derived oxaloacetic acid to form citrate via a reaction catalyzed by mitochondrial citrate synthase in a process called oxidative citrate synthesis. In hypoxic conditions, another pathway of mitochondrial citrate synthesis is activated, where mitochondrial-exclusive isocitrate dehydrogenase 2 (IDH2) enzyme converts glutamate-derived α-ketoglutarate to isocitrate/citrate. Once exported, citrate is converted to acetyl-CoA in the cytoplasm by ATP-citrate lyase (ACL) (Ward & Thompson, 2012). One of the most frequently activated pathways that play diverse roles in human cancers, including melanomas, is the phosphatidylinositol-3 kinase (PI3K/AKT) pathway (Fresno Vara et al., 2004). Several studies have reported that AKT directly phosphorylates and activates ACL enzymes, diverting mitochondrial citrate from entering the TCA cycle to acetyl-CoA production and *de novo* lipogenesis (Bauer, Hatzivassiliou, Zhao, Andreadis, & Thompson, 2005; Berwick, Hers, Heesom, Moule, & Tavare, 2002). A growing number of studies have demonstrated the crucial roles of mitochondrial citrate synthesis and ACL-mediated lipid biosynthesis in different aspects of cancer tumorigenesis, as reviewed here (Khwairakpam et al., 2015; Zaidi, Swinnen, & Smans, 2012).

Downstream of PI3K/AKT are well-characterized signaling regulators, the mammalian/mechanistic target of rapamycin (mTOR) complexes (mTOR1, mTOR2). These proteins serve as stress sensors that integrate environmental cues to regulate cancer cell growth, proliferation, survival, and metabolism (L. C. Kim, Cook, & Chen, 2017; Saxton & Sabatini, 2017). In addition to enhancing and regulating protein synthesis, emerging studies have identified mTOR1 as a critical regulator of mitochondrial biogenesis, mass, and metabolism, in part by targeting the transcriptional coactivator peroxisome proliferator-activated receptor gamma coactivator-1 alpha (PGC-1α) (Bentzinger et al., 2008; Cunningham et al., 2007). More recent studies have revealed that mTOR1 can manipulate mitochondrial bioenergetics in the quest to adapt to targeted therapies and tumor microenvironments in different types of cancers, including melanomas. For example, the resistance of specific subsets of human melanomas, harboring BRAF and NRAS mutations, to MEK inhibitors has been shown to be partially mediated by mTOR1/2-induced PGC-1α upregulation. Different mTOR1/2 inhibitors re-sensitize these mutant cell lines to the MEK inhibitor selumetinib (Gopal et al., 2014; Haq et al., 2013). Investigating the role of mitochondria in tumor adaptation and resistance, Viale *et al*. reported that withdrawal of doxycycline treatment of KRAS-mutant pancreatic ductal adenocarcinoma (PDAC) in mice resulted in a tumor relapse caused by a subpopulation of surviving cells with increased PGC-1α and activated mitochondrial OXPHOS. Inhibition of OXPHOS with oligomycin specifically targeted the surviving cells and prevented tumor relapse following KRAS ablation (Viale et al., 2014). In addition to regulating mitochondrial biogenesis, mTOR1 also has been shown to control other equally essential processes involved in cancer progression, including *de* *novo* lipogenesis (Duvel et al., 2010), glutaminolysis (Csibi et al., 2013), and *de novo* purine synthesis (Ben-Sahra, Hoxhaj, Ricoult, Asara, & Manning, 2016). Findings of these studies highlight the pivotal role of mitochondria in cancer cell bioenergetic homeostasis and metabolic reprogramming to ensure survival under harsh conditions. In the next chapter, I will demonstrate how perturbing mitochondrial bioenergetics could serve as a potential therapeutic target in melanomas with different $BRAF^{V600E}$ status.

Mitochondria-derived ROS in Cancer

As described above, the physiological function of mitochondrial ETC results in the transfer of a single electron to approximately 1-2% of consumed O_2 and to generate $O_2^{\cdot-}$ (Handy & Loscalzo, 2012). While early investigations focused on the oxidative damage caused by these reactive species, advances in cancer research have begun to illuminate the crucial roles that mitochondria-derived ROS play as signaling molecules to promote tumorigenesis. Cancer cells display higher basal levels of ROS than their normal counterparts. To avoid cellular damage, cancer cells uniquely keep ROS levels below that of oxidative stress by upregulating antioxidant defenses, which either detoxify ROS (degradation) or control their production (ROS production and clearance will be discussed in detail in Chapter 3) (Schumacker, 2015). The transcription factor NRF2, also known as nuclear factor (erythroid-derived-2)-like 2 (NFE2L2), has emerged as a prominent up-regulator of the transcript of several downstream antioxidant genes in response to different endogenous and exogenous oxidative insults. NRF2 activity is negatively regulated by its suppressor Kelch-like ECH-associated protein 1 (KEAP1) (Menegon, Columbano, & Giordano, 2016). At the protein level, one of the mechanisms by which NRF2 activity is enhanced in response to oxidative stress is by ROS-mediated oxidation of sensitive cysteine residues on KEAP1, leading to NRF2 stabilization and translocation to the nucleus (Fourquet, Guerois, Biard, & Toledano, 2010; Zhang & Hannink, 2003). Several deregulated oncogenes, such as *c*-myc, BRAF, and KRAS, have been shown to directly upregulate NRF2 to maintain ROS levels within a window that promote tumorigenesis without causing cellular damage (DeNicola et al., 2011; Satoh, Moriguchi, Takai, Ebina, & Yamamoto, 2013).

Elevated ROS levels have been implicated in the initial stages of different cancers including melanoma, as well as metastatic phenotypes and responsiveness to chemotherapy and other targeted therapies, as they can promote tumorigenic mutations by causing DNA damage (Wittgen & van Kempen, 2007). Generally speaking, the rate of nuclear DNA mutations is far less than that of mitochondrial DNA mutations. Mitochondrial DNA is more vulnerable to oxidation by ROS because it is near ROS production sites and is not protected by histones (Sabharwal & Schumacker, 2014). Although excessive production of ROS can cause genomic instability and damage of cellular components, a controlled increase in ROS can provide signaling messengers that regulate different proteins and signaling cascades to promote the tumorigenic progression of cancer cells.

ROS and Tumorigenic Signaling

Controlled elevation of mitochondria-derived ROS has been reported to regulate multiple signaling pathways frequently activated in many types of cancer, melanoma included. For example, one of the well-known oncogenic pathways is the hyperactivation of the PI3K/AKT pathway. This pathway has been implicated in different hallmarks of cancer, including proliferation and suppression of apoptosis. PI3Ks mainly phosphorylate phosphatidylinositol-4,5-bisphosphate (PIP2) to generate the second messenger phosphatidylinositol-3,4,5-trisphosphate (PIP3), which binds AKT, thereby facilitating its plasma membrane localization and phosphorylation. Phosphatase and tensin homolog deleted on chromosome 10 (PTEN) is a tumor suppressor gene that negatively regulates AKT by converting PIP3 to the inactive form, PIP2 (Chalhoub & Baker, 2009). Previous studies have reported that exogenous H_2O_2 oxidized cysteine residues in the active site of PTEN, resulting in loss of function and subsequent activation of PI3K/AKT pathway (Lee et al., 2002; Leslie et al., 2003). Mitochondria-derived ROS has also been shown to activate the AKT pathway by targeting and inactivating PTEN in cancer cells (Connor et al., 2005; Pelicano et al., 2006). Other AKT-associated phosphatases, such as protein phosphatase 2A (PP2A) and protein tyrosine phosphatase 1B (PTP1B), have been identified as targets for ROS-induced oxidative inactivation, resulting in continuous activation of AKT (Lou et al., 2008; Ostman, Frijhoff, Sandin, & Bohmer, 2011; Rao & Clayton, 2002; Salmeen et al., 2003).

Another equally important pathway shown to be responsive to the mitochondria-derived ROS is the hypoxia-responsive pathway. Due to the high proliferative demands and the lack of blood supply and thus O_2 *in vivo* (hypoxic conditions), tumor cells tend to adapt to such harsh conditions by promoting the stabilization of hypoxia-inducible factors (HIF_S) (Semenza, 2010). Under normoxic conditions, the α subunits of HIF1 and HIF2 are hydroxylated, destabilized, and targeted for proteasomal degradation by prolyl hydroxylase domain-containing protein 2 (PHD2) (Kaelin & Ratcliffe, 2008). Several lines of studies have observed that when cells are depleted of mitochondria or treated with ETC inhibitors, mitochondria-derived ROS was diminished and stabilization of HIF α subunits was inhibited under hypoxic conditions (Chandel et al., 1998; Chandel et al., 2000; Chandel & Schumacker, 1999). A few years later, mechanistic studies revealed that the hypoxia-induced increase in mitochondria-derived ROS (originating from complex III) stabilized HIF α subunits by inhibiting PHD2 activity (Brunelle et al., 2005; Guzy et al., 2005; Mansfield et al., 2005). In a recent study, unlike other tumors, malignant melanoma cells displayed a ROS-dependent, constitutively active HIF1α under normoxic conditions (Kuphal, Winklmeier, Warnecke, & Bosserhoff, 2010). Hence, the stabilization and activation of critical players in a hypoxia-response pathway via mitochondria-derived ROS is another example of the crucial roles of mitochondria in promoting the growth and survival of tumor cells.

REFERENCES

Anandatheerthavarada, H. K., Biswas, G., Robin, M. A., & Avadhani, N. G. (2003). Mitochondrial targeting and a novel transmembrane arrest of Alzheimer's amyloid precursor protein impairs mitochondrial function in neuronal cells. J Cell Biol, 161(1), 41-54.

Andreyev, A. Y., Kushnareva, Y. E., & Starkov, A. A. (2005). Mitochondrial metabolism of reactive oxygen species. Biochemistry (Mosc), 70(2), 200-214.

Bauer, D. E., Hatzivassiliou, G., Zhao, F., Andreadis, C., & Thompson, C. B. (2005). ATP citrate lyase is an important component of cell growth and transformation. Oncogene, 24(41), 6314-6322.

Beloribi-Djefaflia, S., Vasseur, S., & Guillaumond, F. (2016). Lipid metabolic reprogramming in cancer cells. Oncogenesis, 5, e189.

Ben-Sahra, I., Hoxhaj, G., Ricoult, S. J. H., Asara, J. M., & Manning, B. D. (2016). mTORC1 induces purine synthesis through control of the mitochondrial tetrahydrofolate cycle. Science, 351(6274), 728-733.

Bentzinger, C. F., Romanino, K., Cloetta, D., Lin, S., Mascarenhas, J. B., Oliveri, F., . . . Ruegg, M. A. (2008). Skeletal muscle-specific ablation of raptor, but not of rictor, causes metabolic changes and results in muscle dystrophy. Cell Metab, 8(5), 411-424.

Berwick, D. C., Hers, I., Heesom, K. J., Moule, S. K., & Tavare, J. M. (2002). The identification of ATP-citrate lyase as a protein kinase B (Akt) substrate in primary adipocytes. J Biol Chem, 277(37), 33895-33900.

Betarbet, R., Sherer, T. B., MacKenzie, G., Garcia-Osuna, M., Panov, A. V., & Greenamyre, J. T. (2000). Chronic systemic pesticide exposure reproduces features of Parkinson's disease. Nat Neurosci, 3(12), 1301-1306.

Borghi, R., Patriarca, S., Traverso, N., Piccini, A., Storace, D., Garuti, A., . . . Massimo, T. (2007). The increased activity of BACE1 correlates with oxidative stress in Alzheimer's disease. Neurobiol Aging, 28(7), 1009-1014.

Brunelle, J. K., Bell, E. L., Quesada, N. M., Vercauteren, K., Tiranti, V., Zeviani, M., . . . Chandel, N. S. (2005). Oxygen sensing requires mitochondrial ROS but not oxidative phosphorylation. Cell Metab, 1(6), 409-414.

Cadonic, C., Sabbir, M. G., & Albensi, B. C. (2016). Mechanisms of Mitochondrial Dysfunction in Alzheimer's Disease. Mol Neurobiol, 53(9), 6078-6090.

Casley, C. S., Canevari, L., Land, J. M., Clark, J. B., & Sharpe, M. A. (2002). Beta-amyloid inhibits integrated mitochondrial respiration and key enzyme activities. J Neurochem, 80(1), 91-100.

Chalhoub, N., & Baker, S. J. (2009). PTEN and the PI3-kinase pathway in cancer. Annu Rev Pathol, 4, 127-150.

Chandel, N. S., Maltepe, E., Goldwasser, E., Mathieu, C. E., Simon, M. C., & Schumacker, P. T. (1998). Mitochondrial reactive oxygen species trigger hypoxia-induced transcription. Proc Natl Acad Sci U S A, 95(20), 11715-11720.

Chandel, N. S., McClintock, D. S., Feliciano, C. E., Wood, T. M., Melendez, J. A., Rodriguez, A. M., & Schumacker, P. T. (2000). Reactive oxygen species generated at mitochondrial complex III stabilize hypoxia-inducible factor-1alpha during hypoxia: a mechanism of O2 sensing. J Biol Chem, 275(33), 25130-25138.

Chandel, N. S., & Schumacker, P. T. (1999). Cells depleted of mitochondrial DNA (rho0) yield insight into physiological mechanisms. FEBS Lett, 454(3), 173-176.

Chaturvedi, R. K., & Flint Beal, M. (2013). Mitochondrial diseases of the brain. Free Radic Biol Med, 63, 1-29.

Christofk, H. R., Vander Heiden, M. G., Harris, M. H., Ramanathan, A., Gerszten, R. E., Wei, R., . . . Cantley, L. C. (2008). The M2 splice isoform of pyruvate kinase is important for cancer metabolism and tumour growth. Nature, 452(7184), 230-233.

Connor, K. M., Subbaram, S., Regan, K. J., Nelson, K. K., Mazurkiewicz, J. E., Bartholomew, P. J., . . . Melendez, J. A. (2005). Mitochondrial H2O2 regulates the angiogenic phenotype via PTEN oxidation. J Biol Chem, 280(17), 16916-16924.

Crouch, P. J., Blake, R., Duce, J. A., Ciccotosto, G. D., Li, Q. X., Barnham, K. J., . . . Trounce, I. A. (2005). Copper-dependent inhibition of human cytochrome c oxidase by a dimeric conformer of amyloid-beta1-42. J Neurosci, 25(3), 672-679.

Csibi, A., Fendt, S. M., Li, C., Poulogiannis, G., Choo, A. Y., Chapski, D. J., . . . Blenis, J. (2013). The mTORC1 pathway stimulates glutamine metabolism and cell proliferation by repressing SIRT4. Cell, 153(4), 840-854.

Cunningham, J. T., Rodgers, J. T., Arlow, D. H., Vazquez, F., Mootha, V. K., & Puigserver, P. (2007). mTOR controls mitochondrial oxidative function through a YY1-PGC-1alpha transcriptional complex. Nature, 450(7170), 736-740.

De Vitto, H., Perez-Valencia, J., & Radosevich, J. A. (2016). Glutamine at focus: versatile roles in cancer. Tumour Biol, 37(2), 1541-1558.

DeNicola, G. M., Karreth, F. A., Humpton, T. J., Gopinathan, A., Wei, C., Frese, K., . . . Tuveson, D. A. (2011). Oncogene-induced Nrf2 transcription promotes ROS detoxification and tumorigenesis. Nature, 475(7354), 106-109.

Devi, L., Prabhu, B. M., Galati, D. F., Avadhani, N. G., & Anandatheerthavarada, H. K. (2006). Accumulation of amyloid precursor protein in the mitochondrial import channels of human Alzheimer's disease brain is associated with mitochondrial dysfunction. J Neurosci, 26(35), 9057-9068.

Duvel, K., Yecies, J. L., Menon, S., Raman, P., Lipovsky, A. I., Souza, A. L., . . . Manning, B. D. (2010). Activation of a metabolic gene regulatory network downstream of mTOR complex 1. Mol Cell, 39(2), 171-183.

Eckert, A., Hauptmann, S., Scherping, I., Rhein, V., Muller-Spahn, F., Gotz, J., & Muller, W. E. (2008). Soluble beta-amyloid leads to mitochondrial defects in amyloid precursor protein and tau transgenic mice. Neurodegener Dis, 5(3-4), 157-159.

Ernster, L., & Schatz, G. (1981). Mitochondria: a historical review. J Cell Biol, 91(3 Pt 2), 227s-255s.

Ferreiro, E., Oliveira, C. R., & Pereira, C. M. (2008). The release of calcium from the endoplasmic reticulum induced by amyloid-beta and prion peptides activates the mitochondrial apoptotic pathway. Neurobiol Dis, 30(3), 331-342.

Filipp, F. V., Ratnikov, B., De Ingeniis, J., Smith, J. W., Osterman, A. L., & Scott, D. A. (2012). Glutamine-fueled mitochondrial metabolism is decoupled from glycolysis in melanoma. Pigment Cell Melanoma Res, 25(6), 732-739.

Fornai, F., Schluter, O. M., Lenzi, P., Gesi, M., Ruffoli, R., Ferrucci, M., . . . Sudhof, T. C. (2005). Parkinson-like syndrome induced by continuous MPTP infusion: convergent roles of the ubiquitin-proteasome system and alpha-synuclein. Proc Natl Acad Sci U S A, 102(9), 3413-3418.

Fourquet, S., Guerois, R., Biard, D., & Toledano, M. B. (2010). Activation of NRF2 by nitrosative agents and H2O2 involves KEAP1 disulfide formation. J Biol Chem, 285(11), 8463-8471.

Fresno Vara, J. A., Casado, E., de Castro, J., Cejas, P., Belda-Iniesta, C., & Gonzalez-Baron, M. (2004). PI3K/Akt signalling pathway and cancer. Cancer Treat Rev, 30(2), 193-204.

Friedman, J. R., & Nunnari, J. (2014). Mitochondrial form and function. Nature, 505(7483), 335-343.

Gao, P., Tchernyshyov, I., Chang, T. C., Lee, Y. S., Kita, K., Ochi, T., . . . Dang, C. V. (2009). c-Myc suppression of miR-23a/b enhances mitochondrial glutaminase expression and glutamine metabolism. Nature, 458(7239), 762-765.

Gopal, Y. N., Rizos, H., Chen, G., Deng, W., Frederick, D. T., Cooper, Z. A., . . . Davies, M. A. (2014). Inhibition of mTORC1/2 overcomes resistance to MAPK pathway inhibitors mediated by PGC1alpha and oxidative phosphorylation in melanoma. Cancer Res, 74(23), 7037-7047.

Greenamyre, J. T., Sherer, T. B., Betarbet, R., & Panov, A. V. (2001). Complex I and Parkinson's disease. IUBMB Life, 52(3-5), 135-141.

Guzy, R. D., Hoyos, B., Robin, E., Chen, H., Liu, L., Mansfield, K. D., . . . Schumacker, P. T. (2005). Mitochondrial complex III is required for hypoxia-induced ROS production and cellular oxygen sensing. Cell Metab, 1(6), 401-408.

Handy, D. E., & Loscalzo, J. (2012). Redox regulation of mitochondrial function. Antioxid Redox Signal, 16(11), 1323-1367.

Haq, R., Shoag, J., Andreu-Perez, P., Yokoyama, S., Edelman, H., Rowe, G. C., . . . Widlund, H. R. (2013). Oncogenic BRAF regulates oxidative metabolism via PGC1alpha and MITF. Cancer Cell, 23(3), 302-315.

Hardy, J. A., & Higgins, G. A. (1992). Alzheimer's disease: the amyloid cascade hypothesis. Science, 256(5054), 184-185.

Hattori, N., Tanaka, M., Ozawa, T., & Mizuno, Y. (1991). Immunohistochemical studies on complexes I, II, III, and IV of mitochondria in Parkinson's disease. Ann Neurol, 30(4), 563-571.

Janetzky, B., Hauck, S., Youdim, M. B., Riederer, P., Jellinger, K., Pantucek, F., . . . Reichmann, H. (1994). Unaltered aconitase activity, but decreased complex I activity in substantia nigra pars compacta of patients with Parkinson's disease. Neurosci Lett, 169(1-2), 126-128.

Kaelin, W. G., Jr., & Ratcliffe, P. J. (2008). Oxygen sensing by metazoans: the central role of the HIF hydroxylase pathway. Mol Cell, 30(4), 393-402.

Kann, O., & Kovacs, R. (2007). Mitochondria and neuronal activity. Am J Physiol Cell Physiol, 292(2), C641-657.

Kao, S. C., Krichevsky, A. M., Kosik, K. S., & Tsai, L. H. (2004). BACE1 suppression by RNA interference in primary cortical neurons. J Biol Chem, 279(3), 1942-1949.

Kaplon, J., Zheng, L., Meissl, K., Chaneton, B., Selivanov, V. A., Mackay, G., . . . Peeper, D. S. (2013). A key role for mitochondrial gatekeeper pyruvate dehydrogenase in oncogene-induced senescence. Nature, 498(7452), 109-112.

Kawamata, H., & Manfredi, G. (2017). Correction: Proteinopathies and OXPHOS dysfunction in neurodegenerative diseases. J Cell Biol.

Keeney, P. M., Xie, J., Capaldi, R. A., & Bennett, J. P., Jr. (2006). Parkinson's disease brain mitochondrial complex I has oxidatively damaged subunits and is functionally impaired and misassembled. J Neurosci, 26(19), 5256-5264.

Khwairakpam, A. D., Shyamananda, M. S., Sailo, B. L., Rathnakaram, S. R., Padmavathi, G., Kotoky, J., & Kunnumakkara, A. B. (2015). ATP citrate lyase (ACLY): a promising target for cancer prevention and treatment. Curr Drug Targets, 16(2), 156-163.

Kim, J. W., Tchernyshyov, I., Semenza, G. L., & Dang, C. V. (2006). HIF-1-mediated expression of pyruvate dehydrogenase kinase: a metabolic switch required for cellular adaptation to hypoxia. Cell Metab, 3(3), 177-185.

Kim, L. C., Cook, R. S., & Chen, J. (2017). mTORC1 and mTORC2 in cancer and the tumor microenvironment. Oncogene, 36(16), 2191-2201.

Knott, A. B., Perkins, G., Schwarzenbacher, R., & Bossy-Wetzel, E. (2008). Mitochondrial fragmentation in neurodegeneration. Nat Rev Neurosci, 9(7), 505-518.

Kuhlbrandt, W. (2015). Structure and function of mitochondrial membrane protein complexes. BMC Biol, 13, 89.

Kuphal, S., Winklmeier, A., Warnecke, C., & Bosserhoff, A. K. (2010). Constitutive HIF-1 activity in malignant melanoma. Eur J Cancer, 46(6), 1159-1169.

Lee, S. R., Yang, K. S., Kwon, J., Lee, C., Jeong, W., & Rhee, S. G. (2002). Reversible inactivation of the tumor suppressor PTEN by H_2O_2. J Biol Chem, 277(23), 20336-20342.

Leslie, N. R., Bennett, D., Lindsay, Y. E., Stewart, H., Gray, A., & Downes, C. P. (2003). Redox regulation of PI 3-kinase signalling via inactivation of PTEN. EMBO J, 22(20), 5501-5510.

Li, F., Calingasan, N. Y., Yu, F., Mauck, W. M., Toidze, M., Almeida, C. G., . . . Gouras, G. K. (2004). Increased plaque burden in brains of APP mutant MnSOD heterozygous knockout mice. J Neurochem, 89(5), 1308-1312.

Lin, M. T., & Beal, M. F. (2006). Mitochondrial dysfunction and oxidative stress in neurodegenerative diseases. Nature, 443(7113), 787-795.

Lin, X., Sun, R., Zhao, X., Zhu, D., Zhao, X., Gu, Q., . . . Sun, B. (2017). C-myc overexpression drives melanoma metastasis by promoting vasculogenic mimicry via c-myc/snail/Bax signaling. J Mol Med (Berl), 95(1), 53-67.

Liu, Y., Fiskum, G., & Schubert, D. (2002). Generation of reactive oxygen species by the mitochondrial electron transport chain. J Neurochem, 80(5), 780-787.

Lou, Y. W., Chen, Y. Y., Hsu, S. F., Chen, R. K., Lee, C. L., Khoo, K. H., . . . Meng, T. C. (2008). Redox regulation of the protein tyrosine phosphatase PTP1B in cancer cells. FEBS J, 275(1), 69-88.

Manczak, M., Anekonda, T. S., Henson, E., Park, B. S., Quinn, J., & Reddy, P. H. (2006). Mitochondria are a direct site of A beta accumulation in Alzheimer's disease neurons: implications for free radical generation and oxidative damage in disease progression. Hum Mol Genet, 15(9), 1437-1449.

Mannava, S., Grachtchouk, V., Wheeler, L. J., Im, M., Zhuang, D., Slavina, E. G., . . . Nikiforov, M. A. (2008). Direct role of nucleotide metabolism in C-MYC-dependent proliferation of melanoma cells. Cell Cycle, 7(15), 2392-2400.

Mansfield, K. D., Guzy, R. D., Pan, Y., Young, R. M., Cash, T. P., Schumacker, P. T., & Simon, M. C. (2005). Mitochondrial dysfunction resulting from loss of cytochrome c impairs cellular oxygen sensing and hypoxic HIF-alpha activation. Cell Metab, 1(6), 393-399.

Masters, C. L., Bateman, R., Blennow, K., Rowe, C. C., Sperling, R. A., & Cummings, J. L. (2015). Alzheimer's disease. Nat Rev Dis Primers, 1, 15056.

McFate, T., Mohyeldin, A., Lu, H., Thakar, J., Henriques, J., Halim, N. D., . . . Verma, A. (2008). Pyruvate dehydrogenase complex activity controls metabolic and malignant phenotype in cancer cells. J Biol Chem, 283(33), 22700-22708.

Menegon, S., Columbano, A., & Giordano, S. (2016). The Dual Roles of NRF2 in Cancer. Trends Mol Med, 22(7), 578-593.

Miller, D. M., Thomas, S. D., Islam, A., Muench, D., & Sedoris, K. (2012). c-Myc and cancer metabolism. Clin Cancer Res, 18(20), 5546-5553.

Miller, W. L. (2013). Steroid hormone synthesis in mitochondria. Mol Cell Endocrinol, 379(1-2), 62-73.

Mizuno, Y., Ohta, S., Tanaka, M., Takamiya, S., Suzuki, K., Sato, T., . . . Kagawa, Y. (1989). Deficiencies in complex I subunits of the respiratory chain in Parkinson's disease. Biochem Biophys Res Commun, 163(3), 1450-1455.

Nicklas, W. J., Vyas, I., & Heikkila, R. E. (1985). Inhibition of NADH-linked oxidation in brain mitochondria by 1-methyl-4-phenyl-pyridine, a metabolite of the neurotoxin, 1-methyl-4-phenyl-1,2,5,6-tetrahydropyridine. Life Sci, 36(26), 2503-2508.

Nicklin, P., Bergman, P., Zhang, B., Triantafellow, E., Wang, H., Nyfeler, B., . . . Murphy, L. O. (2009). Bidirectional transport of amino acids regulates mTOR and autophagy. Cell, 136(3), 521-534.

Nunnari, J., & Suomalainen, A. (2012). Mitochondria: in sickness and in health. Cell, 148(6), 1145-1159.

Ohyagi, Y., Yamada, T., Nishioka, K., Clarke, N. J., Tomlinson, A. J., Naylor, S., . . . Younkin, S. G. (2000). Selective increase in cellular A beta 42 is related to apoptosis but not necrosis. Neuroreport, 11(1), 167-171.

Ostman, A., Frijhoff, J., Sandin, A., & Bohmer, F. D. (2011). Regulation of protein tyrosine phosphatases by reversible oxidation. J Biochem, 150(4), 345-356.

Parker, W. D., Jr., Parks, J. K., & Swerdlow, R. H. (2008). Complex I deficiency in Parkinson's disease frontal cortex. Brain Res, 1189, 215-218.

Pavlova, N. N., & Thompson, C. B. (2016). The emerging hallmarks of cancer metabolism. Cell Metab, 23(1), 27-47.

Pelicano, H., Xu, R. H., Du, M., Feng, L., Sasaki, R., Carew, J. S., . . . Huang, P. (2006). Mitochondrial respiration defects in cancer cells cause activation of Akt survival pathway through a redox-mediated mechanism. J Cell Biol, 175(6), 913-923.

Perry, T. L., Godin, D. V., & Hansen, S. (1982). Parkinson's disease: a disorder due to nigral glutathione deficiency? Neurosci Lett, 33(3), 305-310.

Poewe, W., Seppi, K., Tanner, C. M., Halliday, G. M., Brundin, P., Volkmann, J., . . . Lang, A. E. (2017). Parkinson disease. Nat Rev Dis Primers, 3, 17013.

Rao, R. K., & Clayton, L. W. (2002). Regulation of protein phosphatase 2A by hydrogen peroxide and glutathionylation. Biochem Biophys Res Commun, 293(1), 610-616.

Ray, P. D., Huang, B. W., & Tsuji, Y. (2012). Reactive oxygen species (ROS) homeostasis and redox regulation in cellular signaling. Cell Signal, 24(5), 981-990.

Ren, R., Zhang, Y., Li, B., Wu, Y., & Li, B. (2011). Effect of beta-amyloid (25-35) on mitochondrial function and expression of mitochondrial permeability transition pore proteins in rat hippocampal neurons. J Cell Biochem, 112(5), 1450-1457.

Rhein, V., Song, X., Wiesner, A., Ittner, L. M., Baysang, G., Meier, F., . . . Eckert, A. (2009). Amyloid-beta and tau synergistically impair the oxidative phosphorylation system in triple transgenic Alzheimer's disease mice. Proc Natl Acad Sci U S A, 106(47), 20057-20062.

Ronnback, A., Pavlov, P. F., Mansory, M., Gonze, P., Marliere, N., Winblad, B., . . . Behbahani, H. (2016). Mitochondrial dysfunction in a transgenic mouse model expressing human amyloid precursor protein (APP) with the Arctic mutation. J Neurochem, 136(3), 497-502.

Sabharwal, S. S., & Schumacker, P. T. (2014). Mitochondrial ROS in cancer: initiators, amplifiers or an Achilles' heel? Nat Rev Cancer, 14(11), 709-721.

Salmeen, A., Andersen, J. N., Myers, M. P., Meng, T. C., Hinks, J. A., Tonks, N. K., & Barford, D. (2003). Redox regulation of protein tyrosine phosphatase 1B involves a sulphenyl-amide intermediate. Nature, 423(6941), 769-773.

Satoh, H., Moriguchi, T., Takai, J., Ebina, M., & Yamamoto, M. (2013). Nrf2 prevents initiation but accelerates progression through the Kras signaling pathway during lung carcinogenesis. Cancer Res, 73(13), 4158-4168.

Saxton, R. A., & Sabatini, D. M. (2017). mTOR Signaling in Growth, Metabolism, and Disease. Cell, 168(6), 960-976.

Schapira, A. H., Cooper, J. M., Dexter, D., Clark, J. B., Jenner, P., & Marsden, C. D. (1990). Mitochondrial complex I deficiency in Parkinson's disease. J Neurochem, 54(3), 823-827.

Schell, J. C., Olson, K. A., Jiang, L., Hawkins, A. J., Van Vranken, J. G., Xie, J., . . . Rutter, J. (2014). A role for the mitochondrial pyruvate carrier as a repressor of the Warburg effect and colon cancer cell growth. Mol Cell, 56(3), 400-413.

Schumacker, P. T. (2015). Reactive oxygen species in cancer: a dance with the devil. Cancer Cell, 27(2), 156-157.

Semenza, G. L. (2010). Defining the role of hypoxia-inducible factor 1 in cancer biology and therapeutics. Oncogene, 29(5), 625-634.

Sherer, T. B., Betarbet, R., Testa, C. M., Seo, B. B., Richardson, J. R., Kim, J. H., . . . Greenamyre, J. T. (2003). Mechanism of toxicity in rotenone models of Parkinson's disease. J Neurosci, 23(34), 10756-10764.

Sian, J., Dexter, D. T., Lees, A. J., Daniel, S., Agid, Y., Javoy-Agid, F., . . . Marsden, C. D. (1994). Alterations in glutathione levels in Parkinson's disease and other neurodegenerative disorders affecting basal ganglia. Ann Neurol, 36(3), 348-355.

Sofic, E., Lange, K. W., Jellinger, K., & Riederer, P. (1992). Reduced and oxidized glutathione in the substantia nigra of patients with Parkinson's disease. Neurosci Lett, 142(2), 128-130.

Sradhanjali, S., Tripathy, D., Rath, S., Mittal, R., & Reddy, M. M. (2017). Overexpression of pyruvate dehydrogenase kinase 1 in retinoblastoma: A potential therapeutic opportunity for targeting vitreous seeds and hypoxic regions. PLoS One, 12(5), e0177744.

Swerdlow, R. H., Burns, J. M., & Khan, S. M. (2014). The Alzheimer's disease mitochondrial cascade hypothesis: progress and perspectives. Biochim Biophys Acta, 1842(8), 1219-1231.

Taanman, J. W. (1999). The mitochondrial genome: structure, transcription, translation and replication. Biochim Biophys Acta, 1410(2), 103-123.

Tamagno, E., Bardini, P., Obbili, A., Vitali, A., Borghi, R., Zaccheo, D., . . . Tabaton, M. (2002). Oxidative stress increases expression and activity of BACE in NT2 neurons. Neurobiol Dis, 10(3), 279-288.

Tamagno, E., Guglielmotto, M., Aragno, M., Borghi, R., Autelli, R., Giliberto, L., . . . Tabaton, M. (2008). Oxidative stress activates a positive feedback between the gamma- and beta-secretase cleavages of the beta-amyloid precursor protein. J Neurochem, 104(3), 683-695.

Tamagno, E., Guglielmotto, M., Bardini, P., Santoro, G., Davit, A., Di Simone, D., . . . Tabaton, M. (2003). Dehydroepiandrosterone reduces expression and activity of BACE in NT2 neurons exposed to oxidative stress. Neurobiol Dis, 14(2), 291-301.

Tamagno, E., Parola, M., Bardini, P., Piccini, A., Borghi, R., Guglielmotto, M., . . . Tabaton, M. (2005). Beta-site APP cleaving enzyme up-regulation induced by 4-hydroxynonenal is mediated by stress-activated protein kinases pathways. J Neurochem, 92(3), 628-636.

Tong, Y., Zhou, W., Fung, V., Christensen, M. A., Qing, H., Sun, X., & Song, W. (2005). Oxidative stress potentiates BACE1 gene expression and Abeta generation. J Neural Transm (Vienna), 112(3), 455-469.

Velliquette, R. A., O'Connor, T., & Vassar, R. (2005). Energy inhibition elevates beta-secretase levels and activity and is potentially amyloidogenic in APP transgenic mice: possible early events in Alzheimer's disease pathogenesis. J Neurosci, 25(47), 10874-10883.

Viale, A., Pettazzoni, P., Lyssiotis, C. A., Ying, H., Sanchez, N., Marchesini, M., . . . Draetta, G. F. (2014). Oncogene ablation-resistant pancreatic cancer cells depend on mitochondrial function. Nature, 514(7524), 628-632.

Wallace, D. C. (2005). A mitochondrial paradigm of metabolic and degenerative diseases, aging, and cancer: a dawn for evolutionary medicine. Annu Rev Genet, 39, 359-407.

Warburg, O. (1956a). On respiratory impairment in cancer cells. Science, 124(3215), 269-270.

Warburg, O. (1956b). On the origin of cancer cells. Science, 123(3191), 309-314.

Ward, P. S., & Thompson, C. B. (2012). Metabolic reprogramming: a cancer hallmark even warburg did not anticipate. Cancer Cell, 21(3), 297-308.

Wittgen, H. G., & van Kempen, L. C. (2007). Reactive oxygen species in melanoma and its therapeutic implications. Melanoma Res, 17(6), 400-409.

Zaidi, N., Swinnen, J. V., & Smans, K. (2012). ATP-citrate lyase: a key player in cancer metabolism. Cancer Res, 72(15), 3709-3714.

Zhang, D. D., & Hannink, M. (2003). Distinct cysteine residues in Keap1 are required for Keap1-dependent ubiquitination of Nrf2 and for stabilization of Nrf2 by chemopreventive agents and oxidative stress. Mol Cell Biol, 23(22), 8137-8151.

Zhuang, D., Mannava, S., Grachtchouk, V., Tang, W. H., Patil, S., Wawrzyniak, J. A., . . . Nikiforov, M. A. (2008). C-MYC overexpression is required for continuous suppression of oncogene-induced senescence in melanoma cells. Oncogene, 27(52), 6623-6634.

Zong, W. X., Rabinowitz, J. D., & White, E. (2016). Mitochondria and Cancer. Mol Cell, 61(5), 667-676.

CHAPTER 2

INHIBITING LACTATE DEHYDROGENASE A ENHANCES THE CYTOTOXICITY OF THE MITOCHONDRIA ACCUMULATING ANTIOXIDANT, MITOQUINONE, IN MELANOMA CELLS [*]

[*] Alshamrani, A. A., Franklin, J. L., Beedle, A. M., & Murph, M. M. (2016). Inhibiting Lactate Dehydrogenase A Enhances the Cytotoxicity of the Mitochondria Accumulating Antioxidant, Mitoquinone, in Melanoma Cells. In *Human Skin Cancer, Potential Biomarkers and Therapeutic Targets*. InTech.

Abstract

Limited options exist for inhibitors targeted against melanoma tumors with mutation subtypes other than BRAF. We investigated the cytotoxic activity of mitoquinone (MitoQ), an antioxidant and ubiquinone derivative, on various human melanoma cell lines, alone or in combination with other agents to perturb cellular bioenergetics. This lipophilic cation crosses the cell membrane, enters and accumulates in the mitochondria where it can disrupt mitochondrial function at micromolar concentrations or act as an antioxidant to preserve membrane integrity at nanomolar concentrations. Consistent with previous studies, cells treated with 12.5 μM MitoQ show significantly reduced viability versus control treatments. Although all melanoma cells were susceptible to cytotoxicity induced by MitoQ, cells with wild-type BRAF were responsive to lower doses, compared to cells with activating mutations in BRAF. Mechanistically, the positively charged lipophilic moiety of the MitoQ induced a dose-dependent collapse of the mitochondrial membrane potential ($\Delta\psi m$) and significantly reduced the mitochondrial ATP production and reduced oxygen consumption rate, suggesting mitochondrial dysfunction. We also combined MitoQ with a glycolytic lactate dehydrogenase A inhibitor (FX-11) and observed an enhanced reduction in viability, but not other therapies examined. To summarize, the data suggest that FX-11 enhances the cytotoxic effects of MitoQ in cells with wild-type BRAF.

1. Introduction

Mitoquinone (MitoQ) is a synthetic compound and functional antioxidant that enters the mitochondria and accumulates there. Low doses thwart lipid peroxidation, whereas doses above 1 μM can disrupt mitochondria membrane integrity [1, 2]. MitoQ has a ubiquinone moiety covalently connected through a 10-carbon alkyl chain to a lipophilic cation triphenylphosphonium (TPP^+) moiety [3, 4]. Recently, this TPP^+ moiety has also been shown to inhibit the mitochondrial electron transport chain and induce mitochondrial proton leak [5].

However, additional molecular mechanisms by which these lipophilic cations induce antitumorigenic effects likely exist. Previously, such mitochondria-targeted lipophilic cations displayed cytotoxic activity against hepatocellular carcinoma and breast cancer using cell culture and/or animal models of malignancy [6–8]. Unfortunately, controversy surrounds whether MitoQ can be utilized to prevent age-associated diseases, since some clinical trials showed a lack of efficacy in models outside of cancer [9, 10].

The mitochondria are the cell's powerhouse, responsible for the production of adenosine triphosphate (ATP), the energy required by the cell, utilizing a process called oxidative phosphorylation. Although mechanisms of aerobic cellular respiration are far more efficient in the production of ATP, many tumorigenic cells curiously switch to anaerobic metabolism (glycolysis) during malignant transformation, despite the presence of oxygen, which can be referred to as the "Warburg effect" [11]. This abnormal reprogramming of energy metabolism is therefore a hallmark of cancer [12]. However, not all cancer cells utilize glycolysis, which provides far less ATP, but at a much faster rate. At least prostate and breast cancers, as well as leukemias, likely require oxidative phosphorylation [13].

Intriguingly, studies also suggest that melanoma cells are dependent upon oxidative phosphorylation and show significantly more oxygen consumption than their normal counterparts, the melanocytes [13]. Alternatively, other studies suggest that melanoma cells may vacillate between utilizing either oxidative phosphorylation or glycolysis, depending on the environmental conditions [14]. Since cells found within tumors are highly heterogenic, it is likely that both conditions could be found at different locations when sampling the same tumor specimen.

Malignant cells reprogram or vacillate their cellular metabolism to meet the anabolic requirements for growth and proliferation while also sustaining their survival and viability amid harsh microenvironments with limited nutrients [15]. Among melanoma cells, this bioenergetic switch has been suggested to be a direct consequence of an oncogenic activating mutation in BRAF [13]. This further insinuates that melanomas expressing wild-type BRAF versus mutant BRAF proteins would respond differently to compounds that target the mitochondria. Since 2011, the armamentarium has grown tremendously for small molecule inhibitors targeting BRAF melanomas, including vemurafenib, cobimetinib, dabrafenib, and trametinib, but there is a lack of targeted therapeutics for those cancer subtypes without the BRAF mutation.

In this study, we sought to investigate whether MitoQ has cytotoxic activity against human melanoma cell lines, both wild-type and BRAF mutant melanomas, alone or in combination with other agents to perturb cellular bioenergetics. We observed that cells treated with MitoQ have significantly less viability than controls and display enhanced mitochondrial dysfunction due to a decrease in mitochondrial metabolism. Our results also demonstrate that the cytotoxic effect was mediated by the positively charged lipophilic moiety of the MitoQ, since (1-Decyl) triphenylphosphonium bromide (dTPP) recapitulated the reduction in cell viability. Furthermore, we found that MitoQ displayed lower IC_{50} when combined with the FX-11, a small molecule that inhibits lactate dehydrogenase A, compared to single agent treatment.

2. Materials and Methods

2.1. Cell Culture

BRAF wild-type (MeWo) and BRAF mutant (A375) human melanoma cell lines were originally purchased from the American Type Culture Collection (ATCC®, Manassas, VA). BRAF wild-type (SB-2) and BRAF mutant (SK-MEL-5) human melanoma cell lines were obtained from The University of Texas MD Anderson Cancer Center (Houston, TX) and the National Cancer Institute NCI/NIH (Frederick, MD), respectively. All cell culture materials were purchased from Life Technologies®, Thermo Fisher Scientific Inc. (Waltham, MA). SB-2 and SK-MEL-5 cells were grown in DMEM while MeWo and A375 cells were grown in Roswell Park Memorial Institute (RPMI 1640) medium supplemented with 5% fetal bovine serum, or without for serum-free medium, and 1% penicillin/streptomycin was used to culture and maintain cell lines (Gibco® and Thermo Fisher Scientific Inc.). Cells were cultured at 37°C in an atmosphere of 95% humidity and 5% CO_2. The medium was changed every 48 h. Cells were maintained for at least three subsequent passages after thawing prior to conducting the experiments to ensure the stability of their physiochemical properties. For the no-glucose media, we used RPMI 1640 deprived of glucose and HEPES buffer (Invitrogen®, Carlsbad, CA) that contained 2 mM L-glutamine and was supplemented with 5% FBS and 1% penicillin/streptomycin. For the high-glucose media, we used no-glucose media (above) supplemented with 25 mM glucose. For the galactose media, we used no-glucose media (above) supplemented with 10 mM galactose. The 100 mM glucose and galactose stock solutions were prepared by dissolving 1.8016 g of glucose or galactose powders into a 50 mL deionized water, volume to 100 mL, and then either sterilized by autoclaving (glucose solution) or filtration (galactose solution) to make it suitable for cell culturing purposes.

2.2. Chemicals

The mitochondrial antioxidant MitoQ was kindly provided by Dr. Michael P. Murphy, Medical Research Council Mitochondrial Biology Unit, Cambridge, United Kingdom, to J.L.F. Chemotherapeutic agents cis-diamineplatinum(II) dichloride and Dacarbazine were purchased from Sigma-Aldrich® (St Louis, MO). The lipophilic cation (1-Decyl) triphenylphosphonium bromide (dTPP) was purchased from Santa Cruz Biotechnology® (Dallas, TX). The LPA1/3 receptor antagonist, Ki16425 was purchased from Selleck® Chemicals (Houston, TX). The autotaxin inhibitors HA-130 and PF-8380, along with the lactate dehydrogenase A inhibitor FX-11 were purchased from Calbiochem®/EMD Millipore (Billerica, MA). The oxidative stress and apoptosis inducer Elesclomol was purchased from ApexBio® Technology LLC (Houston, TX).

2.3. Cell Viability Assay

MeWo, SB-2, SK-MEL-5, and A375 cells were seeded into standard, flat-bottom, clear 96-well plates at 5000-10,000 cells per well. Twenty-four hours after seeding, cells were maintained in either high glucose or galactose media for 48 h as previously described [16]. For drug treatments, compound stock solutions were prepared in distilled water (MitoQ, dTPP, Ki16425) or dimethyl sulfoxide (DMSO – cisplatin, DTIC, Elesclomol, FX-11, HA-130, and PF-8380), and then added to the wells to give the final drug concentrations (ranging from 0.1 to 200 μM) using different conditioned media where indicated. Cells were then incubated for 24 h and cell viability was measured using the CellTiter-Blue® viability assay Promega (Madison, WI) as previously described [17–20]. For combination experiments, MeWo cells were treated with the IC_{50} of FX-11, HA-130 or PF-8380 in combination with increasing concentrations of the MitoQ (0.8–50 μM) and incubated for 24 h in serum-free medium.

2.4. Mitochondrial Toxicity Assay

MeWo cells were plated at 5000 cells/well on standard, flat-bottom, clear 96-well plates with a final media volume of 100 μL/well. After 24 h, cells were then maintained in either high glucose or galactose media for 48 h as previously described prior to treatment with different compounds. Cells were then treated with MitoQ at different concentrations ranging from 1 to 200 μM in different conditioned media as specified above. In addition, cells were treated with a positive control toxic compound, digitonin (200 μM) and then both groups were incubated for 3 h at 37°C in an atmosphere of 95% humidity and 5% CO_2. Cellular toxicity profiles were generated using the Mitochondrial

ToxGlo™ Assay Promega (Madison, WI) following the manufacturer's protocol. Next, an ATP detection reagent that consists of luciferin, ATPase inhibitors, and thermostable Ultra-Glo™ luciferase was utilized to lyse viable cells and assess their ATP levels. This combination of reagents generates a luminescent signal proportional to the amount of ATP present.

2.5. Oxygen Consumption Rate Assay

MeWo cells were seeded at 15,000 cells/well on standard, flat-bottom, clear 96-well plates, and incubated for 24 h. Cells were treated with increasing concentrations of MitoQ (6.25–100 μM) for 20 min prior to the assessment of cellular respiration using Oxygen Consumption Rate Assay Kit MitoXpress®-Xtra HS Method, Cayman Chemicals (Ann Arbor, MI) following the manufacturer's protocol. The phosphorescent oxygen probe provided by the kit is quenched by oxygen in the extracellular medium. Therefore, the signal intensity obtained using this kit is proportional to the increase in the oxygen consumption rate by cells.

2.6. Assessment of the Mitochondrial Membrane Potential (Δψm)

MeWo cells were plated at 3000 cells/well in standard, flat-bottom, clear 96-well plates, and incubated for 24 h. Cells were washed twice with warm phosphate buffered saline and the nuclei were stained using NucBlue® live cell Hoechst 33342 stain following the manufacturer's protocol. Cells were then washed one time with warm PBS and then incubated in warm live cell imaging solution containing 20 nM tetramethylrhodamine methyl ester (TMRM) dye (Molecular Probes™, Thermo Fisher

Scientific) for 30 min in the dark at room temperature prior to the treatment with MitoQ (12.5–100 μM) or left untreated. Fluorescent imaging was performed to visualize nuclear (Hoechst) and mitochondrial (TMRM) staining with DAPI and TRITC filters, respectively, using an X71 inverted fluorescent microscope (Olympus, Center Valley, PA).

2.7. Fluorescence Images Analysis

MeWo cells were viewed using an Olympus X71 inverted epifluorescent microscope (40× objective) with an ND25 neutral density filter and images were captured using a DP-72 camera with identical black balance correction and exposure time in the CellSens Software (Olympus). Fluorescence microscopy experiments were repeated three times and three random pictures per condition per experiment were used to quantify the TMRM dye fluorescence intensity ($n = 3$) using Image-Pro® Insight 8.0 (MediaCybernetics®, Rockville, MD). The TMRM corrected fluorescence intensity was calculated for each image by normalizing the total red fluorescence of each entire 40× image (total TMRM intensity) by the number of cells in the same image (determined by the number of DAPI nuclei counted by manual tag in Image-Pro® Insight) to eliminate the impact of the differences in cell numbers between wells on our interpretation of data. Cells per image ranged from 135 to 270. Average TMRM corrected intensities for each dosing condition were expressed as relative percentage of the fluorescence intensities of untreated cells.

2.8. Statistical Analysis

The statistical differences in experimental data were analyzed using analysis of variance (ANOVA) test, followed by either Tukey's or Bonferroni's multiple comparisons tests between groups using GraphPad Prism (La Jolla, CA). Student's t-test was used when only two groups are compared. $*p < 0.05$, $**p < 0.01$, and $***p < 0.001$ indicate the levels of significance.

3. Results

To study the cytotoxic effects of the mitochondria-targeted lipophilic cation MitoQ in melanoma cells, we treated BRAF wild-type melanoma cells, MeWo and SB-2, or melanoma cells with BRAF activating mutations, A375 or SK-MEL-5, with increasing concentrations of MitoQ (0.8–50 μM) for 24 h (white bars) or 48 h (red bars). The data suggest that incubation with MitoQ during this period significantly suppresses the viability of all cell lines in a dose-dependent manner (Figure 1.1A). Notably, MeWo and SB-2 cells are more sensitive to lower concentrations of MitoQ (0.8–12.5 μM at 24 h; $p < 0.001$), when compared to A375 or SK-MEL-5 cells (Figure 1.1B). We assessed cell viability 24 h posttreatment in MeWo cells with increasing concentrations (0.8–200 μM) of Cisplatin, Dacarbazine, Ki16425, PF-8380, and HA-130 and Elesclomol to evaluate the cytotoxic potency of MitoQ in comparison with other chemotherapeutics (as negative controls) or investigational compounds (Figure 1.1C). MitoQ significantly affected cell viability at lower concentrations (3.1–50 μM) in MeWo cells when compared with other agents ($*p < 0.05$).

Since MeWo cells are more sensitive to MitoQ treatment than A375 or SK-MEL-5 cells, we used MeWo cells to examine whether the MitoQ-induced cytotoxicity of melanoma cells is resultant from dysfunctional mitochondria. For this assay, cells were treated with increasing concentrations (0.8–200 μM) of MitoQ in the presence of high glucose or glucose-deprived/galactose-supplemented medium. Replacing glucose with galactose in the medium is a well-established approach to study the effect of mitochondrial toxins in cancer cells [16, 21–23]. The purpose of this switch is to augment the susceptibility of cells to the MitoQ-mediated mitochondrial toxicity. Indeed, replacing glucose with galactose significantly exacerbates the cytotoxic effects of MitoQ after 24 or 48 h of treatment (Figure 1.2A). As a correlative, we measured the intracellular ATP levels after a 3 h treatment with increasing concentrations of MitoQ. MeWo cells cultured in galactose-supplemented medium exhibited significant reduction (***$p < 0.001$) among intracellular ATP levels with MitoQ treatment (Figure 1.2B).

We then assessed the cell membrane integrity using a fluorogenic peptide substrate (bis-AAFR110) that measures dead-cell protease activity. This peptide cannot cross the intact cell membranes of live cells and, therefore, the fluorescence signal is proportional to the non-live cells with compromised cell membranes. MitoQ treatment did not change cell membrane integrity in conditioned medium, unlike the cytotoxic compound digitonin, which is a detergent that can dissolve cell membranes, block ATP production, and subsequently cause cell death. Here, the positive control Digitonin caused a significant reduction in ATP (Figure 1.2C) and a twofold change in the cell membrane integrity (Figure 1.2D). Taken together, these data suggest that the cytotoxicity mediated via MitoQ potently affects mitochondria; however, it does not indicate the moiety responsible. Thus, we treated cells with dTPP, the positively charged lipophilic cation contained within the structure of MitoQ. Indeed, cells in galactose-containing medium were not viable in the presence of 0.8 μM dTPP at 24 or 48 h (Figure 1.2E), suggesting this component is responsible for the MitoQ-induced cytotoxicity.

To further confirm this mechanism, we measured the oxygen consumption rate of MeWo cells in response to acute exposure. The data show that MitoQ (20 min to 1 h) causes a significant reduction in the respiratory capacity of the mitochondria (Figure 1.3A). In addition, we assessed the impact of MitoQ on the mitochondrial membrane potential ($\Delta\psi m$) using fluorescent TMRM dye, which reflects the level of mitochondrial transmembrane potential—an indication of functional respiratory chain complexes. Data show the dose-dependent (Figure 1.3B) and rapid (15 min) collapse (Figure 1.3C) of the mitochondrial membrane potential ($\Delta\psi m$) in treated MeWo cells. Unlike staurosporine, the potent protein kinase inhibitor that is cytotoxic to mammalian tumor cell lines, which induced an apparent maximal reduction in the $\Delta\psi m$ at different concentrations (12.5–50 μM), MitoQ caused a dose-dependent collapse of the $\Delta\psi m$ (Figure 1.3D). These data show that MitoQ disrupted the mitochondrial respiratory chain and oxidative phosphorylation prior to decreases in cell viability, suggesting that these events lead to the subsequent melanoma cell cytotoxicity.

Since melanoma cells can reprogram their metabolism toward aerobic glycolysis to survive in case of mitochondrial dysfunction, we hypothesized that inhibition of the lactate dehydrogenase A (LDHA) enzyme would force the cells to rely on the mitochondria. Thus, this would increase vulnerability to MitoQ-induced cytotoxicity. Indeed, inhibition of LDHA using FX-11 enhanced the cytotoxic effects of MitoQ among

MeWo, A375, SB-2, and SK-MEL-5 cells after 24 h of incubation (Figure 1.4A). Interestingly, the combination of MitoQ with investigational autotaxin inhibitors PF-8380 and HA-130 for 24 h reduced, rather than enhanced, the cytotoxic capabilities of MitoQ (Figure 1.4B). The significant difference among treated groups is clearly demonstrated at 12.5 and 25 μM (Figure 1.4C). The IC_{50} values further reflect the increase in cytotoxicity with combinations between MitoQ and FX-11 against other comparisons (Table 1.1). These data suggest that disruption of the cellular metabolic machinery serves as a potential cytotoxic strategy against melanoma *in vitro* and warrants further investigation *in vivo*.

4. Discussion

The data suggest that melanoma cells are susceptible to cytotoxicity mediated by the functional antioxidant, MitoQ, by inducing a dose-dependent reduction in the basal oxygen consumption rate and a rapid depolarization of the mitochondrial membrane potential. Culturing MeWo cells in galactose-supplemented medium significantly reduces intracellular ATP levels in response to MitoQ treatment, compared with culturing in glucose-containing medium. The data show that MitoQ did not affect the plasma membrane integrity, unlike the cell membrane permeabilizing compound, digitonin. Importantly, our study demonstrates that dual disruption of the metabolic machinery enhances the cytotoxicity of MitoQ using FX-11 (Figure 1.5).

The ability of cancer cells, melanoma cells in particular, to reprogram their metabolism has emerged as a major factor that leads to the development of resistance to many existing therapeutics [15, 24]. Recent studies have demonstrated that high levels of lactate dehydrogenase (LDH), an enzyme that converts the cytosolic pyruvate into lactate, could be utilized as a predictor of disease progression and chemotherapy response in addition to its involvement in the resistance of different types of cancer cells, including melanoma cells to chemotherapeutic drugs [25, 26]. Results from a recent Phase III clinical trial revealed that metastatic melanoma patients with high serum levels of LDH have shown less favorable responses to Elesclomol, a promising first-in-class, mitochondria-targeted compound that exerts anticancer activity by inducing oxidative stress and subsequent apoptotic cell death [27]. Therefore, we hypothesized that inhibiting cellular aerobic glycolysis would create a synergistic response to the cytotoxic effects of MitoQ an approach conducted by several studies whereby mitochondria-targeted compounds were used in combination with glycolysis inhibitor, 2-deoxyglucose (2-DG). However, due to the high concentration of 2-DG needed to achieve the desirable synergistic cancer cell growth arrest [7, 8, 28], we were eager to find a more potent and irreversible glycolysis inhibitor that could augment MitoQ's cytotoxicity. Thus, in this study we found that the cytotoxic effects of MitoQ were synergistically enhanced when combined with a subtoxic (5 μM) concentration of FX-11, a selective suppressor of lactate dehydrogenase A. These data suggest that FX-11-treated cells were forced to rely more on mitochondrial oxidative phosphorylation to survive, which made them more vulnerable to the effects of the lipophilic cation MitoQ.

Recently, Trnka *et al*. have shown that longer aliphatic chains that link the positively charged triphenylphosphonium with any biologically active compound to target mitochondria inhibited the mitochondrial electron transport chain and induced mitochondrial proton leak [5]. Herein we observed that the MitoQ-induced cytotoxicity was mediated by the lipophilic cation dTPP moiety of MitoQ, rather than the redox cycling of the antioxidant moiety (ubiquinone). If dTPP is more potent than MitoQ, this is suggestive that the ubiquinone moiety may be protecting against the toxic effect of dTPP. Lastly, our results are in agreement with other publications [3, 5] showing the massive mitochondrial accumulation of the lipophilic cation moiety disrupts cellular respiratory capacities and induces cytotoxicity.

Surprisingly, autotaxin inhibitors reduced, rather than increased, the potency of MitoQ. Since autotaxin inhibitors have shown superior activity in melanoma models [18, 20, 29], we hypothesize that this reduction in MitoQ potency could have resulted from the disruption of mitochondrial membrane potential by autotaxin inhibitors. If so, this would affect the integration and accumulation of MitoQ into the mitochondria of melanoma cells and reduce the compound's efficacy. Our observation is in agreement with previous studies in which autotaxin has been reported to protect breast cancer and melanoma cells against Taxol-induced cell death through maintaining their mitochondrial membrane potential [30].

Consistent with previous studies showing that BRAF wild-type cells, including MeWo cells, display enhanced oxidative phosphorylation capabilities and mitochondrial capacity [31], we observed that these cells are more sensitive to MitoQ treatment than A375 cells, which possess an activating BRAF mutation. Therefore, our study is relevant to developing targeted strategies against wild-type BRAF melanomas, which includes the subtypes RAS, NF1, and Triple-WT [32], with the most relevance to Triple-WT. Although the majority of melanoma patients have tumors with activating mutations in BRAF, and thus are candidates for BRAF inhibitors like Vemurafenib, Trametinib, Dabrafenib, and Cobimetinib, those patients that have tumors with wild-type BRAF lack a clear strategy for targeted therapy. BRAF status of melanoma cells has been directly linked to cellular metabolism and the bioenergetic switch between mitochondrial oxidative phosphorylation and aerobic glycolysis [13, 15]. Given the ability of MitoQ to accumulate at large concentrations in the mitochondria [3], it is not altogether surprising that MitoQ has a profound effect on the viability of cells with increased mitochondrial respiratory capacities. In summary, more research is needed to investigate molecular vulnerabilities among these subgroups.

Table 1.1. Cell viability IC_{50} values after 24 or 48 h of treatment with MitoQ and FX-11.

Cell line	MitoQ Ave IC_{50} (µM) 24 h	MitoQ 95% CI	MitoQ + FX-11 Ave IC_{50} (µM) 24 h	MitoQ + FX-11 95% CI
MeWo	8.4	6.8 – 10.3	4.9	3.5 – 6.9
SB-2	5.1	2.6 – 9.8	2.8	2 – 4
A375	18.4	8.3 – 40.9	4.5	2.1 – 9.6
SK-MEL-5	10.6	4.6 –24.3	1.3	0.6 – 2.6

Cell line	MitoQ Ave IC_{50} (µM) 48 h	MitoQ 95% CI	MitoQ + FX-11 Ave IC_{50} (µM) 48 h	MitoQ + FX-11 95% CI
MeWo	13	9.3 – 18	8	5.2 – 12.2
SB-2	11	3.6 – 32.8	6.5	3.1 – 13.2
A375	21.4	8.5 – 53.7	5.2	2.3 – 11.8
SK-MEL-5	26	9.4 – 71.4	7.3	4.2 – 12.6

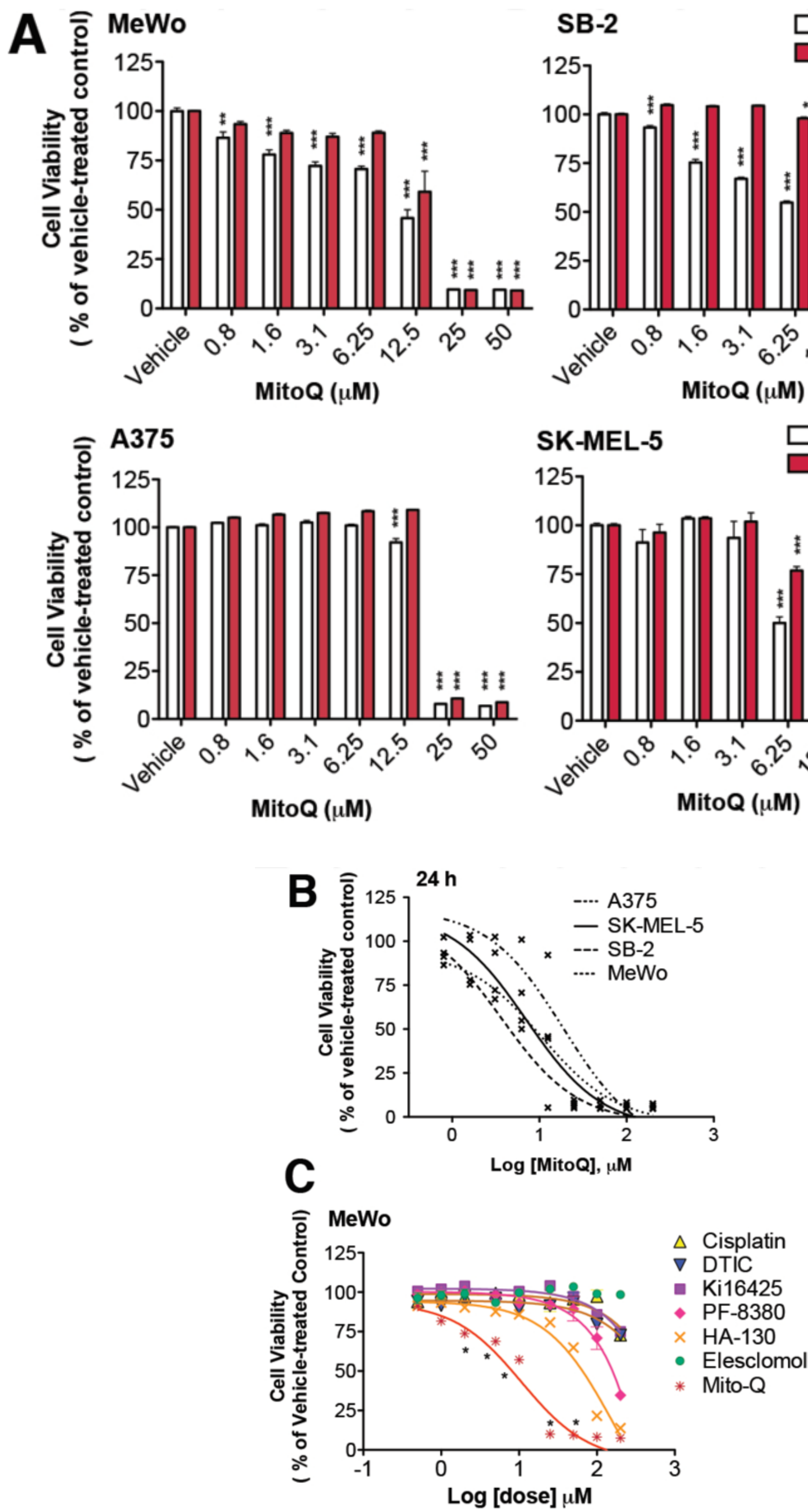
A
MeWo
SB-2
A375
SK-MEL-5
24h MitoQ
48h MitoQ
Cell Viability
(% of vehicle-treated control)
Vehicle
0.8
1.6
3.1
6.25
12.5
25
50
MitoQ (μM)
B
24 h
A375
SK-MEL-5
SB-2
MeWo
Log [MitoQ], μM
C
MeWo
Cisplatin
DTIC
Ki16425
PF-8380
HA-130
Elesclomol
Mito-Q
(% of Vehicle-treated Control)
Log [dose] μM

Figure 1.1. The viability of melanoma cells is significantly impacted after MitoQ treatment. To evaluate the potential cytotoxic effects of MitoQ in melanoma cells, (A) BRAF wild-type cells, MeWo and SB-2, or BRAF mutant cells, A375 and SK-MEL-5, were treated with increasing concentrations for 24 h (white bars) or 48 h (red bars) prior to determining cell viability. The data are expressed as the percentage of vehicle-treated controls (set at 100%) within each experiment and the mean ± SEM, n = 3 per treatment group (**$p < 0.01$; ***$p < 0.001$) indicate significant differences between vehicle versus treatment conditions. (B) The 24 h treatment data are also presented in logarithmic scale as a comparison between cell lines. (C) To assess the cytotoxicity of MitoQ in comparison with other approved drugs or investigational compounds, MeWo cells were treated with increasing concentrations (0.8–50 μM) for 24 h prior to the assessment of viability.

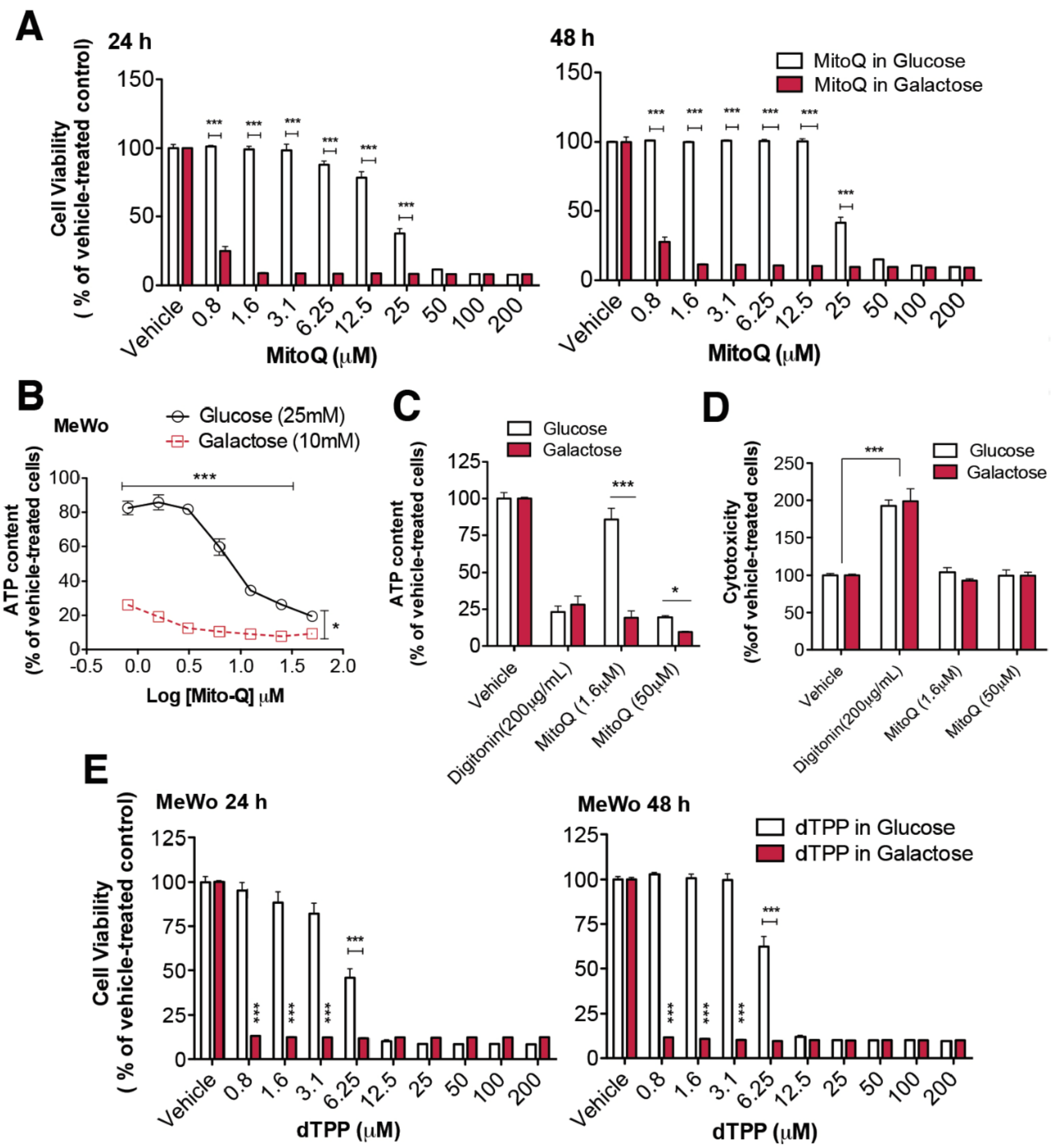

Figure 1.2. Replacing cell culture medium containing glucose with galactose increases susceptibility to MitoQ-mediated cytotoxicity. To determine whether the MitoQ-induced cytotoxicity is the result of dysfunctional mitochondria, we maintained MeWo cells in high glucose (25 mM) or galactose (10 mM)-supplemented medium for (A) 24 or 48 h prior to MitoQ treatment. Cells cultured in galactose-supplemented media

rely on the mitochondria to generate ATP and sustain viability, which make them more suitable to mitochondrial toxicants. (B) ATP levels of MeWo cells were measured using ToxGlo™ Assay after 3 h exposure to increasing concentrations of MitoQ with cells cultured in different medium. (C) Results are also shown as the percentage of vehicle-treated controls (set at 100%) within experiments using the indicated concentrations of MitoQ or digitonin. (D) Plasma membrane cytotoxicity was assessed using the indicated concentrations of MitoQ or digitonin. (E) The viability of MeWo cells was measured in the presence of dTPP with cells cultured in either glucose (black bars) or galactose (red bars) for 24 or 48 h as indicated. Data are expressed as means ± SEM, n = 3 per treatment group. *$p < 0.05$ and ***$p < 0.001$ indicate significant differences between groups.

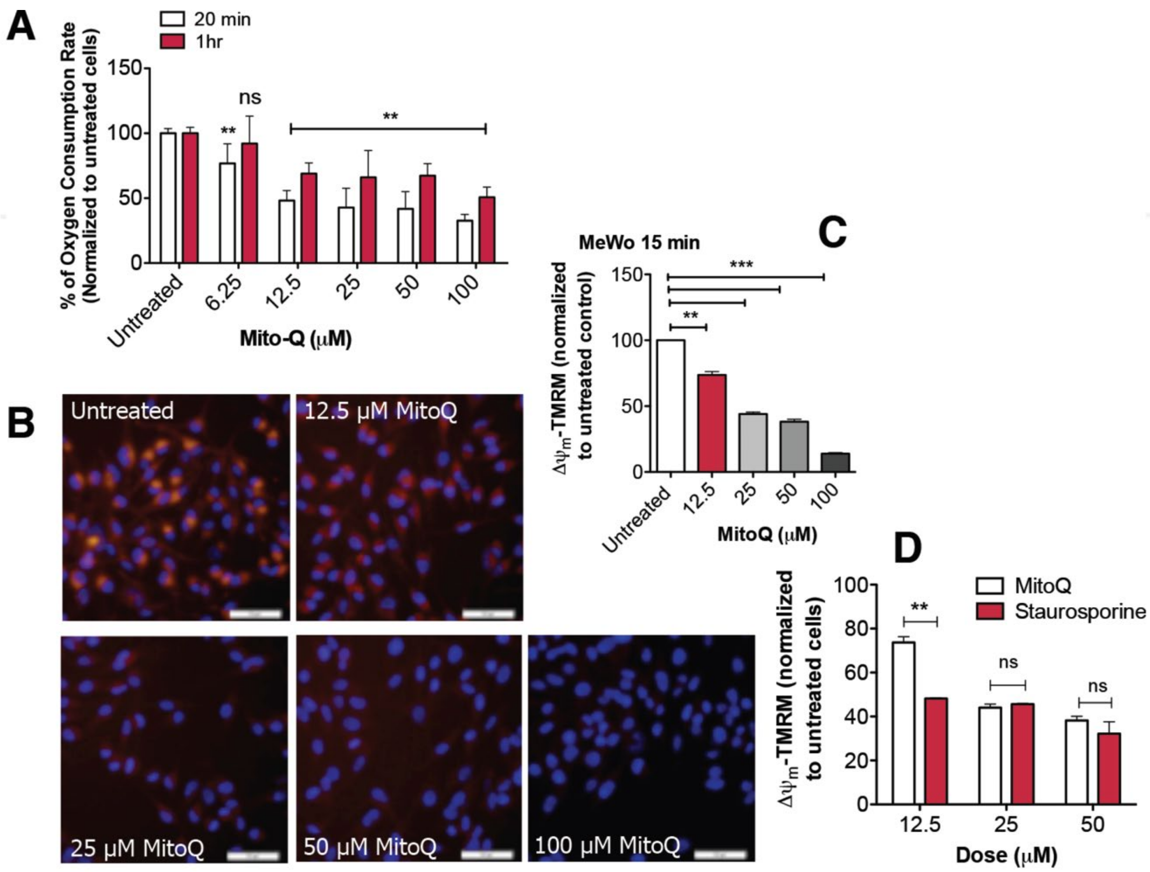

Figure 1.3. MitoQ induces a dose-dependent reduction in the mitochondrial transmembrane potential in melanoma cells. (A) The oxygen consumption rate was measured in untreated or MeWo cells treated with increasing concentrations of MitoQ for 20 min (white bars) or 1 h (red bars). (B) Representative fluorescence microscopic images of MeWo cells are shown after staining with TMRM (20 nM) and nuclear DAPI stain in the absence or presence of MitoQ (12.5, 25, 50, and 100 μM). (C) The bar graph shows quantification of TMRM signals after incubation for 30 min followed by 15 min treatment with MitoQ. The intensity of TMRM reflects the level of mitochondrial transmembrane potential, which indicate functional respiratory chain complexes. Treating MeWo cells with MitoQ resulted in a significant, dose-dependent reduction in the

mitochondrial transmembrane potential, further suggesting mitochondrial dysfunction. (D) The bar graph shows TMRM intensity of MitoQ-treated cells is compared to staurosporine treatments. All data are expressed as mean ± SEM. Scale bar: 50 μm. $^{**}p < 0.01$, $^{***}p < 0.001$ indicate a significant difference between MitoQ treated and untreated cells.

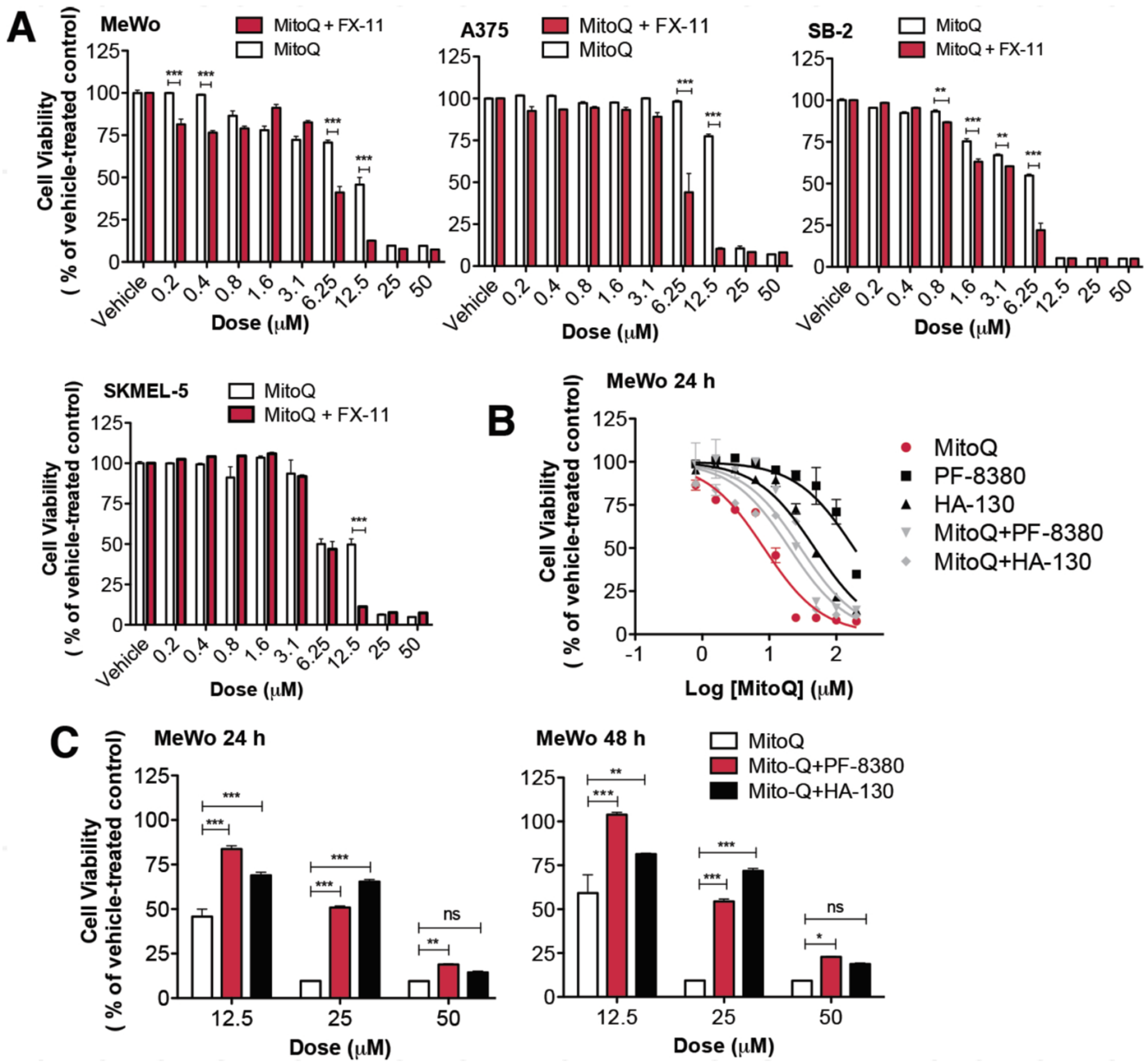

Figure 1.4. Inhibiting lactate dehydrogenase A enhances the cytotoxicity induced by MitoQ in melanoma cells. (A) MeWo, A375, SB-2, and SK-MEL-5 cells were treated with increasing concentrations of MitoQ for 24 h in the absence (white bars) and presence (red bars) of the lactate dehydrogenase inhibitor (FX-11, 5 μM). (B) Treatment of MeWo cells with 24 h MitoQ in combination with the autotaxin inhibitors, PF-8380 and HA-130 reduces, rather than enhances, the cytotoxic effects of MitoQ. (C) The viability of MeWo cells treated with the highest concentrations (12.5, 25, and 50 μM) of MitoQ alone or in combination with different autotaxin inhibitors for 24 and 48 h are

shown. Cell viability is shown as percentage of vehicle-treated controls (set at 100%) within all experiments. Data shown represent the mean ± SEM, n = 3 per treatment group. *$p < 0.05$, **$p < 0.01$, and ***$p < 0.001$ indicate significant differences between single and combination therapies.

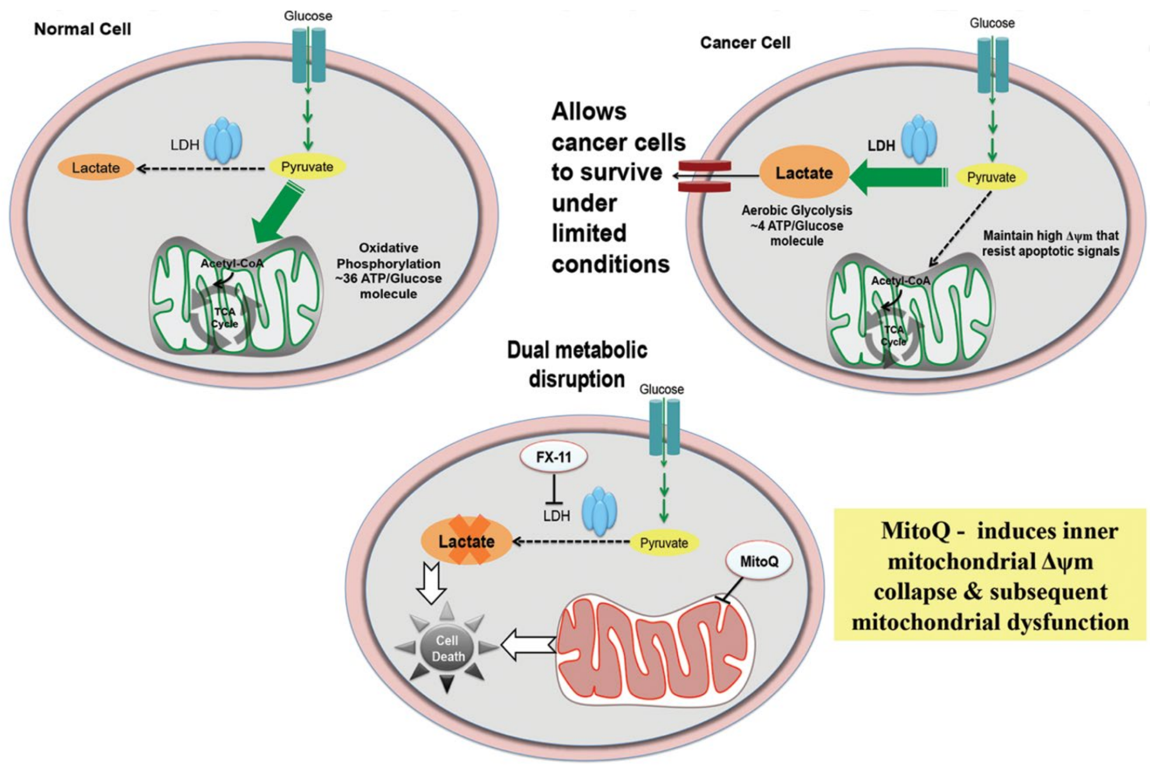

Figure 1.5. Working model of the observed treatment effects. This schematic illustration represents how targeting lactate metabolism enhances the cytotoxic effects of the mitochondria-targeted lipophilic cation MitoQ in melanoma cells. The normal cell depicted here is generating ATP through mitochondrial oxidative phosphorylation. During malignant transformation, cancer cells tend to strategically reprogram their metabolism toward aerobic glycolysis to produce lactate in order to acidify the surrounding tumor microenvironment and to survive in the harsh and metabolically limiting conditions, which is illustrated here by the cancer cell. In addition, the cancer cell is also maintaining functional mitochondria to resist apoptotic signals. The bottom cell shows our working model with dual disruption of metabolic machinery using a combination of MitoQ and FX-11 to counteract the melanoma cell’s viability.

REFERENCES

[1] Murphy MP: Selective targeting of bioactive compounds to mitochondria. Trend Biotechnol 1997, 15(8):326–330.

[2] Cocheme HM, Kelso GF, James AM, Ross MF, Trnka J, Mahendiran T, Asin Cayuela J, Blaikie FH, Manas AR, Porteous CM et al: Mitochondrial targeting of quinones: therapeutic implications. Mitochondrion 2007, 7(Suppl):S94–S102.

[3] Murphy MP, Smith RA: Targeting antioxidants to mitochondria by conjugation to lipophilic cations. Annu Rev Pharmacol Toxicol 2007, 47:629–656.

[4] Kelso GF, Porteous CM, Coulter CV, Hughes G, Porteous WK, Ledgerwood EC, Smith RA, Murphy MP: Selective targeting of a redox-active ubiquinone to mitochondria within cells: antioxidant and antiapoptotic properties. J Biol Chem 2001, 276(7):4588-4596.

[5] Trnka J, Elkalaf M, Andel M: Lipophilic triphenylphosphonium cations inhibit mitochondrial electron transport chain and induce mitochondrial proton leak. PLoS One 2015, 10(4):e0121837.

[6] Gonzalez Y, Aryal B, Chehab L, Rao VA: Atg7- and Keap1-dependent autophagy protects breast cancer cell lines against mitoquinone-induced oxidative stress. Oncotarget 2014, 5(6):1526–1537.

[7] Dilip A, Cheng G, Joseph J, Kunnimalaiyaan S, Kalyanaraman B, Kunnimalaiyaan M, Gamblin TC: Mitochondria-targeted antioxidant and glycolysis inhibition:

synergistic therapy in hepatocellular carcinoma. Anticancer Drugs 2013, 24(9):881–888.

[8] Cheng G, Zielonka J, Dranka BP, McAllister D, Mackinnon AC Jr., Joseph J, Kalyanaraman B: Mitochondria-targeted drugs synergize with 2-deoxyglucose to trigger breast cancer cell death. Cancer Res 2012, 72(10):2634–2644.

[9] Smith RA, Murphy MP: Animal and human studies with the mitochondria-targeted antioxidant MitoQ. Ann N Y Acad Sci 2010, 1201:96–103.

[10] Oyewole AO, Birch-Machin MA: Mitochondria-targeted antioxidants. FASEB J 2015, 29(12):4766–4771.

[11] Warburg O: On respiratory impairment in cancer cells. Science 1956, 124(3215):269–270.

[12] Hanahan D, Weinberg RA: Hallmarks of cancer: the next generation. Cell 2011, 144(5): 646–674.

[13] Haq R, Fisher DE, Widlund HR: Molecular pathways: BRAF induces bioenergetic adaptation by attenuating oxidative phosphorylation. Clin Cancer Res 2014, 20(9):2257–2263.

[14] Theodosakis N, Micevic G, Kelly DP, Bosenberg M: Mitochondrial function in melanoma. Arch Biochem Biophys 2014, 563:56–59.

[15] Abildgaard C, Guldberg P: Molecular drivers of cellular metabolic reprogramming in melanoma. Trends Mol Med 2015, 21(3):164–171.

[16] Marroquin LD, Hynes J, Dykens JA, Jamieson JD, Will Y: Circumventing the Crabtree effect: replacing media glucose with galactose increases susceptibility of HepG2 cells to mitochondrial toxicants. Toxicol Sci 2007, 97(2):539–547.

[17] Hasegawa Y, Murph M, Yu S, Tigyi G, Mills GB: Lysophosphatidic acid (LPA)-induced vasodilator-stimulated phosphoprotein mediates lamellipodia formation to initiate motility in PC-3 prostate cancer cells. Mol Oncol 2008, 2(1):54–69.

[18] Altman MK, Gopal V, Jia W, Yu S, Hall H, Mills GB, McGinnis AC, Bartlett MG, Jiang G, Madan D et al: Targeting melanoma growth and viability reveals dualistic functionality of the phosphonothionate analogue of carba cyclic phosphatidic acid. Mol Cancer 2010, 9:140.

[19] Hooks SB, Callihan P, Altman MK, Hurst JH, Ali MW, Murph MM: Regulators of GProtein signaling RGS10 and RGS17 regulate chemoresistance in ovarian cancer cells. Mol Cancer 2010, 9:289.

[20] Murph MM, Jiang GW, Altman MK, Jia W, Nguyen DT, Fambrough JM, Hardman WJ, Nguyen HT, Tran SK, Alshamrani AA et al: Vinyl sulfone analogs of lysophosphatidylcholine irreversibly inhibit autotaxin and prevent angiogenesis in melanoma. Bioorg Med Chem. 2015 Sep 1;23(17):5999–6013.

[21] Rossignol R, Gilkerson R, Aggeler R, Yamagata K, Remington SJ, Capaldi RA: Energy substrate modulates mitochondrial structure and oxidative capacity in cancer cells. Cancer Res 2004, 64(3):985–993.

[22] Dykens JA, Jamieson J, Marroquin L, Nadanaciva S, Billis PA, Will Y: Biguanideinduced mitochondrial dysfunction yields increased lactate production and cytotoxicity of aerobically-poised HepG2 cells and human hepatocytes in vitro. Toxicol Appl Pharmacol 2008, 233(2):203–210.

[23] Rana P, Nadanaciva S, Will Y: Mitochondrial membrane potential measurement of H9c2 cells grown in high-glucose and galactose-containing media does not

provide additional predictivity towards mitochondrial assessment. Toxicol In Vitro 2011, 25(2):580–587.

[24] Zhao Y, Butler EB, Tan M: Targeting cellular metabolism to improve cancer therapeutics. Cell Death Dis 2013, 4:e532.

[25] Zhuang L, Scolyer RA, Murali R, McCarthy SW, Zhang XD, Thompson JF, Hersey P: Lactate dehydrogenase 5 expression in melanoma increases with disease progression and is associated with expression of Bcl-XL and Mcl-1, but not Bcl-2 proteins. Mod Pathol 2010, 23(1):45–53.

[26] Doherty JR, Cleveland JL: Targeting lactate metabolism for cancer therapeutics. J Clin Invest 2013, 123(9):3685–3692.

[27] O'Day SJ, Eggermont AM, Chiarion-Sileni V, Kefford R, Grob JJ, Mortier L, Robert C, Schachter J, Testori A, Mackiewicz J et al: Final results of phase III SYMMETRY study: randomized, double-blind trial of elesclomol plus paclitaxel versus paclitaxel alone as treatment for chemotherapy-naive patients with advanced melanoma. J Clin Oncol 2013, 31(9):1211–1218.

[28] Cheng G, Zielonka J, McAllister DM, Mackinnon AC, Jr., Joseph J, Dwinell MB, Kalyanaraman B: Mitochondria-targeted vitamin E analogs inhibit breast cancer cell energy metabolism and promote cell death. BMC Cancer 2013, 13:285.

[29] Baker DL, Fujiwara Y, Pigg KR, Tsukahara R, Kobayashi S, Murofushi H, Uchiyama A, Murakami-Murofushi K, Koh E, Bandle RW et al: Carba analogs of cyclic phosphatidic acid are selective inhibitors of autotaxin and cancer cell invasion and metastasis. J Biol Chem 2006, 281(32):22786–22793.

[30] Samadi N, Gaetano C, Goping IS, Brindley DN: Autotaxin protects MCF-7 breast cancer and MDA-MB-435 melanoma cells against Taxol-induced apoptosis. Oncogene 2009, 28(7):1028–1039.

[31] Vazquez F, Lim JH, Chim H, Bhalla K, Girnun G, Pierce K, Clish CB, Granter SR, Widlund HR, Spiegelman BM et al: PGC1alpha expression defines a subset of human melanoma tumors with increased mitochondrial capacity and resistance to oxidative stress. Cancer Cell 2013, 23(3):287–301.

[32] Cancer Genome Atlas N: Genomic classification of cutaneous melanoma. Cell 2015, 161(7):1681–1696.

CHAPTER 3

MITOCHONDRIAL REGULATION OF THE DEATH OF NEUROTROPHIN-DEPRIVED NEURONS

Features of Programmed Cell Death in Neuronal Development

Apoptosis is a unique form of programmed cell death (PCD) that has been implicated in various physiological processes such as normal cell turnover, immune system maintenance and response. It is also implicated during both normal development of the nervous system and pathological developments such as cancers and several neurodegenerative diseases, as previously mentioned in Chapter 1 (Elmore, 2007; Yuan & Yankner, 2000). Unlike the suggested nomenclature "regulated cell death," which is mainly induced by pathological conditions or toxic insults, "PCD" indicates naturally occurring or developmentally programmed cell death in embryonic and postembryonic life (Galluzzi et al., 2015; Galluzzi et al., 2012). Distinctive morphological characteristics distinguish apoptosis from other types of cell death, including asymmetric but still-intact plasma membrane at early stages, plasma membrane blebbing, chromatin condensation, DNA fragmentation, cytoplasmic shrinkage and fragmentation at later stages, and neurotic degradation. Eventually, dying cells are rapidly engulfed by phagocytic cells to prevent inflammatory responses (Kerr, Wyllie, & Currie, 1972).

One of the well-established physiological functions of apoptosis occurs during the development of the vertebrate nervous system. Soon after exiting the cell cycle early in development, and at the time when post-mitotic neurons start to innervate (form synaptic contact with) their target organs, roughly 50% of neurons undergo apoptotic death to match the number of neurons to the size of the organ they innervate (Oppenheim, 1991). The number of neurons in the peripheral nervous system (PNS), and some areas in the central nervous system (CNS), surviving this event has been primarily linked to the availability and sufficiency of organ-produced neurotrophic factors. The proposed coordination between organ size, the quantities of neurotrophic substances produced, and the number of innervated neurons were the bases of the “neurotrophic theory” (Cowan, 2001; Oppenheim, 1991; Purves, Snider, & Voyvodic, 1988). The initial recognition of the tyrosine kinase receptor tropomyosin receptor kinase A (TrkA) as a receptor necessary for nerve growth factor (NGF)-induced survival (Klein, Jing, Nanduri, O'Rourke, & Barbacid, 1991), along with its expression patterns, supports this theory in the PNS (Glebova & Ginty, 2005).

Unlike neurons in the PNS, the majority of developing neurons in the CNS seem to be less dependent on either the expression of receptors or the availability of neurotrophic factors, as the knockdown or deletion of the highly expressed, closely related receptor (TrKB) or the brain-derived neurotrophic factor (BDNF), respectively, affect only a subset of CNS neuronal populations (Ernfors, Lee, & Jaenisch, 1994; Jones, Farinas, Backus, & Reichardt, 1994; Nikoletopoulou et al., 2010; Rauskolb et al., 2010; Southwell et al., 2012). The following section will discuss several *in vitro* models used to recapitulate this form of developmental cell death.

In Vitro Models of the Apoptotic Death of Developing Neurons

The physiological significance of developmental cell death has been investigated over the last 70 years (Glucksmann, 1951). The role of neurotrophic factors in the elimination of overproduced neurons during the PNS development, or “the neurotrophic theory,” is considered one of the most prominent and well-characterized examples of the involvement of cell death in vertebrate development (Yamaguchi & Miura, 2015). In search of understanding the molecular mechanisms underlying the apoptotic death during neuronal development, several *in vitro* models have been established to recapitulate the features of neurons undergoing physiological death *in vivo*. Among these are rat- and mouse-derived cultures of NGF-deprived sympathetic neurons, cultures of serum-starved/repolarized cerebellar granule neurons (CGNs), cultures of toxin-treated cortical neurons, and trophic factor-deprived chick motoneurons (D'Mello, Galli, Ciotti, & Calissano, 1993; Deckwerth & Johnson, 1993; Desagher et al., 2005; Deshmukh & Johnson, 1998; Miller & Johnson, 1996; Milligan, Oppenheim, & Schwartz, 1994; Wong et al., 2005). Since the early 1980s, sympathetic neurons dissected from the superior cervical ganglion (SCG) have become the most extensively studied model of neuronal death. Even though yielding a low number of cells to work with, the accessibility and size of the SCG makes it relatively easier to dissect (Johnson & Argiro, 1983), as illustrated in Figure 2.1. Late embryonic and early postnatal sympathetic neurons dissected from rat or mice SCGs show apoptotic hallmarks within 48-72 h when deprived of NGF (Deckwerth & Johnson, 1993; Edwards & Tolkovsky, 1994; Martin et al., 1988). The sequence of biochemical and morphological changes following NGF withdrawal-induced death of sympathetic neurons, which will be discussed in detail in the following sections, is summarized in Figure 2.2.

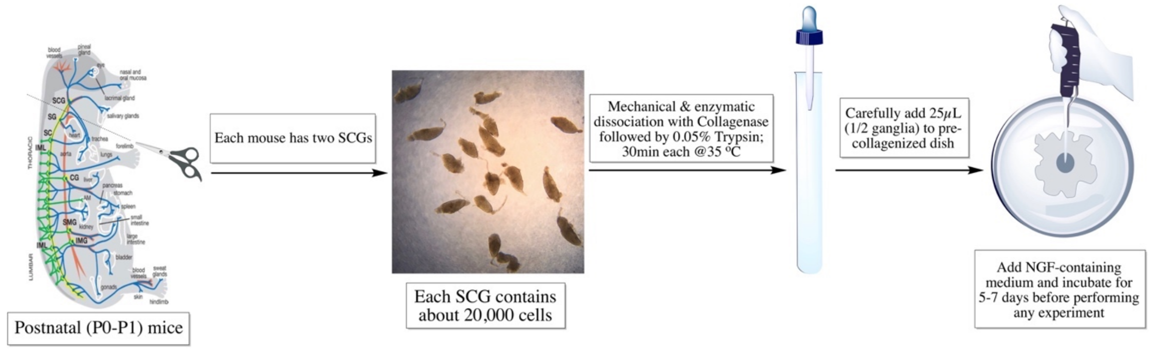

Figure 2.1. Dissecting and culturing sympathetic neurons from a day$_0$ - or day$_1$-old mouse. The size and location of the mouse superior cervical ganglia (SCG) make it easier to dissect than other sympathetic ganglia*. The SCG is stereotypically located in the bifurcation between the internal and external carotid arteries and can be distinguished from the surrounding fat tissues as a white to translucent, spindle-shaped mass. As shown above, mice are decapitated as close to the "shoulder" area as possible to avoid losing any parts of the SCG. Following dissection, removing excess fat tissues and blood vesicles is crucial to ensure culturing debris-free neurons. The SCG are then subjected to an optimized multistep dissociation process (*for details see methods section in Chapter 4*) to retrieve the highest number of cells possible. Neurons are allowed to attach to a collagenized surface for one hour at 37 ^{0}C and 5% CO_2. Cultures are then maintained in a NGF-containing medium for 5-7 days to restore their physiochemical properties.

**The schematic representation of the mouse sympathetic nervous system anatomy was adopted from (Glebova & Ginty, 2005), with permission.*

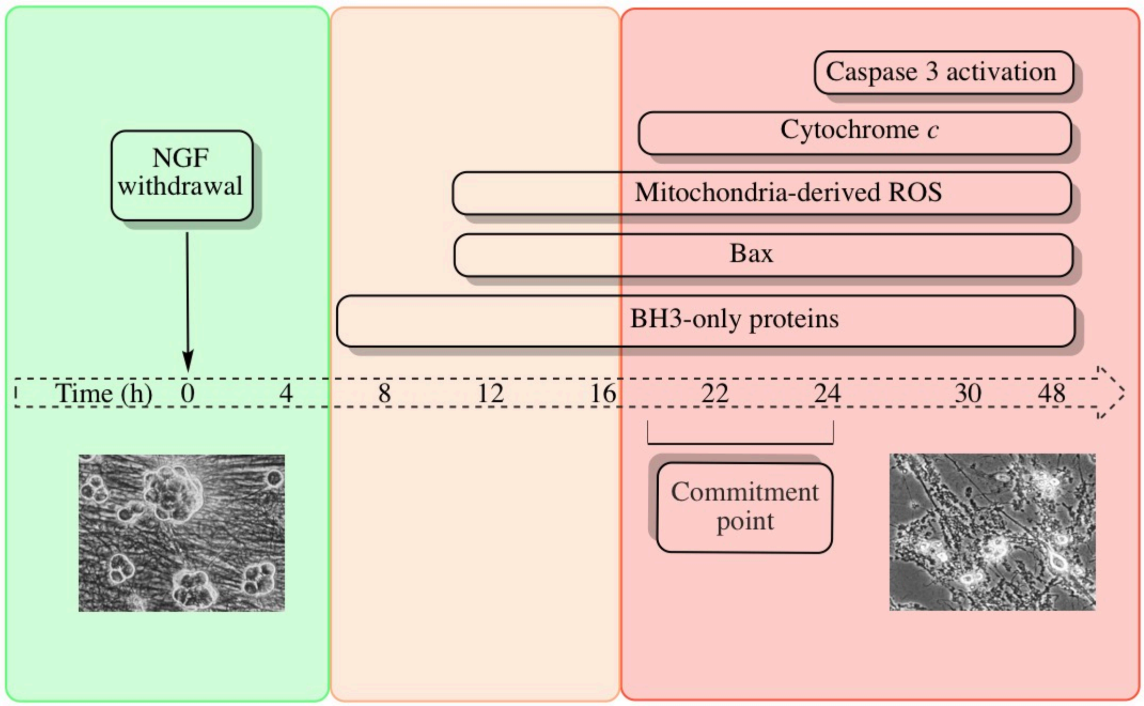

Figure 2.2. Illustrative timeline of morphological and biochemical changes during the apoptotic death of NGF-deprived mouse sympathetic neurons *in vitro*. The sequence of events begins approximately 6 hours after NGF withdrawal when the transcriptional and protein levels of BH3-only pro-apoptotic proteins start to rise. The elevation in Bax-dependent ROS derived mainly from the mitochondria starts as early as 12 hours post deprivation and is sustained throughout the apoptotic process. The release of cytochrome *c* and subsequent caspase 3 activation occurs between approximately 18-24 hours after withdrawal. It is within this window that only 50% of the neurons can be rescued by the NGF re-addition (about 50% of neurons committed to die).

Key Players in the Intrinsic Death of NGF-Deprived Neurons

The molecular mechanisms of apoptosis are tightly regulated, energy-dependent cascades of events that eventually lead to proteolytic activation of an evolutionarily conserved family of cysteine proteases called caspases. The effector or “executioner” caspases (such as caspase 3, 6, 7), which cause the actual damage by cleaving various cellular substrates, are activated when cleaved by the initiator caspases (e.g., 8, 9, and 10). Based on the type of stimulus and the degree of mitochondrial involvement, there are two distinct yet connected pathways by which the initiator caspases are activated: the extrinsic (death receptor pathway) and the intrinsic (mitochondrial pathway) (Figure 2.3). As the name implies, the extrinsic pathway involves binding of an extracellular death ligand belonging to the tumor necrosis factor (TNF) superfamily (e.g., FasL, TNF-α) to a trans-membrane death receptor such as FasR or TNFR1. Upon binding, the cytoplasmic trimeric death domain of FasL/FasR or TNF-α/TNFR1 recruits the corresponding adaptor proteins FADD (Fas-associated protein with death domain) or TRAAD (TNFR-associated death domain protein). The initiator caspases 8, 10 are cleaved and activated when three molecules of either caspase bind the adaptor protein, forming a complex known as DISC (death-inducing signaling complex). DISC-activated caspases 8, 10 can trigger apoptotic death, for example, by cleaving the pro-caspase 3 into the executor caspase 3. In addition, caspase 8 can activate the mitochondrial pathway by cleaving the pro-apoptotic Bcl-2 family member Bid into the truncated Bid (*t*Bid), which triggers cytochrome *c* release by activating Bax-mediated mitochondrial permeabilization (Elmore, 2007; Ott, Norberg, et al., 2007).

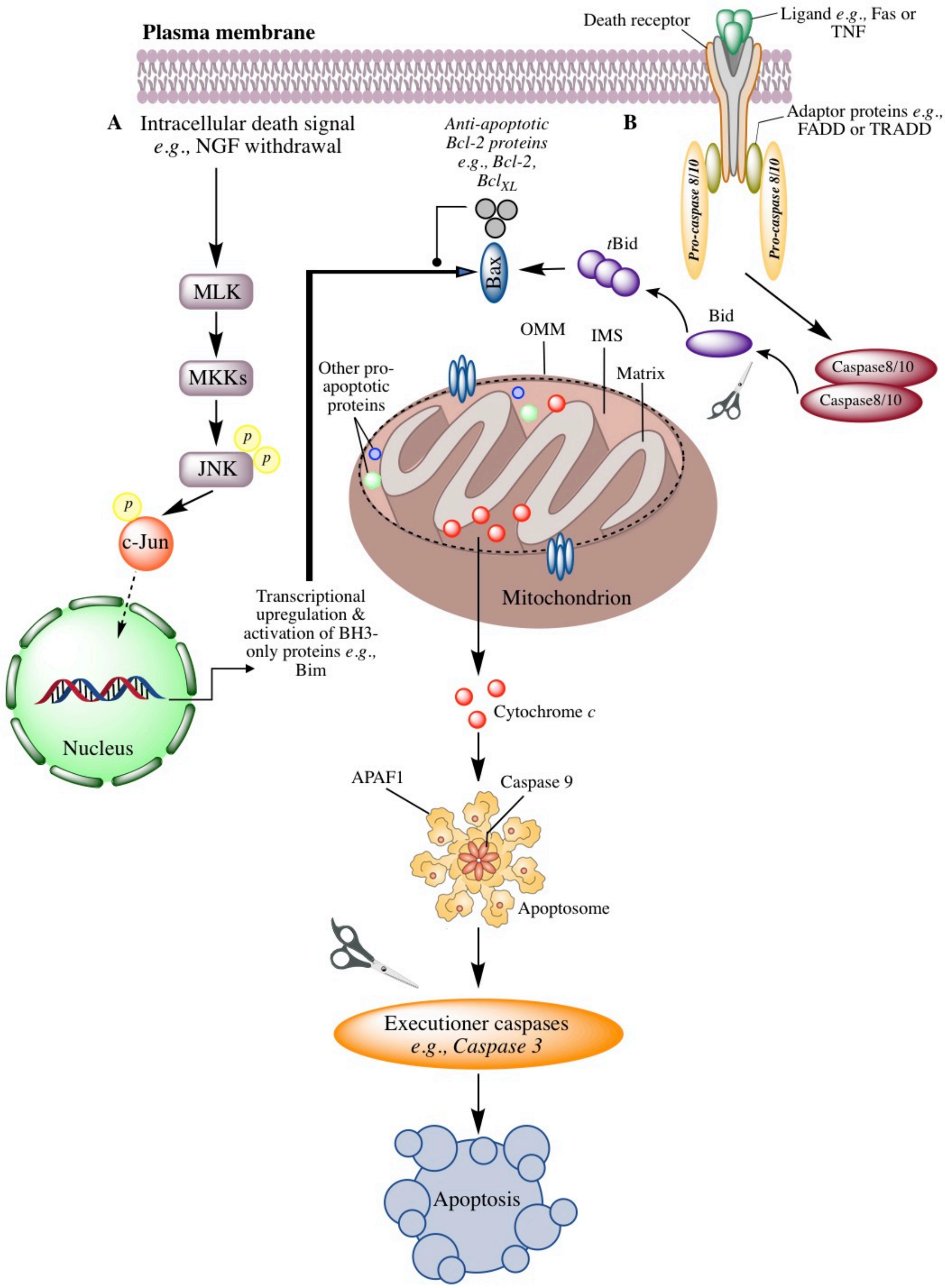
Plasma membrane
Death receptor
Ligand e.g., Fas or TNF
A
Intracellular death signal e.g., NGF withdrawal
Anti-apoptotic Bcl-2 proteins e.g., Bcl-2, Bcl$_{XL}$
B
Adaptor proteins e.g., FADD or TRADD
Pro-caspase 8/10
Pro-caspase 8/10
tBid
Bax
MLK
MKKs
JNK
p
p
p
c-Jun
Bid
OMM
IMS
Matrix
Other pro-apoptotic proteins
Caspase8/10
Caspase8/10
Mitochondrion
Nucleus
Transcriptional upregulation & activation of BH3-only proteins e.g., Bim
Cytochrome c
APAF1
Caspase 9
Apoptosome
Executioner caspases e.g., Caspase 3
Apoptosis

Figure 2.3. Key steps in apoptotic signaling: the intrinsic vs. extrinsic pathways. A. During neuronal development, the lack of target organ-derived neurotrophins (e.g., nerve growth factor, NGF) triggers the intrinsic (mitochondria-regulated) form of apoptotic death. In sympathetic neurons, NGF withdrawal activates the stress-responsive mixed-lineage kinase-c-Jun N-terminal kinase-Jun (MLK-JNK-*c*-Jun) protein kinase cascade. In addition to the activity of other transcription factors, the N-terminal phosphorylation of *c*-Jun enhances its transcriptional activity and results in increasing the transcription of the initiator proteins, Bcl-2 homologous 3 (BH3-only) family members such as Bim and Puma, among others. These proteins enable the activation of the pro-apoptotic effector, BCL-2-associated X protein (Bax), that translocates to the mitochondria to permeabilize the outer membrane (OMM) (see Figure 2.4 for details), allowing the exit of some pro-apoptotic proteins such as cytochrome *c* from the mitochondrial intermembrane space (IMS). The released cytochrome *c* binds the apoptotic protease-activating factor 1 (Apaf-1) scaffold protein, inducing its oligomerization into a heptameric structure called “apoptosome*” that recruits and activates the initiator caspase 9, which cleaves and activates executioner caspases, caspase 3 and 7, to induce apoptosis. **B.** In neuronal pathologies rather than developmental cell death, binding of an extracellular ligand with its corresponding cell-surface death receptor initiates the extrinsic form of apoptotic death of these cells. Such binding recruit specific adaptor molecules to activate downstream initiator caspases (caspase 8/10). The resultant dimerization and activation of the initiator caspases can either directly cleave and activate executioner caspases 3/7 or

proteolyze the BH3-only protein Bid to engage the mitochondrial pathway, leading to apoptosis.

Note: **The apoptosome schematic representation was adopted from (Tait & Green, 2010), with permission.*

Conversely, the intrinsic pathway is a non-receptor-initiated pathway that is mainly regulated by the mitochondria in response to several intracellular stimuli including ionizing radiation, DNA damage, and growth factor deprivation, among other cellular stresses. The mitochondrial intermembrane space contains several pro-apoptotic proteins, among which is cytochrome *c*, which redistributes to the cytosol in response to different stimuli. In the absence of apoptotic stimuli, cytochrome *c* resides at the inner membrane of the mitochondria (IMM), serving as the primary carrier of electrons from respiratory complex III (bc1 complex) to complex IV (cytochrome oxidase) in the ETC, an indispensable step in the OXPHOS and mitochondrial metabolism, as discussed in Chapter 1. The apoptotic signal mediates the activation and mitochondrial translocation of pro-apoptotic family effector members (e.g., Bax). The oligomerization and insertion of BCL-2-associated X protein (Bax) permeabilizes the outer mitochondrial membrane (OMM), allowing cytochrome *c* redistribution into the cytoplasm. Each molecule of the released cytochrome *c* binds seven molecules of apoptotic protease-activating factor 1 (Apaf-1). In the presence of dATP, this heptameric complex (known as an apoptosome) then recruits and cleaves pro-caspase 9 into the initiator active caspase 9, which then cleaves and activates executor caspases 3, 7 (Huttemann et al., 2011). The first part of this review will discuss the mitochondrial (intrinsic) pathway of the apoptotic death of developing neurons, using SCG-derived sympathetic neurons as an *in vitro* model.

Extensive studies, including ours, suggest that developing neurons die primarily by activating the intrinsic pathway in response to neurotrophic factor deprivation (Deshmukh & Johnson, 1997). For example, both *in vitro* and *in vivo* studies reported that NGF withdrawal-induced death of sympathetic neurons requires activation of caspase 3. Such death was prevented using different broad-spectrum caspase inhibitors, such as BAF (boc-aspartyl-(OMe)-fluoromethyl-ketone) and zVAD-fmk (carbobenzoxy-valyl-alanylaspartyl-[O methyl]- fluoromethylketone) (Deshmukh, Kuida, & Johnson, 2000; Deshmukh et al., 1996; McCarthy, Rubin, & Philpott, 1997). More recently, sympathetic neurons derived from caspase 3-null animals survived NGF deprivation (Kirkland, Saavedra, Cummings, & Franklin, 2010). This study, in addition to the finding that the other executor caspase-7 is not expressed in sympathetic neurons (Wright, Vaughn, & Deshmukh, 2007), strongly suggests the indispensable role of caspase 3 in the death of developing neurons. Upstream from the caspase 3 activation cascade in NGF-deprived sympathetic neurons lies another key player of the intrinsic pathway, cytochrome *c*. Over the last two decades, cell fractionation, immunoblotting, and immunocytochemistry studies have demonstrated cytochrome *c* redistribution into the cytosol of sympathetic neurons following NGF withdrawal. In support, microinjection of neutralizing cytochrome *c* antibody prevented the death of NGF-deprived sympathetic neurons. In addition to the observation that NGF-deprived sympathetic neurons restore their mitochondrial cytochrome *c* levels after NGF re-addition (Martinou et al., 1999), these studies suggest that cytochrome *c* is functionally important in the apoptotic death of sympathetic neurons following NGF withdrawal. Despite numerous research efforts proposing several pathways (Gogvadze, Orrenius, & Zhivotovsky, 2006), the precise mechanism by which mitochondrial cytochrome *c* is redistributed remains elusive. However, considering the current literature, Bax activation and oligomerization appears to be a critical step, at least in different types of neuronal *in vitro* and *in vivo* models (Deckwerth et al., 1996; Miller & Johnson, 1996; Xiang et al., 1998).

In sympathetic neurons, the NGF withdrawal-induced release of apoptogenic factors into the cytosol, particularly cytochrome *c*, is tightly governed by the multidomain pro-apoptotic effector protein Bax, and, although less likely, the BCL-2 antagonist or killer, Bak (Putcha et al., 2002). In healthy cells, Bax mostly resides in the cytosol in a monomeric state, with some loosely attached to the OMM. Apoptotic signals trigger Bax activation and translocation to the mitochondria, where it oligomerizes, inserts itself into, and permeabilizes the OMM, creating an exit route for cytochrome *c* (Putcha, Deshmukh, & Johnson, 1999; Wolter et al., 1997). Microinjecting Bax into NGF-maintained sympathetic neurons causes cytochrome *c* release and apoptotic cell death (Vekrellis et al., 1997; Whitfield, Neame, Paquet, Bernard, & Ham, 2001). Sympathetic neurons derived from Bax-deficient SCG mice survive for more extended periods of time in NGF-deprived medium, and their soma morphology and neurite outgrowth were restored upon NGF re-addition. Furthermore, the number of isolated sympathetic neurons from day-one Bax-deficient mice was higher compared with wild-type mice, suggesting that the death of sympathetic neurons deprived of NGF is most likely Bax-dependent (Deckwerth et al., 1996).

Role of BH3-Only Pro-Apoptotic Proteins in Neuronal Apoptosis

The B cell lymphoma 2 (BCL-2) family of proteins is divided into three main groups based on their structural and sequence homology: the multidomain pro-survival proteins (e.g., BCL-2, BCL_{XL}), the multidomain pro-apoptotic effector proteins (e.g., Bax, Bak), and the BCL-2 homology 3 (BH3-only) initiator proteins (e.g., Bim, Puma, Bmf, Dp5/Hrk) (Figure 2.4a). There are two suggested mechanisms by which BH3-only proteins regulate Bax translocation to the mitochondria during apoptotic cell death. In the first model, Bax is proposed to be constitutively active in the cytosol but happens to be sequestered by one of the multidomain pro-survival proteins. One BH3-only protein is sufficient to directly and competitively bind the pro-survival protein, allowing active Bax to translocate to the mitochondria. The second indirect model proposes that two sets of BH3-only proteins are needed to activate and release Bax, either by directly interacting with Bax or by neutralizing the bound pro-survival protein, respectively (Figure 2.4b) (Czabotar, Lessene, Strasser, & Adams, 2014; Tait & Green, 2010). The reported findings that Bax expression does not change following NGF deprivation (Putcha et al., 2002; Whitfield et al., 2001), and that the protein synthesis inhibitor, cycloheximide, suppresses Bax translocation and cytochrome *c* release, could suggest that *de novo* protein synthesis upstream of Bax is required for the apoptotic death of NGF-deprived neurons (Franklin & Johnson, 1998; Martin et al., 1988; Neame, Rubin, & Philpott, 1998).

Several models of neurotrophic factor-mediated neuronal death, including NGF-deprived sympathetic neurons, displayed a significant rise in the transcriptional and protein levels of multiple BH3-only proteins (Besirli et al., 2005; Harris & Johnson, 2001; Kristiansen et al., 2011; Putcha et al., 2001; Whitfield et al., 2001). Neuronal death protein (Dp5), a rodent homolog of the human Harakiri protein (Hrk), was the first BH3-only protein to be identified and demonstrated to have a role in the apoptotic death of NGF-deprived sympathetic neurons. Microinjecting rat sympathetic neurons with full-length Dp5 induces apoptosis (Imaizumi et al., 1997). Mice deficient in Dp5 ($Dp5^{-/-}$) were viable and showed no anatomical anomalies in the nervous system during postnatal development. Sympathetic neurons derived from Dp5$^{-/-}$ mice exhibited a slightly delayed, but not completely suppressed, death when deprived of NGF (Imaizumi et al., 2004). This finding suggests that other more potent BH3-only proteins might also be involved in the NGF withdrawal-induced death of sympathetic neurons. The Bcl-2 interacting mediator of cell death (Bim_{EL}) and the p53-upregulated modulator of apoptosis (Puma) are probably the most potent among the BH3-only proteins (Wyttenbach & Tolkovsky, 2006). There are three splice variants of Bim that have different degrees of apoptotic potency: Bim_S > Bim_L > Bim_{EL} (O'Connor et al., 1998). The apoptotic potencies of Bim_L and Bim_{EL} are better regulated than Bim_S because they are mostly bound with the cytoplasmic dynein light chain 1 (LC8), a component of the dynein motor complex associated with the microtubule cytoskeleton (Puthalakath, Huang, O'Reilly, King, & Strasser, 1999). The post-translational modifications the Bim_{EL} undergoes makes it the best-regulated splice variant among the three isoforms, which will be discussed in further detail later in this chapter. Neuronal populations, including sympathetic neurons, CGNs and dorsal root ganglion (DRG) neurons, predominantly express the extra-long isoform of Bim (Bim_{EL}) when receiving an apoptotic signal. For instance, the function of the Bim_{EL} protein in neurons has been studied in gain-of-function and loss-of-function experiments in both *in vitro* and *in vivo* models. Overexpressing Bim_{EL} in sympathetic neurons and CGNs can induce cytochrome *c* release and apoptosis in the presence of NGF. In addition, reducing the level of Bim_{EL} expression via microinjection of Bim antisense oligonucleotides can significantly, but not completely, protect sympathetic neurons against NGF deprivation-induced death (Putcha et al., 2001; Whitfield et al., 2001). It is likely that more than one BH3-only protein must be simultaneously upregulated to achieve efficient activation of the intrinsic pathway of developing neurons following neurotrophic factor withdrawal. Puma is another BH3-only protein that has also been implicated in this type of cell death and proposed to partially compensate for the loss of Bim. In one study, CGNs derived from $Bim^{-/-}$, $Puma^{-/-}$ double knockout mice displayed more resistance to apoptotic death induced by KCl deprivation than that achieved by deleting individual proteins (Ren et al., 2010). The probability that multiple BH3-only proteins are required to sufficiently translocate Bax to the mitochondria is supported by the observation that, unlike knocking out individual BH3-only proteins, Bax deletion prevented, not merely delayed, the NGF withdrawal-induced death of sympathetic neurons (Deckwerth et al., 1996). The reason why NGF-deprived neurons upregulate more than one BH3-only pro-apoptotic proteins remains elusive. Previous evidence demonstrated that members of the BH3-only family proteins exhibit different binding specificities to different anti-apoptotic proteins, where more potent proteins (e.g., Bim and Puma) can interact with multiple pro-survival proteins (e.g., BCL-2, BCL_{XL}) (Figure 2.4c) (Chen et al., 2005; Kuwana et al., 2005). This characteristic will presumably efficiently inhibit the pro-survival proteins and activate the key pro-apoptotic protein, Bax.

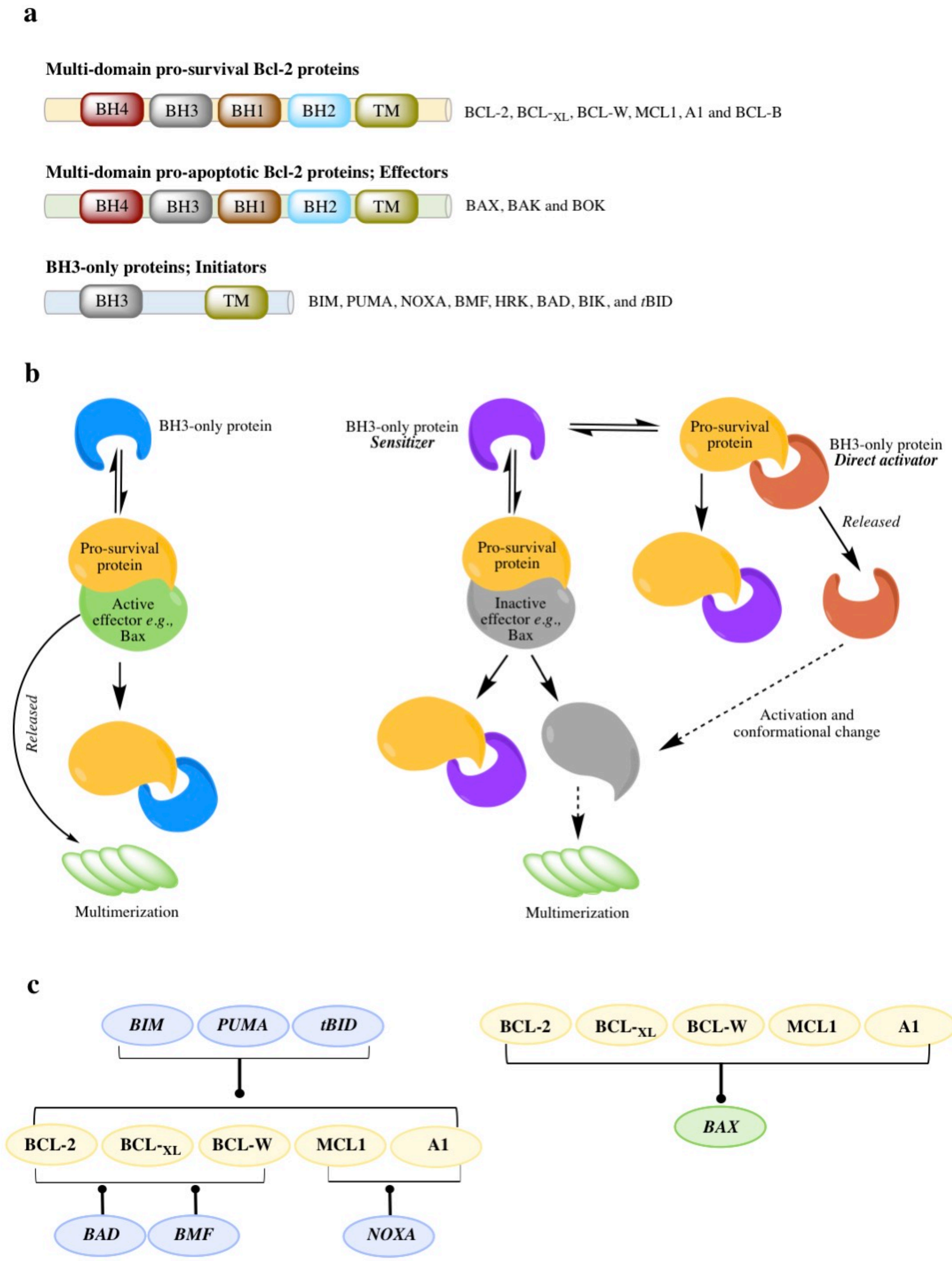

Figure 2.4. Structures, models of activation, and interaction selectivity of the Bcl-2 family proteins. Based on the Bcl-2 homology (BH) domain organization, the B cell

lymphoma 2 (BCL-2) family of proteins is divided into two major groups: the multi-domain group and the single-domain group. Multi-domain family members, including pro-survival (e.g., Bcl-2, Bcl_{XL}) and pro-apoptotic protein "effectors" (e.g., Bax), share (BH1-BH4) domains, whereas the "initiator" pro-apoptotic proteins (e.g., Bim) (proteins that activate the effectors) contain only the BH3 amphipathic helix. Members of both major groups share a transmembrane (TM) domain that helps to anchor them to cellular organelles, such as mitochondria **(a)**. Two prominent models addressing how BH3-only proteins activate the pro-apoptotic effector proteins are shown: the indirect model (*left*) and the de-repression-direct activation model (*right*). In the indirect model, the active pro-apoptotic effector protein (e.g., Bax) is sequestered to a pro-survival protein (e.g., Bcl_{XL}) in the cytosol. A release of the constitutively active Bax is achieved when a BH3-only protein (e.g., Bim) competitively interacts with Bcl_{XL}, allowing Bax multimerization and mitochondrial membrane permeabilization. On the other hand, the de-repression-direct activation model requires multiple BH3-only proteins to work simultaneously to achieve such an outcome. First, a sensitizer BH3-only protein (e.g., Puma) is needed to bind to pro-survival proteins (e.g., Bcl_{XL}) that are sequestering both inactive BAX and the direct activators of Bax (e.g., Bim). Once the inactive Bax is free, a second subset of BH3-only proteins (e.g., Bim) is required to directly activate Bax, allowing its transformation and translocation to the mitochondria **(b)**. Some BH3-only proteins (e.g., Bim, Puma) can bind to and neutralize all pro-survival proteins, whereas others (e.g., Noxa, Bad or Bmf) can neutralize only a limited subset of pro-survival proteins. All pro-survival proteins can probably sequester Bax to the cytosol (Czabotar, Peter E., et al. 2014)

Roles of Redox Cycling and Mitochondria-derived Reactive Oxygen Species in the Death of Neurotrophic Factor-Deprived Neurons

In this part of Chapter 3, I will discuss the roles of mitochondria-derived ROS in the release of pro-apoptotic factors from mitochondria of neurotrophic factor-deprived neurons, as well as which antioxidant pathways are activated during the survival of neurotrophic factor-maintained neurons. As described in Chapter 1, in addition to the NADPH oxidase-mediated superoxide production (Bedard & Krause, 2007; Tammariello, Quinn, & Estus, 2000), $O_2^{\cdot-}$ is primarily produced during the OXPHOS process of many types of cells, including neurons. The produced $O_2^{\cdot-}$ is then rapidly converted into hydrogen peroxide (H_2O_2), which is subsequently converted into water, as shown in Figure 2.5 (Ray, Huang, & Tsuji, 2012). Over the last two decades, considerable evidence has indicated the central role of mitochondria-derived ROS in apoptotic neuronal death following neurotrophic factor withdrawal. For example, NGF-deprived rat sympathetic neurons showed a significant increase in ROS levels that preceded the commitment to die point (18h after deprivation). Microinjecting these cells with the human copper/zinc superoxide dismutase protein (SOD), an enzyme that catalyzes the conversion of $O_2^{\cdot-}$ into H_2O_2, delayed their death following NGF withdrawal. The same study showed that inhibiting cellular SOD using antisense vector re-sensitized these cells to NGF-deprivation-induced death (Greenlund, Deckwerth, & Johnson, 1995). In support of this study, Ferrari G. *et al*. reported that both D- and L-stereoisomers of the antioxidant N-acetylcysteine prevented death in two different models of apoptotic death caused by loss of trophic support, neuroblast-like PC12 cells deprived of serum/NGF, and sympathetic neurons deprived of NGF (Ferrari, Yan, & Greene, 1995). Such findings led to the resurgence of interest in the role of ROS in the apoptotic death of developing neurons.

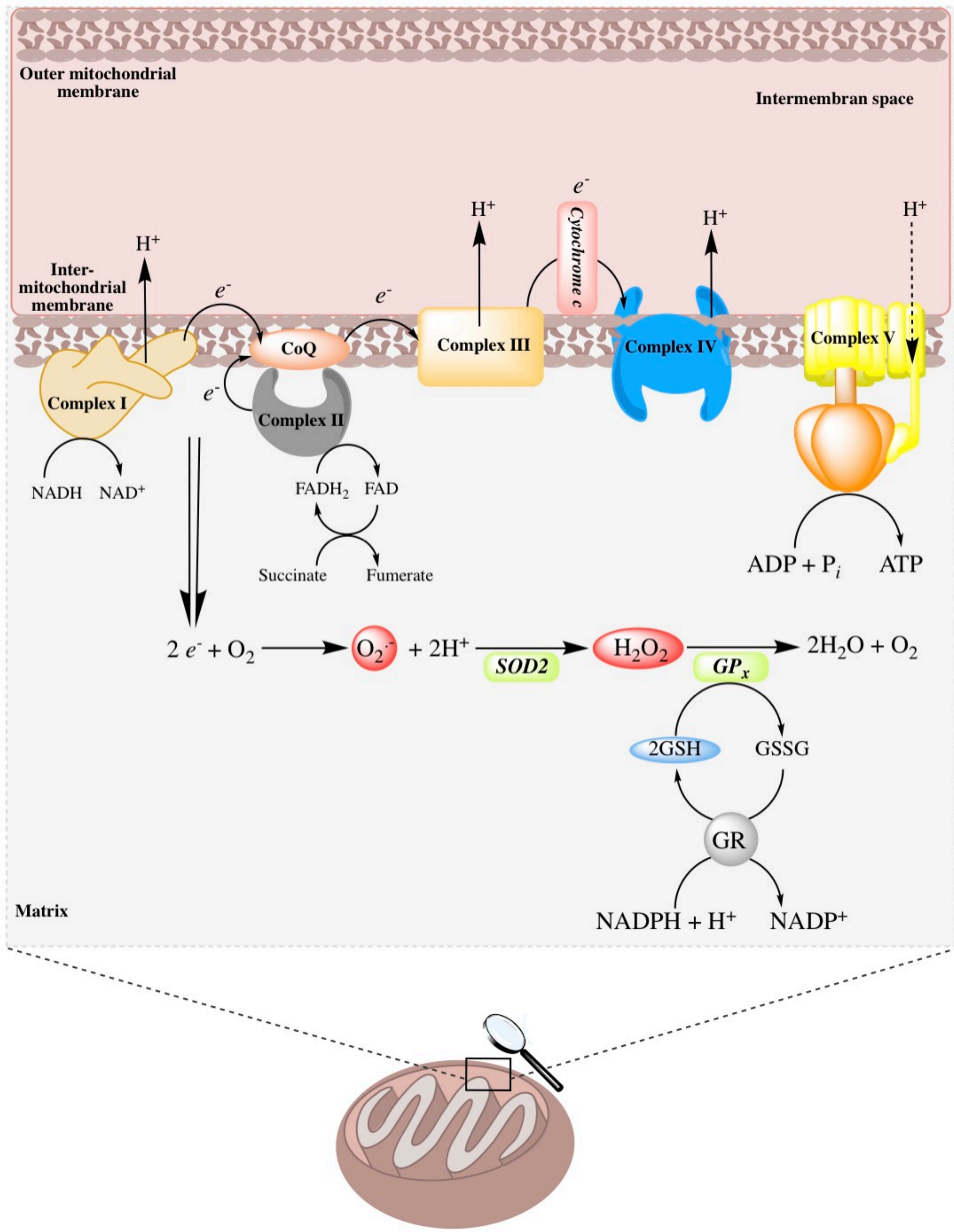

Figure 2.5. Mitochondrial production and clearance of ROS. Within the mitochondrial intermembrane, electrons (e^-) are continuously shuttled through ETC

complexes during the OXPHOS process. Electron leakage at complex I and II results in superoxide ($O_2^{\cdot-}$) production, as they reduce diatomic oxygen (O_2). Mitochondrial superoxide dismutase 2 (SOD2), also known as manganese-dependent superoxide dismutase (MnSOD), rapidly converts most of the produced $O_2^{\cdot-}$ into hydrogen peroxide (H_2O_2), which can sometimes transform into other ROS (e.g., hydroxyl radicals, $OH^{\cdot}$) in the absence of antioxidant defenses. The detoxification of H_2O_2 into water is achieved by glutathione peroxidase (GP_x), an enzyme that catalyzes the oxidation of the reduced form of the tripeptide glutathione (GSH) into the oxidized form (GSSG). More reduced GSH (antioxidant form) is formed by glutathione reductase enzyme (GR), using NADPH as electrons donor.

Several lines of evidence (Kirkland & Franklin, 2001; Kirkland, Saavedra, & Franklin, 2007; Kirkland, Windelborn, Kasprzak, & Franklin, 2002) have shown that cytochrome *c* release during the apoptotic death of NGF-deprived sympathetic neurons is tightly regulated by the redox states of these cells. The redox-sensitive dye 5 (and 6)-carboxy-2′,7′-dichlorodihydrofluorescein diacetate bis (acetoxymethyl) ester (CM-H_2DCFDA) (Royall & Ischiropoulos, 1993) was utilized in conjunction with confocal microscopy to demonstrate that depriving rat sympathetic neurons of NGF caused a biphasic (early and late) rise in ROS levels that persisted throughout the rest of the apoptotic process (Kirkland & Franklin, 2001). A similar increase in the production of mitochondria-derived ROS has also been reported in another *in vitro* model of developmental neuronal death, serum-starved/repolarized CGNs (Kirkland, Windelborn, et al., 2002). Confocal microscopy experiments revealed that re-addition of NGF to cultures of NGF-deprived rat and mouse SCG sympathetic neurons rapidly suppresses (within 10-20 min of exposure) the elevated levels of H_2O_2-associated ROS, as detected with dihydrorhodamine and CM-H_2DCFDA, respectively (Dugan, Creedon, Johnson, & Holtzman, 1997; Kirkland et al., 2007). Surprisingly, in the later study, they demonstrated that $O_2^{\cdot -}$ production had not diminished upon re-addition of NGF, suggesting that ROS clearance (or antioxidant defenses) rather than production is affected by NGF. In an attempt to investigate the role of redox cycling in NGF-mediated rescue of neurons, treatment of sympathetic neurons deprived of NGF for 24 hours with N,N′-bis (2-chloroethyl)-N-nitrosourea (BCNU), an inhibitor of glutathione reductase and thus glutathione (GSH) (Figure 2.5), suppressed the ability of NGF to inhibit ROS detoxification and cytochrome *c* redistribution (Kirkland et al., 2007). Furthermore, the

NGF withdrawal-induced elevation in ROS levels, the subsequent release of cytochrome *c*, and the activation of the intrinsic apoptotic cascade in sympathetic neurons were blocked using antioxidants such as N-acetyl-l cysteine and GSH ethyl ester, a membrane-permeant form of glutathione. The GSH levels also significantly increased, and the ROS burst was blocked by the protein synthesis inhibitor, cycloheximide, by shunting cysteine from incorporation into protein to GSH synthesis (Ferrari et al., 1995; Kirkland & Franklin, 2001; Kirkland, Windelborn, et al., 2002; Ratan, Murphy, & Baraban, 1994). These studies further suggest the pivotal roles of ROS and GSH cycling in the apoptotic death of developing neuron models.

Compelling evidence implicates electron leakage for mitochondrial ETC as a primary source of elevated levels of $O_2^{\cdot-}$ and other downstream ROS in apoptotic sympathetic neurons. The mitochondrial un-coupler carbonyl cyanide *p*-trifluoromethoxyphenylhydrazone (FCCP) dissipates the proton gradient across the IMM, which presumably prevents electron leakage by accelerating their transmission through ETC. FCCP treatment abolishes the rise of ROS in NGF-deprived rat and mouse sympathetic neurons, as measured by the redox-sensitive dye CM-H_2DCFDA (Kirkland & Franklin, 2001; Kirkland, Windelborn, et al., 2002). These findings were supported using the mitochondria-targeted redox-sensitive dye MitoSOX™ Red. The positively charged triphenylphosphonium cation targets the MitoSOX™ to the mitochondrial matrix. This accumulation is driven by the high membrane potential across the IMM. MitoSOX™ becomes intensely fluorescent when oxidized by $O_2^{\cdot-}$, more so than other ROS, including the downstream dismutation product, H_2O_2, which makes it more indicative of the mitochondrial production of $O_2^{\cdot-}$ than CM-H_2DCFDA (Robinson et al., 2006; Zhao et al., 2003). In support of the validity of MitoSOX™ as a tool to test mitochondrial production of $O_2^{\cdot -}$ in neurons, Kirkland R.A. *et al.* reported that while H_2O_2 treatment had no effect, MitoSOX™ fluorescence intensity increased after treatment with menadione, a membrane-permeant compound that generates $O_2^{\cdot -}$ intracellularly by transferring electrons from NADH or NADPH to O_2. More importantly, they found that withdrawing NGF caused a significant increase in both redox-sensitive dyes in mouse sympathetic neurons. This increase was blocked by FCCP, strongly suggesting a mitochondrial origin of produced $O_2^{\cdot -}$ and downstream ROS during the apoptotic death of developing neurons (Kirkland et al., 2007).

Bax and Caspase-Mediated Prooxidant State during Neuronal Apoptosis

After the discovery that a mitochondria-derived pro-oxidant state triggers cytochrome *c* release and thus apoptotic death of neurotrophic factor-derived neurons, and that cytochrome *c* release and subsequent activation of cytosolic caspases is Bax-dependent, it was of great importance to investigate the relationship between ROS and Bax in NGF-deprived neurons. A study by Kirkland R.A. *et al.* reported findings that NGF-deprived sympathetic neurons and repolarized/serum-starved CG neurons derived from Bax-null mice showed a complete suppression of ROS bursts occurring during the apoptotic death of their Bax-wild-type counterparts (Kirkland, Windelborn, et al., 2002). They used the mitochondria-targeted redox-sensitive dyes MitoSOX™ Red and CM-H_2DCFDA in conjunction with confocal microscopy to demonstrate that non-apoptotic SCG-derived sympathetic and CG neurons had lower $O_2^{\cdot -}$ and H_2O_2-associated ROS levels, respectively, when Bax was genetically deleted (Kirkland et al., 2010). These data suggest that Bax lies upstream of most or all increased mitochondria-derived ROS production occurring during the apoptotic death of neurons following neurotrophic factor withdrawal. How a Bax-induced pro-oxidant state regulates cytochrome *c* release from mitochondria is an open question that has yet to be answered. Evidence suggests that cytochrome *c* release is more complex than simply OMM pores formed by Bax (Garrido et al., 2006; Gogvadze et al., 2006; Tait & Green, 2010). Cytochrome *c* is closely associated with cardiolipin (CL), a mitochondria-specific phospholipid at the outer leaflet of the IMM that has been implicated as a critical key player in apoptotic cell death (Gonzalvez & Gottlieb, 2007; Ott, Gogvadze, Orrenius, & Zhivotovsky, 2007; Petrosillo, Casanova, Matera, Ruggiero, & Paradies, 2006). Evidence suggests that the dissociation of cytochrome *c* from CL, and thus cytochrome *c* liberation from the IMM, is initiated by CL peroxidation (Orrenius & Zhivotovsky, 2005; Ott, Robertson, Gogvadze, Zhivotovsky, & Orrenius, 2002; Shidoji, Hayashi, Komura, Ohishi, & Yagi, 1999). Previous studies have shown that Bax-mediated production of ROS causes CL peroxidation and subsequent cytochrome *c* release in different models of apoptotic death, including rat sympathetic neurons deprived of NGF (Jiang et al., 2008; Kirkland, Adibhatla, Hatcher, & Franklin, 2002).

The central role of caspase 3 in neuronal death following neurotrophic factor deprivation makes it another ideal candidate that could mechanistically contribute to the rise of ROS during such death. In an attempt to determine such a correlation, NGF-deprived sympathetic neurons were treated with broad-spectrum caspase inhibitors BAF or zVAD-fmk. Confocal microscopy revealed that caspase inhibitors significantly attenuated, but did not prevent, the increased levels of $O_2^{\cdot-}$ and H_2O_2-associated ROS, as detected by the redox-sensitive dyes MitoSOX™ and CM-H_2DCFDA, respectively (Kirkland & Franklin, 2001; Kirkland et al., 2010). In the later study, NGF-deprived sympathetic neurons derived from caspase 3-null mice showed lower levels of mitochondria-produced $O_2^{\cdot -}$ compared with wild-type cells. These data suggest that much of mitochondria-derived ROS is probably caspase 3-dependent.

Suppression of the Apoptotic Death of Developmental Neurons by Chronic Membrane Depolarization

In addition to the neurotrophic factor-mediated survival (or suppression of PCD) of different neuronal populations during nervous system development, considerable evidence suggests electrical activity as another crucial factor that determines such a fate. For instance, both *in vitro* and *in vivo* studies have shown that disrupting synaptic transmission or electrical signals, either pharmacologically or mechanistically (by removing afferent input), suppresses the growth and induces the apoptotic death of several types of neurons (Baker, Ruijter, & Bingmann, 1991; Linden, 1994; Pasic & Rubel, 1989; Schmidt & Kater, 1993). While numerous studies have demonstrated how neurotrophic factors control which neurons survive during development, few efforts have been aimed toward understanding how electrical activity promotes the survival or suppresses the death of neurons at this stage of embryonic development. In this section, I will provide up-to-date knowledge about how chronically depolarized neurons survive neurotrophic factor-induced death.

The phenomenon that elevated concentrations of potassium ($[K^+]_E$) maintain neuronal survival in the absence of neurotrophic factors has been documented since the early 1970s. Scott B.S. and Fisher K.C. were among the first to report that culturing embryonic chicken DRG neurons in high [K^+]-containing medium promotes their survival for extended periods, even though they would normally undergo PCD in physiological $[K^+]_E$ (≈5mM) (Scott & Fisher, 1970). Since then, a large number of studies from different laboratories have reported the same pro-survival effects of elevated $[K^+]_E$ in several types of neuronal populations derived from different species, as summarized in **Table 2.1**. All these studies showed morphological similarities between neurons maintained in the appropriate neurotrophic factor or high $[K^+]_E$-containing medium, as well as similar rates of survival. Furthermore, in the context of neuronal survival *in vitro*, increased $[K^+]_E$ seems to efficiently substitute for the absence of neurotrophic factors, where deprivation of both at the same time triggers apoptotic cell death.

Table 2.1. Examples of neuronal populations where elevated $[K^+]_E$ promoted survival in the absence of the appropriate neurotrophic factors.

Neuronal type	Species	Optimal pro-survival $[K^+]_E$	References
Dorsal root ganglion neurons	Human	20mM	*(Scott, 1971, 1977)*
	Chicken	40mM	*(Chalazonitis & Fischbach, 1980; Scott & Fisher, 1970)*
	Mouse	20mM	*(Scott, 1977)*
	Rat	35mM	*(Eichler, Dubinsky, & Rich, 1992)*
Ciliary ganglion neurons	Chicken	25-40mM	*(Bennett & White, 1979; Collins & Lile, 1989; Collins, Schmidt, Guthrie, & Kater, 1991; Nishi & Berg, 1981)*
Cerebellar ganglion neurons	Rat	25mM	*(Gallo, Kingsbury, Balazs, & Jorgensen, 1987; Lasher & Zagon, 1972)*
Sympathetic neurons	Chicken	45mM	*(Phillipson & Sandler, 1975)*
	Mouse	40mM	*(Putcha et al., 1999)*
	Rat	33-35mM	*(Franklin, Sanz-Rodriguez, Juhasz, Deckwerth, & Johnson, 1995; Koike, Martin, & Johnson, 1989; Koike & Tanaka, 1991)*
Myenteric neurons	Rat	25mM	*(Franklin, Fickbohm, & Willard, 1992)*

The resting membrane potential is determined by the action of multiple ion transporters that set the concentration gradients across the neuronal membrane. Due to the leakiness of potassium ion channels in neurons at resting potential, the relative intracellular to extracellular [K^+] makes it a primary determinant of the membrane potential. A condition where no net K^+ flux occurs across the membrane because of the equal opposing forces of ion concentration gradients and transmembrane potentials is known as an electrochemical equilibrium. The membrane potential at which K^+ ions are at electrochemical equilibrium (equilibrium potential) can be mathematically predicted by the Nernst equation. Assuming that the resting membrane is permeable only to K^+ions, then the Nernst equation predicts that the logarithm of the K^+ concentration gradient across the membrane will proportionally affect the membrane potential (Hille, 2001; Purves D, 2001). This assumption has been subjected to testing by several laboratories in an attempt to understand how elevated $[K^+]_E$ promotes neuronal survival in the absence of neurotrophic factors. Electrophysiological *in vitro* studies revealed that membranes of different types of neurons proportionally depolarize when chronically exposed to elevated $[K^+]_E$. Such depolarization remains as long as the high $[K^+]_E$ is present in the medium. Reducing $[K^+]_E$ to physiological concentration (≈5mM) rapidly repolarizes the membrane potential to resting levels (Chalazonitis & Fischbach, 1980; Franklin et al., 1992; Franklin et al., 1995; Nishi & Berg, 1981; Tolkovsky, Walker, Murrell, & Suidan, 1990). Subsequent works aimed to test whether high $[K^+]_E$ promotes neuronal survival through imitating the effects of the naturally occurring electrical activity. These studies assessed the survival of many types of neurons from both the peripheral and central nervous systems by implementing other membrane depolarizing techniques. Indeed, cultures of neurons deprived of their pro-survival factors survived for extended times when treated with different depolarizing agents other than K^+ (Gallo et al., 1987; Koike et al., 1989; Yan, Ni, Weller, Wood, & Paul, 1994), or when electrically stimulated with an exogenous current (Brosenitsch & Katz, 2001; Corredor & Goldberg, 2009; Heydorn, Frazer, & Weiss, 1981; Kaplan et al., 1988; Sisken & Smith, 1975). These findings strongly suggest that K^+-mediated chronic depolarization likely promotes neuronal survival by imitating some of the effects of electrical activity *in vivo*.

The changes in intracellular free calcium concentration $[Ca^{2+}]i$ is the principal means by which a depolarizing signal (change in the membrane potential) is translated into a biochemical response in neurons. Calcium (Ca^{2+}) is a well-known universal second messenger that regulates several aspects of neuronal functions, including survival. The rise of $[Ca^{2+}]i$ results either from the entrance of extracellular Ca^{2+} through transmembrane voltage-gated Ca^{2+} channels or depletion from intracellular endoplasmic reticulum (ER) stores (Brini, Cali, Ottolini, & Carafoli, 2014; Ghosh & Greenberg, 1995). It was of great interest to investigate the impacts of chronic membrane depolarization on the activity of Ca^{2+} channels of developing neurons. In the early 1980s, Nishi and Berg demonstrated for the first time that K^+-promoted survival of chicken ciliary ganglion neurons (CGNs) was blocked by the non-selective Ca^{2+} channel antagonists verapamil and Mg^{2+} (Nishi & Berg, 1981). In support of these findings, verapamil also induced death of chronically depolarized rat sympathetic neurons (Koike et al., 1989). Measuring $[Ca^{2+}]i$ using the Ca^{2+}-sensitive dye fura (Grynkiewicz, Poenie, & Tsien, 1985) revealed that a sustained rise of Ca^{2+} levels above the baseline was a universal phenomenon in several types of K^+-depolarized neurons, including chicken

CGNs (Collins et al., 1991), rat myenteric neurons (Franklin et al., 1992), rat SCG-derived sympathetic neurons (Franklin et al., 1995; Koike & Tanaka, 1991), and rat CGNs (Bessho, Nawa, & Nakanishi, 1994). Following repolarization with medium containing physiological $[K^+]_E$, the $[Ca^{2+}]i$ rapidly returns to baseline levels in these cells. Subsequent works by several laboratories demonstrated that pharmacological blockage of dihydropyridine-sensitive L-type Ca^{2+} channels with different antagonists reduced the sustained increase in $[Ca^{2+}]i$ and prevented K^+-enhanced survival in a number of types of neurons (Collins & Lile, 1989; Collins et al., 1991; Franklin et al., 1992; Franklin et al., 1995; Thayer, Hirning, & Miller, 1987). In addition, dihydropyridine-sensitive L-type Ca^{2+} channel agonists augment the survival of some of these neurons maintained in sub-optimal $[K^+]_E$ (Gallo et al., 1987; Koike et al., 1989). These data suggest that influx of extracellular Ca^{2+} through voltage-gated L-type Ca^{2+} channels is required for the survival of chronically depolarized neurons. However, the specific mechanisms by which chronically depolarized neurons survive neurotrophic factor deprivation are yet to be discovered.

Summary

Several neuronal populations undergo massive apoptotic death during the development of the vertebrate CNS and PNS *in vivo*. The presence of the appropriate neurotrophic factor and afferent input (electrical stimulation) are prominent determinants of which neurons live and which die both *in vivo* and in cultures. This death is characterized by all features of the intrinsic (mitochondrial) pathway, including upregulation of Bcl-2 pro-apoptotic proteins (e.g., BH3-only proteins), cytochrome *c* release, caspase 3 activation, and oxidative stress. In cultures, the death of neurons deprived of their neurotrophic factor is prevented by high $[K^+]_E$- induced chronic depolarization. Extensive evidence suggests that this survival apparently requires Ca^{2+} influx through dihydropyridine-sensitive L-type, voltage-gated Ca^{2+} channels. However, little is currently known about the exact mechanism(s) by which chronic membrane depolarization promotes neuronal survival. The following research aims to investigate the impacts of chronic depolarization on the BH3-only proteins, mitochondria-derived RS, and antioxidant defenses in the surviving neurons.

REFERENCES

Anandatheerthavarada, H. K., Biswas, G., Robin, M. A., & Avadhani, N. G. (2003). Mitochondrial targeting and a novel transmembrane arrest of Alzheimer's amyloid precursor protein impairs mitochondrial function in neuronal cells. J Cell Biol, 161(1), 41-54.

Andreyev, A. Y., Kushnareva, Y. E., & Starkov, A. A. (2005). Mitochondrial metabolism of reactive oxygen species. Biochemistry (Mosc), 70(2), 200-214.

Baker, R. E., Ruijter, J. M., & Bingmann, D. (1991). Effect of chronic exposure to high magnesium on neuron survival in long-term neocortical explants of neonatal rats in vitro. Int J Dev Neurosci, 9(6), 597-606.

Bauer, D. E., Hatzivassiliou, G., Zhao, F., Andreadis, C., & Thompson, C. B. (2005). ATP citrate lyase is an important component of cell growth and transformation. Oncogene, 24(41), 6314-6322.

Bedard, K., & Krause, K. H. (2007). The NOX family of ROS-generating NADPH oxidases: physiology and pathophysiology. Physiol Rev, 87(1), 245-313.

Beloribi-Djefaflia, S., Vasseur, S., & Guillaumond, F. (2016). Lipid metabolic reprogramming in cancer cells. Oncogenesis, 5, e189.

Ben-Sahra, I., Hoxhaj, G., Ricoult, S. J. H., Asara, J. M., & Manning, B. D. (2016). mTORC1 induces purine synthesis through control of the mitochondrial tetrahydrofolate cycle. Science, 351(6274), 728-733.

Bennett, M. R., & White, W. (1979). The survival and development of cholinergic neurons in potassium-enriched media. Brain Res, 173(3), 549-553.

Bentzinger, C. F., Romanino, K., Cloetta, D., Lin, S., Mascarenhas, J. B., Oliveri, F., . . . Ruegg, M. A. (2008). Skeletal muscle-specific ablation of raptor, but not of rictor, causes metabolic changes and results in muscle dystrophy. Cell Metab, 8(5), 411-424.

Berwick, D. C., Hers, I., Heesom, K. J., Moule, S. K., & Tavare, J. M. (2002). The identification of ATP-citrate lyase as a protein kinase B (Akt) substrate in primary adipocytes. J Biol Chem, 277(37), 33895-33900.

Besirli, C. G., Wagner, E. F., & Johnson, E. M., Jr. (2005). The limited role of NH2-terminal c-Jun phosphorylation in neuronal apoptosis: identification of the nuclear pore complex as a potential target of the JNK pathway. J Cell Biol, 170(3), 401-411.

Bessho, Y., Nawa, H., & Nakanishi, S. (1994). Selective up-regulation of an NMDA receptor subunit mRNA in cultured cerebellar granule cells by K(+)-induced depolarization and NMDA treatment. Neuron, 12(1), 87-95.

Betarbet, R., Sherer, T. B., MacKenzie, G., Garcia-Osuna, M., Panov, A. V., & Greenamyre, J. T. (2000). Chronic systemic pesticide exposure reproduces features of Parkinson's disease. Nat Neurosci, 3(12), 1301-1306.

Borghi, R., Patriarca, S., Traverso, N., Piccini, A., Storace, D., Garuti, A., . . . Massimo, T. (2007). The increased activity of BACE1 correlates with oxidative stress in Alzheimer's disease. Neurobiol Aging, 28(7), 1009-1014.

Brini, M., Cali, T., Ottolini, D., & Carafoli, E. (2014). Neuronal calcium signaling: function and dysfunction. Cell Mol Life Sci, 71(15), 2787-2814.

Brosenitsch, T. A., & Katz, D. M. (2001). Physiological patterns of electrical stimulation can induce neuronal gene expression by activating N-type calcium channels. J Neurosci, 21(8), 2571-2579.

Brunelle, J. K., Bell, E. L., Quesada, N. M., Vercauteren, K., Tiranti, V., Zeviani, M., . . . Chandel, N. S. (2005). Oxygen sensing requires mitochondrial ROS but not oxidative phosphorylation. Cell Metab, 1(6), 409-414.

Cadonic, C., Sabbir, M. G., & Albensi, B. C. (2016). Mechanisms of Mitochondrial Dysfunction in Alzheimer's Disease. Mol Neurobiol, 53(9), 6078-6090.

Casley, C. S., Canevari, L., Land, J. M., Clark, J. B., & Sharpe, M. A. (2002). Beta-amyloid inhibits integrated mitochondrial respiration and key enzyme activities. J Neurochem, 80(1), 91-100.

Chalazonitis, A., & Fischbach, G. D. (1980). Elevated potassium induces morphological differentiation of dorsal root ganglionic neurons in dissociated cell culture. Dev Biol, 78(1), 173-183.

Chalhoub, N., & Baker, S. J. (2009). PTEN and the PI3-kinase pathway in cancer. Annu Rev Pathol, 4, 127-150.

Chandel, N. S., Maltepe, E., Goldwasser, E., Mathieu, C. E., Simon, M. C., & Schumacker, P. T. (1998). Mitochondrial reactive oxygen species trigger hypoxia-induced transcription. Proc Natl Acad Sci U S A, 95(20), 11715-11720.

Chandel, N. S., McClintock, D. S., Feliciano, C. E., Wood, T. M., Melendez, J. A., Rodriguez, A. M., & Schumacker, P. T. (2000). Reactive oxygen species generated at mitochondrial complex III stabilize hypoxia-inducible factor-1alpha during hypoxia: a mechanism of O_2 sensing. J Biol Chem, 275(33), 25130-25138.

Chandel, N. S., & Schumacker, P. T. (1999). Cells depleted of mitochondrial DNA (rho0) yield insight into physiological mechanisms. FEBS Lett, 454(3), 173-176.

Chaturvedi, R. K., & Flint Beal, M. (2013). Mitochondrial diseases of the brain. Free Radic Biol Med, 63, 1-29.

Chen, L., Willis, S. N., Wei, A., Smith, B. J., Fletcher, J. I., Hinds, M. G., . . . Huang, D. C. (2005). Differential targeting of prosurvival Bcl-2 proteins by their BH3-only ligands allows complementary apoptotic function. Mol Cell, 17(3), 393-403.

Christofk, H. R., Vander Heiden, M. G., Harris, M. H., Ramanathan, A., Gerszten, R. E., Wei, R., . . . Cantley, L. C. (2008). The M2 splice isoform of pyruvate kinase is important for cancer metabolism and tumour growth. Nature, 452(7184), 230-233.

Collins, F., & Lile, J. D. (1989). The role of dihydropyridine-sensitive voltage-gated calcium channels in potassium-mediated neuronal survival. Brain Res, 502(1), 99-108.

Collins, F., Schmidt, M. F., Guthrie, P. B., & Kater, S. B. (1991). Sustained increase in intracellular calcium promotes neuronal survival. J Neurosci, 11(8), 2582-2587.

Connor, K. M., Subbaram, S., Regan, K. J., Nelson, K. K., Mazurkiewicz, J. E., Bartholomew, P. J., . . . Melendez, J. A. (2005). Mitochondrial H2O2 regulates the angiogenic phenotype via PTEN oxidation. J Biol Chem, 280(17), 16916-16924.

Corredor, R. G., & Goldberg, J. L. (2009). Electrical activity enhances neuronal survival and regeneration. J Neural Eng, 6(5), 055001.

Cowan, W. M. (2001). Viktor Hamburger and Rita Levi-Montalcini: the path to the discovery of nerve growth factor. Annu Rev Neurosci, 24, 551-600.

Crouch, P. J., Blake, R., Duce, J. A., Ciccotosto, G. D., Li, Q. X., Barnham, K. J., . . . Trounce, I. A. (2005). Copper-dependent inhibition of human cytochrome c oxidase by a dimeric conformer of amyloid-beta1-42. J Neurosci, 25(3), 672-679.

Csibi, A., Fendt, S. M., Li, C., Poulogiannis, G., Choo, A. Y., Chapski, D. J., . . . Blenis, J. (2013). The mTORC1 pathway stimulates glutamine metabolism and cell proliferation by repressing SIRT4. Cell, 153(4), 840-854.

Cunningham, J. T., Rodgers, J. T., Arlow, D. H., Vazquez, F., Mootha, V. K., & Puigserver, P. (2007). mTOR controls mitochondrial oxidative function through a YY1-PGC-1alpha transcriptional complex. Nature, 450(7170), 736-740.

Czabotar, P. E., Lessene, G., Strasser, A., & Adams, J. M. (2014). Control of apoptosis by the BCL-2 protein family: implications for physiology and therapy. Nat Rev Mol Cell Biol, 15(1), 49-63.

D'Mello, S. R., Galli, C., Ciotti, T., & Calissano, P. (1993). Induction of apoptosis in cerebellar granule neurons by low potassium: inhibition of death by insulin-like growth factor I and cAMP. Proc Natl Acad Sci U S A, 90(23), 10989-10993.

De Vitto, H., Perez-Valencia, J., & Radosevich, J. A. (2016). Glutamine at focus: versatile roles in cancer. Tumour Biol, 37(2), 1541-1558.

Deckwerth, T. L., Elliott, J. L., Knudson, C. M., Johnson, E. M., Jr., Snider, W. D., & Korsmeyer, S. J. (1996). BAX is required for neuronal death after trophic factor deprivation and during development. Neuron, 17(3), 401-411.

Deckwerth, T. L., & Johnson, E. M., Jr. (1993). Temporal analysis of events associated with programmed cell death (apoptosis) of sympathetic neurons deprived of nerve growth factor. J Cell Biol, 123(5), 1207-1222.

DeNicola, G. M., Karreth, F. A., Humpton, T. J., Gopinathan, A., Wei, C., Frese, K., . . . Tuveson, D. A. (2011). Oncogene-induced Nrf2 transcription promotes ROS detoxification and tumorigenesis. Nature, 475(7354), 106-109.

Desagher, S., Severac, D., Lipkin, A., Bernis, C., Ritchie, W., Le Digarcher, A., & Journot, L. (2005). Genes regulated in neurons undergoing transcription-dependent apoptosis belong to signaling pathways rather than the apoptotic machinery. J Biol Chem, 280(7), 5693-5702.

Deshmukh, M., & Johnson, E. M., Jr. (1997). Programmed cell death in neurons: focus on the pathway of nerve growth factor deprivation-induced death of sympathetic neurons. Mol Pharmacol, 51(6), 897-906.

Deshmukh, M., & Johnson, E. M., Jr. (1998). Evidence of a novel event during neuronal death: development of competence-to-die in response to cytoplasmic cytochrome c. Neuron, 21(4), 695-705.

Deshmukh, M., Kuida, K., & Johnson, E. M., Jr. (2000). Caspase inhibition extends the commitment to neuronal death beyond cytochrome c release to the point of mitochondrial depolarization. J Cell Biol, 150(1), 131-143.

Deshmukh, M., Vasilakos, J., Deckwerth, T. L., Lampe, P. A., Shivers, B. D., & Johnson, E. M., Jr. (1996). Genetic and metabolic status of NGF-deprived sympathetic neurons saved by an inhibitor of ICE family proteases. J Cell Biol, 135(5), 1341-1354.

Devi, L., Prabhu, B. M., Galati, D. F., Avadhani, N. G., & Anandatheerthavarada, H. K. (2006). Accumulation of amyloid precursor protein in the mitochondrial import channels of human Alzheimer's disease brain is associated with mitochondrial dysfunction. J Neurosci, 26(35), 9057-9068.

Dugan, L. L., Creedon, D. J., Johnson, E. M., Jr., & Holtzman, D. M. (1997). Rapid suppression of free radical formation by nerve growth factor involves the mitogen-activated protein kinase pathway. Proc Natl Acad Sci U S A, 94(8), 4086-4091.

Duvel, K., Yecies, J. L., Menon, S., Raman, P., Lipovsky, A. I., Souza, A. L., . . . Manning, B. D. (2010). Activation of a metabolic gene regulatory network downstream of mTOR complex 1. Mol Cell, 39(2), 171-183.

Eckert, A., Hauptmann, S., Scherping, I., Rhein, V., Muller-Spahn, F., Gotz, J., & Muller, W. E. (2008). Soluble beta-amyloid leads to mitochondrial defects in amyloid precursor protein and tau transgenic mice. Neurodegener Dis, 5(3-4), 157-159.

Edwards, S. N., & Tolkovsky, A. M. (1994). Characterization of apoptosis in cultured rat sympathetic neurons after nerve growth factor withdrawal. J Cell Biol, 124(4), 537-546.

Eichler, M. E., Dubinsky, J. M., & Rich, K. M. (1992). Relationship of intracellular calcium to dependence on nerve growth factor in dorsal root ganglion neurons in cell culture. J Neurochem, 58(1), 263-269.

Elmore, S. (2007). Apoptosis: a review of programmed cell death. Toxicol Pathol, 35(4), 495-516.

Ernfors, P., Lee, K. F., & Jaenisch, R. (1994). Mice lacking brain-derived neurotrophic factor develop with sensory deficits. Nature, 368(6467), 147-150.

Ernster, L., & Schatz, G. (1981). Mitochondria: a historical review. J Cell Biol, 91(3 Pt 2), 227s-255s.

Ferrari, G., Yan, C. Y., & Greene, L. A. (1995). N-acetylcysteine (D- and L-stereoisomers) prevents apoptotic death of neuronal cells. J Neurosci, 15(4), 2857-2866.

Ferreiro, E., Oliveira, C. R., & Pereira, C. M. (2008). The release of calcium from the endoplasmic reticulum induced by amyloid-beta and prion peptides activates the mitochondrial apoptotic pathway. Neurobiol Dis, 30(3), 331-342.

Filipp, F. V., Ratnikov, B., De Ingeniis, J., Smith, J. W., Osterman, A. L., & Scott, D. A. (2012). Glutamine-fueled mitochondrial metabolism is decoupled from glycolysis in melanoma. Pigment Cell Melanoma Res, 25(6), 732-739.

Fornai, F., Schluter, O. M., Lenzi, P., Gesi, M., Ruffoli, R., Ferrucci, M., . . . Sudhof, T. C. (2005). Parkinson-like syndrome induced by continuous MPTP infusion: convergent roles of the ubiquitin-proteasome system and alpha-synuclein. Proc Natl Acad Sci U S A, 102(9), 3413-3418.

Fourquet, S., Guerois, R., Biard, D., & Toledano, M. B. (2010). Activation of NRF2 by nitrosative agents and H2O2 involves KEAP1 disulfide formation. J Biol Chem, 285(11), 8463-8471.

Franklin, J. L., Fickbohm, D. J., & Willard, A. L. (1992). Long-term regulation of neuronal calcium currents by prolonged changes of membrane potential. J Neurosci, 12(5), 1726-1735.

Franklin, J. L., & Johnson, E. M. (1998). Control of neuronal size homeostasis by trophic factor-mediated coupling of protein degradation to protein synthesis. J Cell Biol, 142(5), 1313-1324.

Franklin, J. L., Sanz-Rodriguez, C., Juhasz, A., Deckwerth, T. L., & Johnson, E. M., Jr. (1995). Chronic depolarization prevents programmed death of sympathetic neurons in vitro but does not support growth: requirement for Ca^{2+} influx but not Trk activation. J Neurosci, 15(1 Pt 2), 643-664.

Fresno Vara, J. A., Casado, E., de Castro, J., Cejas, P., Belda-Iniesta, C., & Gonzalez-Baron, M. (2004). PI3K/Akt signalling pathway and cancer. Cancer Treat Rev, 30(2), 193-204.

Friedman, J. R., & Nunnari, J. (2014). Mitochondrial form and function. Nature, 505(7483), 335-343.

Gallo, V., Kingsbury, A., Balazs, R., & Jorgensen, O. S. (1987). The role of depolarization in the survival and differentiation of cerebellar granule cells in culture. J Neurosci, 7(7), 2203-2213.

Galluzzi, L., Bravo-San Pedro, J. M., Vitale, I., Aaronson, S. A., Abrams, J. M., Adam, D., . . . Kroemer, G. (2015). Essential versus accessory aspects of cell death: recommendations of the NCCD 2015. Cell Death Differ, 22(1), 58-73.

Galluzzi, L., Vitale, I., Abrams, J. M., Alnemri, E. S., Baehrecke, E. H., Blagosklonny, M. V., . . . Kroemer, G. (2012). Molecular definitions of cell death subroutines: recommendations of the Nomenclature Committee on Cell Death 2012. Cell Death Differ, 19(1), 107-120.

Gao, P., Tchernyshyov, I., Chang, T. C., Lee, Y. S., Kita, K., Ochi, T., . . . Dang, C. V. (2009). c-Myc suppression of miR-23a/b enhances mitochondrial glutaminase expression and glutamine metabolism. Nature, 458(7239), 762-765.

Garrido, C., Galluzzi, L., Brunet, M., Puig, P. E., Didelot, C., & Kroemer, G. (2006). Mechanisms of cytochrome c release from mitochondria. Cell Death Differ, 13(9), 1423-1433.

Ghosh, A., & Greenberg, M. E. (1995). Calcium signaling in neurons: molecular mechanisms and cellular consequences. Science, 268(5208), 239-247.

Glebova, N. O., & Ginty, D. D. (2005). Growth and survival signals controlling sympathetic nervous system development. Annu Rev Neurosci, 28, 191-222.

Glucksmann, A. (1951). Cell deaths in normal vertebrate ontogeny. Biol Rev Camb Philos Soc, 26(1), 59-86.

Gogvadze, V., Orrenius, S., & Zhivotovsky, B. (2006). Multiple pathways of cytochrome c release from mitochondria in apoptosis. Biochim Biophys Acta, 1757(5-6), 639-647.

Gonzalvez, F., & Gottlieb, E. (2007). Cardiolipin: setting the beat of apoptosis. Apoptosis, 12(5), 877-885.

Gopal, Y. N., Rizos, H., Chen, G., Deng, W., Frederick, D. T., Cooper, Z. A., . . . Davies, M. A. (2014). Inhibition of mTORC1/2 overcomes resistance to MAPK pathway inhibitors mediated by PGC1alpha and oxidative phosphorylation in melanoma. Cancer Res, 74(23), 7037-7047.

Greenamyre, J. T., Sherer, T. B., Betarbet, R., & Panov, A. V. (2001). Complex I and Parkinson's disease. IUBMB Life, 52(3-5), 135-141.

Greenlund, L. J., Deckwerth, T. L., & Johnson, E. M., Jr. (1995). Superoxide dismutase delays neuronal apoptosis: a role for reactive oxygen species in programmed neuronal death. Neuron, 14(2), 303-315.

Grynkiewicz, G., Poenie, M., & Tsien, R. Y. (1985). A new generation of Ca^{2+} indicators with greatly improved fluorescence properties. J Biol Chem, 260(6), 3440-3450.

Guzy, R. D., Hoyos, B., Robin, E., Chen, H., Liu, L., Mansfield, K. D., . . . Schumacker, P. T. (2005). Mitochondrial complex III is required for hypoxia-induced ROS production and cellular oxygen sensing. Cell Metab, 1(6), 401-408.

Handy, D. E., & Loscalzo, J. (2012). Redox regulation of mitochondrial function. Antioxid Redox Signal, 16(11), 1323-1367.

Haq, R., Shoag, J., Andreu-Perez, P., Yokoyama, S., Edelman, H., Rowe, G. C., . . . Widlund, H. R. (2013). Oncogenic BRAF regulates oxidative metabolism via PGC1alpha and MITF. Cancer Cell, 23(3), 302-315.

Hardy, J. A., & Higgins, G. A. (1992). Alzheimer's disease: the amyloid cascade hypothesis. Science, 256(5054), 184-185.

Harris, C. A., & Johnson, E. M., Jr. (2001). BH3-only Bcl-2 family members are coordinately regulated by the JNK pathway and require Bax to induce apoptosis in neurons. J Biol Chem, 276(41), 37754-37760.

Hattori, N., Tanaka, M., Ozawa, T., & Mizuno, Y. (1991). Immunohistochemical studies on complexes I, II, III, and IV of mitochondria in Parkinson's disease. Ann Neurol, 30(4), 563-571.

Heydorn, W. E., Frazer, A., & Weiss, B. (1981). Electrical stimulation of sympathetic nerves increases the concentration of cyclic AMP in rat pineal gland. Proc Natl Acad Sci U S A, 78(11), 7176-7179.

Hille, B. (2001). Ion Channels of Excitable Membranes (Third Edition ed.): SINAUER ASSOCIATES, INC; Sunderland, MA.

Huttemann, M., Pecina, P., Rainbolt, M., Sanderson, T. H., Kagan, V. E., Samavati, L., . . . Lee, I. (2011). The multiple functions of cytochrome c and their regulation in life and death decisions of the mammalian cell: From respiration to apoptosis. Mitochondrion, 11(3), 369-381.

Imaizumi, K., Benito, A., Kiryu-Seo, S., Gonzalez, V., Inohara, N., Lieberman, A. P., . . . Nunez, G. (2004). Critical role for DP5/Harakiri, a Bcl-2 homology domain 3-only Bcl-2 family member, in axotomy-induced neuronal cell death. J Neurosci, 24(15), 3721-3725.

Imaizumi, K., Tsuda, M., Imai, Y., Wanaka, A., Takagi, T., & Tohyama, M. (1997). Molecular cloning of a novel polypeptide, DP5, induced during programmed neuronal death. J Biol Chem, 272(30), 18842-18848.

Janetzky, B., Hauck, S., Youdim, M. B., Riederer, P., Jellinger, K., Pantucek, F., . . . Reichmann, H. (1994). Unaltered aconitase activity, but decreased complex I activity in substantia nigra pars compacta of patients with Parkinson's disease. Neurosci Lett, 169(1-2), 126-128.

Jiang, J., Huang, Z., Zhao, Q., Feng, W., Belikova, N. A., & Kagan, V. E. (2008). Interplay between bax, reactive oxygen species production, and cardiolipin oxidation during apoptosis. Biochem Biophys Res Commun, 368(1), 145-150.

Johnson, M. I., & Argiro, V. (1983). Techniques in the tissue culture of rat sympathetic neurons. Methods Enzymol, 103, 334-347.

Jones, K. R., Farinas, I., Backus, C., & Reichardt, L. F. (1994). Targeted disruption of the BDNF gene perturbs brain and sensory neuron development but not motor neuron development. Cell, 76(6), 989-999.

Kaelin, W. G., Jr., & Ratcliffe, P. J. (2008). Oxygen sensing by metazoans: the central role of the HIF hydroxylase pathway. Mol Cell, 30(4), 393-402.

Kann, O., & Kovacs, R. (2007). Mitochondria and neuronal activity. Am J Physiol Cell Physiol, 292(2), C641-657.

Kao, S. C., Krichevsky, A. M., Kosik, K. S., & Tsai, L. H. (2004). BACE1 suppression by RNA interference in primary cortical neurons. J Biol Chem, 279(3), 1942-1949.

Kaplan, F. S., Maguire, T. G., Lee, V. M., Selzer, M. E., Spindler, K., Black, J., & Brighton, C. T. (1988). Direct extracellular electrical stimulation influences density dependent aggregation of fetal rat cerebrocortical neurons in vitro. Neurosci Lett, 94(1-2), 33-38.

Kaplon, J., Zheng, L., Meissl, K., Chaneton, B., Selivanov, V. A., Mackay, G., . . . Peeper, D. S. (2013). A key role for mitochondrial gatekeeper pyruvate dehydrogenase in oncogene-induced senescence. Nature, 498(7452), 109-112.

Kawamata, H., & Manfredi, G. (2017). Correction: Proteinopathies and OXPHOS dysfunction in neurodegenerative diseases. J Cell Biol.

Keeney, P. M., Xie, J., Capaldi, R. A., & Bennett, J. P., Jr. (2006). Parkinson's disease brain mitochondrial complex I has oxidatively damaged subunits and is functionally impaired and misassembled. J Neurosci, 26(19), 5256-5264.

Kerr, J. F., Wyllie, A. H., & Currie, A. R. (1972). Apoptosis: a basic biological phenomenon with wide-ranging implications in tissue kinetics. Br J Cancer, 26(4), 239-257.

Khwairakpam, A. D., Shyamananda, M. S., Sailo, B. L., Rathnakaram, S. R., Padmavathi, G., Kotoky, J., & Kunnumakkara, A. B. (2015). ATP citrate lyase (ACLY): a promising target for cancer prevention and treatment. Curr Drug Targets, 16(2), 156-163.

Kim, J. W., Tchernyshyov, I., Semenza, G. L., & Dang, C. V. (2006). HIF-1-mediated expression of pyruvate dehydrogenase kinase: a metabolic switch required for cellular adaptation to hypoxia. Cell Metab, 3(3), 177-185.

Kim, L. C., Cook, R. S., & Chen, J. (2017). mTORC1 and mTORC2 in cancer and the tumor microenvironment. Oncogene, 36(16), 2191-2201.

Kirkland, R. A., Adibhatla, R. M., Hatcher, J. F., & Franklin, J. L. (2002). Loss of cardiolipin and mitochondria during programmed neuronal death: evidence of a role for lipid peroxidation and autophagy. Neuroscience, 115(2), 587-602.

Kirkland, R. A., & Franklin, J. L. (2001). Evidence for redox regulation of cytochrome C release during programmed neuronal death: antioxidant effects of protein synthesis and caspase inhibition. J Neurosci, 21(6), 1949-1963.

Kirkland, R. A., Saavedra, G. M., Cummings, B. S., & Franklin, J. L. (2010). Bax regulates production of superoxide in both apoptotic and nonapoptotic neurons: role of caspases. J Neurosci, 30(48), 16114-16127.

Kirkland, R. A., Saavedra, G. M., & Franklin, J. L. (2007). Rapid activation of antioxidant defenses by nerve growth factor suppresses reactive oxygen species during neuronal apoptosis: evidence for a role in cytochrome c redistribution. J Neurosci, 27(42), 11315-11326.

Kirkland, R. A., Windelborn, J. A., Kasprzak, J. M., & Franklin, J. L. (2002). A Bax-induced pro-oxidant state is critical for cytochrome c release during programmed neuronal death. J Neurosci, 22(15), 6480-6490.

Klein, R., Jing, S. Q., Nanduri, V., O'Rourke, E., & Barbacid, M. (1991). The trk proto-oncogene encodes a receptor for nerve growth factor. Cell, 65(1), 189-197.

Knott, A. B., Perkins, G., Schwarzenbacher, R., & Bossy-Wetzel, E. (2008). Mitochondrial fragmentation in neurodegeneration. Nat Rev Neurosci, 9(7), 505-518.

Koike, T., Martin, D. P., & Johnson, E. M., Jr. (1989). Role of Ca^{2+} channels in the ability of membrane depolarization to prevent neuronal death induced by trophic-factor deprivation: evidence that levels of internal Ca^{2+} determine nerve growth factor dependence of sympathetic ganglion cells. Proc Natl Acad Sci U S A, 86(16), 6421-6425.

Koike, T., & Tanaka, S. (1991). Evidence that nerve growth factor dependence of sympathetic neurons for survival in vitro may be determined by levels of cytoplasmic free Ca^{2+}. Proc Natl Acad Sci U S A, 88(9), 3892-3896.

Kristiansen, M., Menghi, F., Hughes, R., Hubank, M., & Ham, J. (2011). Global analysis of gene expression in NGF-deprived sympathetic neurons identifies molecular pathways associated with cell death. BMC Genomics, 12, 551.

Kuhlbrandt, W. (2015). Structure and function of mitochondrial membrane protein complexes. BMC Biol, 13, 89.

Kuphal, S., Winklmeier, A., Warnecke, C., & Bosserhoff, A. K. (2010). Constitutive HIF-1 activity in malignant melanoma. Eur J Cancer, 46(6), 1159-1169.

Kuwana, T., Bouchier-Hayes, L., Chipuk, J. E., Bonzon, C., Sullivan, B. A., Green, D. R., & Newmeyer, D. D. (2005). BH3 domains of BH3-only proteins differentially regulate Bax-mediated mitochondrial membrane permeabilization both directly and indirectly. Mol Cell, 17(4), 525-535.

Lasher, R. S., & Zagon, I. S. (1972). The effect of potassium on neuronal differentiation in cultures of dissociated newborn rat cerebellum. Brain Res, 41(2), 482-488.

Lee, S. R., Yang, K. S., Kwon, J., Lee, C., Jeong, W., & Rhee, S. G. (2002). Reversible inactivation of the tumor suppressor PTEN by H2O2. J Biol Chem, 277(23), 20336-20342.

Leslie, N. R., Bennett, D., Lindsay, Y. E., Stewart, H., Gray, A., & Downes, C. P. (2003). Redox regulation of PI 3-kinase signalling via inactivation of PTEN. EMBO J, 22(20), 5501-5510.

Li, F., Calingasan, N. Y., Yu, F., Mauck, W. M., Toidze, M., Almeida, C. G., . . . Gouras, G. K. (2004). Increased plaque burden in brains of APP mutant MnSOD heterozygous knockout mice. J Neurochem, 89(5), 1308-1312.

Lin, M. T., & Beal, M. F. (2006). Mitochondrial dysfunction and oxidative stress in neurodegenerative diseases. Nature, 443(7113), 787-795.

Lin, X., Sun, R., Zhao, X., Zhu, D., Zhao, X., Gu, Q., . . . Sun, B. (2017). C-myc overexpression drives melanoma metastasis by promoting vasculogenic mimicry via c-myc/snail/Bax signaling. J Mol Med (Berl), 95(1), 53-67.

Linden, R. (1994). The survival of developing neurons: a review of afferent control. Neuroscience, 58(4), 671-682.

Liu, Y., Fiskum, G., & Schubert, D. (2002). Generation of reactive oxygen species by the mitochondrial electron transport chain. J Neurochem, 80(5), 780-787.

Lou, Y. W., Chen, Y. Y., Hsu, S. F., Chen, R. K., Lee, C. L., Khoo, K. H., . . . Meng, T. C. (2008). Redox regulation of the protein tyrosine phosphatase PTP1B in cancer cells. FEBS J, 275(1), 69-88.

Manczak, M., Anekonda, T. S., Henson, E., Park, B. S., Quinn, J., & Reddy, P. H. (2006). Mitochondria are a direct site of A beta accumulation in Alzheimer's disease neurons: implications for free radical generation and oxidative damage in disease progression. Hum Mol Genet, 15(9), 1437-1449.

Mannava, S., Grachtchouk, V., Wheeler, L. J., Im, M., Zhuang, D., Slavina, E. G., . . . Nikiforov, M. A. (2008). Direct role of nucleotide metabolism in C-MYC-dependent proliferation of melanoma cells. Cell Cycle, 7(15), 2392-2400.

Mansfield, K. D., Guzy, R. D., Pan, Y., Young, R. M., Cash, T. P., Schumacker, P. T., & Simon, M. C. (2005). Mitochondrial dysfunction resulting from loss of cytochrome c impairs cellular oxygen sensing and hypoxic HIF-alpha activation. Cell Metab, 1(6), 393-399.

Martin, D. P., Schmidt, R. E., DiStefano, P. S., Lowry, O. H., Carter, J. G., & Johnson, E. M., Jr. (1988). Inhibitors of protein synthesis and RNA synthesis prevent neuronal death caused by nerve growth factor deprivation. J Cell Biol, 106(3), 829-844.

Martinou, I., Desagher, S., Eskes, R., Antonsson, B., Andre, E., Fakan, S., & Martinou, J. C. (1999). The release of cytochrome c from mitochondria during apoptosis of NGF-deprived sympathetic neurons is a reversible event. J Cell Biol, 144(5), 883-889.

Masters, C. L., Bateman, R., Blennow, K., Rowe, C. C., Sperling, R. A., & Cummings, J. L. (2015). Alzheimer's disease. Nat Rev Dis Primers, 1, 15056.

McCarthy, M. J., Rubin, L. L., & Philpott, K. L. (1997). Involvement of caspases in sympathetic neuron apoptosis. J Cell Sci, 110 (Pt 18), 2165-2173.

McFate, T., Mohyeldin, A., Lu, H., Thakar, J., Henriques, J., Halim, N. D., . . . Verma, A. (2008). Pyruvate dehydrogenase complex activity controls metabolic and malignant phenotype in cancer cells. J Biol Chem, 283(33), 22700-22708.

Menegon, S., Columbano, A., & Giordano, S. (2016). The Dual Roles of NRF2 in Cancer. Trends Mol Med, 22(7), 578-593.

Miller, D. M., Thomas, S. D., Islam, A., Muench, D., & Sedoris, K. (2012). c-Myc and cancer metabolism. Clin Cancer Res, 18(20), 5546-5553.

Miller, T. M., & Johnson, E. M., Jr. (1996). Metabolic and genetic analyses of apoptosis in potassium/serum-deprived rat cerebellar granule cells. J Neurosci, 16(23), 7487-7495.

Miller, W. L. (2013). Steroid hormone synthesis in mitochondria. Mol Cell Endocrinol, 379(1-2), 62-73.

Milligan, C. E., Oppenheim, R. W., & Schwartz, L. M. (1994). Motoneurons deprived of trophic support in vitro require new gene expression to undergo programmed cell death. J Neurobiol, 25(8), 1005-1016.

Mizuno, Y., Ohta, S., Tanaka, M., Takamiya, S., Suzuki, K., Sato, T., . . . Kagawa, Y. (1989). Deficiencies in complex I subunits of the respiratory chain in Parkinson's disease. Biochem Biophys Res Commun, 163(3), 1450-1455.

Neame, S. J., Rubin, L. L., & Philpott, K. L. (1998). Blocking cytochrome c activity within intact neurons inhibits apoptosis. J Cell Biol, 142(6), 1583-1593.

Nicklas, W. J., Vyas, I., & Heikkila, R. E. (1985). Inhibition of NADH-linked oxidation in brain mitochondria by 1-methyl-4-phenyl-pyridine, a metabolite of the neurotoxin, 1-methyl-4-phenyl-1,2,5,6-tetrahydropyridine. Life Sci, 36(26), 2503-2508.

Nicklin, P., Bergman, P., Zhang, B., Triantafellow, E., Wang, H., Nyfeler, B., . . . Murphy, L. O. (2009). Bidirectional transport of amino acids regulates mTOR and autophagy. Cell, 136(3), 521-534.

Nikoletopoulou, V., Lickert, H., Frade, J. M., Rencurel, C., Giallonardo, P., Zhang, L., . . . Barde, Y. A. (2010). Neurotrophin receptors TrkA and TrkC cause neuronal death whereas TrkB does not. Nature, 467(7311), 59-63.

Nishi, R., & Berg, D. K. (1981). Effects of high K+ concentrations on the growth and development of ciliary ganglion neurons in cell culture. Dev Biol, 87(2), 301-307.

Nunnari, J., & Suomalainen, A. (2012). Mitochondria: in sickness and in health. Cell, 148(6), 1145-1159.

O'Connor, L., Strasser, A., O'Reilly, L. A., Hausmann, G., Adams, J. M., Cory, S., & Huang, D. C. (1998). Bim: a novel member of the Bcl-2 family that promotes apoptosis. EMBO J, 17(2), 384-395.

Ohyagi, Y., Yamada, T., Nishioka, K., Clarke, N. J., Tomlinson, A. J., Naylor, S., . . . Younkin, S. G. (2000). Selective increase in cellular A beta 42 is related to apoptosis but not necrosis. Neuroreport, 11(1), 167-171.

Oppenheim, R. W. (1991). Cell death during development of the nervous system. Annu Rev Neurosci, 14, 453-501.

Orrenius, S., & Zhivotovsky, B. (2005). Cardiolipin oxidation sets cytochrome c free. Nat Chem Biol, 1(4), 188-189.

Ostman, A., Frijhoff, J., Sandin, A., & Bohmer, F. D. (2011). Regulation of protein tyrosine phosphatases by reversible oxidation. J Biochem, 150(4), 345-356.

Ott, M., Gogvadze, V., Orrenius, S., & Zhivotovsky, B. (2007). Mitochondria, oxidative stress and cell death. Apoptosis, 12(5), 913-922.

Ott, M., Norberg, E., Walter, K. M., Schreiner, P., Kemper, C., Rapaport, D., . . . Orrenius, S. (2007). The mitochondrial TOM complex is required for tBid/Bax-induced cytochrome c release. J Biol Chem, 282(38), 27633-27639.

Ott, M., Robertson, J. D., Gogvadze, V., Zhivotovsky, B., & Orrenius, S. (2002). Cytochrome c release from mitochondria proceeds by a two-step process. Proc Natl Acad Sci U S A, 99(3), 1259-1263.

Parker, W. D., Jr., Parks, J. K., & Swerdlow, R. H. (2008). Complex I deficiency in Parkinson's disease frontal cortex. Brain Res, 1189, 215-218.

Pasic, T. R., & Rubel, E. W. (1989). Rapid changes in cochlear nucleus cell size following blockade of auditory nerve electrical activity in gerbils. J Comp Neurol, 283(4), 474-480.

Pavlova, N. N., & Thompson, C. B. (2016). The Emerging Hallmarks of Cancer Metabolism. Cell Metab, 23(1), 27-47.

Pelicano, H., Xu, R. H., Du, M., Feng, L., Sasaki, R., Carew, J. S., . . . Huang, P. (2006). Mitochondrial respiration defects in cancer cells cause activation of Akt survival pathway through a redox-mediated mechanism. J Cell Biol, 175(6), 913-923.

Perry, T. L., Godin, D. V., & Hansen, S. (1982). Parkinson's disease: a disorder due to nigral glutathione deficiency? Neurosci Lett, 33(3), 305-310.

Petrosillo, G., Casanova, G., Matera, M., Ruggiero, F. M., & Paradies, G. (2006). Interaction of peroxidized cardiolipin with rat-heart mitochondrial membranes: induction of permeability transition and cytochrome c release. FEBS Lett, 580(27), 6311-6316.

Phillipson, O. T., & Sandler, M. (1975). The influence of nerve growth factor, potassium depolarization and dibutyryl (cyclic) adenosine 3',5'-monophosphate on explant cultures of chick embryo sympathetic ganglia. Brain Res, 90(2), 273-281.

Poewe, W., Seppi, K., Tanner, C. M., Halliday, G. M., Brundin, P., Volkmann, J., . . . Lang, A. E. (2017). Parkinson disease. Nat Rev Dis Primers, 3, 17013.

Purves D, A. G., Fitzpatrick D, et al., editors. (2001). The Ionic Basis of the Resting Membrane PotentialNeuroscience. 2nd edition: Sunderland (MA): Sinauer Associates.

Purves, D., Snider, W. D., & Voyvodic, J. T. (1988). Trophic regulation of nerve cell morphology and innervation in the autonomic nervous system. Nature, 336(6195), 123-128.

Putcha, G. V., Deshmukh, M., & Johnson, E. M., Jr. (1999). BAX translocation is a critical event in neuronal apoptosis: regulation by neuroprotectants, BCL-2, and caspases. J Neurosci, 19(17), 7476-7485.

Putcha, G. V., Harris, C. A., Moulder, K. L., Easton, R. M., Thompson, C. B., & Johnson, E. M., Jr. (2002). Intrinsic and extrinsic pathway signaling during neuronal apoptosis: lessons from the analysis of mutant mice. J Cell Biol, 157(3), 441-453.

Putcha, G. V., Moulder, K. L., Golden, J. P., Bouillet, P., Adams, J. A., Strasser, A., & Johnson, E. M. (2001). Induction of BIM, a proapoptotic BH3-only BCL-2 family member, is critical for neuronal apoptosis. Neuron, 29(3), 615-628.

Puthalakath, H., Huang, D. C., O'Reilly, L. A., King, S. M., & Strasser, A. (1999). The proapoptotic activity of the Bcl-2 family member Bim is regulated by interaction with the dynein motor complex. Mol Cell, 3(3), 287-296.

Rao, R. K., & Clayton, L. W. (2002). Regulation of protein phosphatase 2A by hydrogen peroxide and glutathionylation. Biochem Biophys Res Commun, 293(1), 610-616.

Ratan, R. R., Murphy, T. H., & Baraban, J. M. (1994). Macromolecular synthesis inhibitors prevent oxidative stress-induced apoptosis in embryonic cortical neurons by shunting cysteine from protein synthesis to glutathione. J Neurosci, 14(7), 4385-4392.

Rauskolb, S., Zagrebelsky, M., Dreznjak, A., Deogracias, R., Matsumoto, T., Wiese, S., . . . Barde, Y. A. (2010). Global deprivation of brain-derived neurotrophic factor in the CNS reveals an area-specific requirement for dendritic growth. J Neurosci, 30(5), 1739-1749.

Ray, P. D., Huang, B. W., & Tsuji, Y. (2012). Reactive oxygen species (ROS) homeostasis and redox regulation in cellular signaling. Cell Signal, 24(5), 981-990.

Ren, D., Tu, H. C., Kim, H., Wang, G. X., Bean, G. R., Takeuchi, O., . . . Cheng, E. H. (2010). BID, BIM, and PUMA are essential for activation of the BAX- and BAK-dependent cell death program. Science, 330(6009), 1390-1393.

Ren, R., Zhang, Y., Li, B., Wu, Y., & Li, B. (2011). Effect of beta-amyloid (25-35) on mitochondrial function and expression of mitochondrial permeability transition pore proteins in rat hippocampal neurons. J Cell Biochem, 112(5), 1450-1457.

Rhein, V., Song, X., Wiesner, A., Ittner, L. M., Baysang, G., Meier, F., . . . Eckert, A. (2009). Amyloid-beta and tau synergistically impair the oxidative phosphorylation system in triple transgenic Alzheimer's disease mice. Proc Natl Acad Sci U S A, 106(47), 20057-20062.

Robinson, K. M., Janes, M. S., Pehar, M., Monette, J. S., Ross, M. F., Hagen, T. M., . . . Beckman, J. S. (2006). Selective fluorescent imaging of superoxide in vivo using ethidium-based probes. Proc Natl Acad Sci U S A, 103(41), 15038-15043.

Ronnback, A., Pavlov, P. F., Mansory, M., Gonze, P., Marliere, N., Winblad, B., . . . Behbahani, H. (2016). Mitochondrial dysfunction in a transgenic mouse model expressing human amyloid precursor protein (APP) with the Arctic mutation. J Neurochem, 136(3), 497-502.

Royall, J. A., & Ischiropoulos, H. (1993). Evaluation of 2',7'-dichlorofluorescin and dihydrorhodamine 123 as fluorescent probes for intracellular H_2O_2 in cultured endothelial cells. Arch Biochem Biophys, 302(2), 348-355.

Sabharwal, S. S., & Schumacker, P. T. (2014). Mitochondrial ROS in cancer: initiators, amplifiers or an Achilles' heel? Nat Rev Cancer, 14(11), 709-721.

Salmeen, A., Andersen, J. N., Myers, M. P., Meng, T. C., Hinks, J. A., Tonks, N. K., & Barford, D. (2003). Redox regulation of protein tyrosine phosphatase 1B involves a sulphenyl-amide intermediate. Nature, 423(6941), 769-773.

Satoh, H., Moriguchi, T., Takai, J., Ebina, M., & Yamamoto, M. (2013). Nrf2 prevents initiation but accelerates progression through the Kras signaling pathway during lung carcinogenesis. Cancer Res, 73(13), 4158-4168.

Saxton, R. A., & Sabatini, D. M. (2017). mTOR Signaling in Growth, Metabolism, and Disease. Cell, 168(6), 960-976.

Schapira, A. H., Cooper, J. M., Dexter, D., Clark, J. B., Jenner, P., & Marsden, C. D. (1990). Mitochondrial complex I deficiency in Parkinson's disease. J Neurochem, 54(3), 823-827.

Schell, J. C., Olson, K. A., Jiang, L., Hawkins, A. J., Van Vranken, J. G., Xie, J., . . . Rutter, J. (2014). A role for the mitochondrial pyruvate carrier as a repressor of the Warburg effect and colon cancer cell growth. Mol Cell, 56(3), 400-413.

Schmidt, M. F., & Kater, S. B. (1993). Fibroblast growth factors, depolarization, and substratum interact in a combinatorial way to promote neuronal survival. Dev Biol, 158(1), 228-237.

Schumacker, P. T. (2015). Reactive oxygen species in cancer: a dance with the devil. Cancer Cell, 27(2), 156-157.

Scott, B. S. (1971). Effect of potassium on neuron survival in cultures of dissociated human nervous tissue. Exp Neurol, 30(2), 297-308.

Scott, B. S. (1977). The effect of elevated potassium on the time course of neuron survival in cultures of dissociated dorsal root ganglia. J Cell Physiol, 91(2), 305-316.

Scott, B. S., & Fisher, K. C. (1970). Potassium concentration and number of neurons in cultures of dissociated ganglia. Exp Neurol, 27(1), 16-22.

Semenza, G. L. (2010). Defining the role of hypoxia-inducible factor 1 in cancer biology and therapeutics. Oncogene, 29(5), 625-634.

Sherer, T. B., Betarbet, R., Testa, C. M., Seo, B. B., Richardson, J. R., Kim, J. H., . . . Greenamyre, J. T. (2003). Mechanism of toxicity in rotenone models of Parkinson's disease. J Neurosci, 23(34), 10756-10764.

Shidoji, Y., Hayashi, K., Komura, S., Ohishi, N., & Yagi, K. (1999). Loss of molecular interaction between cytochrome c and cardiolipin due to lipid peroxidation. Biochem Biophys Res Commun, 264(2), 343-347.

Sian, J., Dexter, D. T., Lees, A. J., Daniel, S., Agid, Y., Javoy-Agid, F., . . . Marsden, C. D. (1994). Alterations in glutathione levels in Parkinson's disease and other neurodegenerative disorders affecting basal ganglia. Ann Neurol, 36(3), 348-355.

Sisken, B. F., & Smith, S. D. (1975). The effects of minute direct electrical currents on cultured chick embryo trigeminal ganglia. J Embryol Exp Morphol, 33(1), 29-41.

Sofic, E., Lange, K. W., Jellinger, K., & Riederer, P. (1992). Reduced and oxidized glutathione in the substantia nigra of patients with Parkinson's disease. Neurosci Lett, 142(2), 128-130.

Southwell, D. G., Paredes, M. F., Galvao, R. P., Jones, D. L., Froemke, R. C., Sebe, J. Y., . . . Alvarez-Buylla, A. (2012). Intrinsically determined cell death of developing cortical interneurons. Nature, 491(7422), 109-113.

Sradhanjali, S., Tripathy, D., Rath, S., Mittal, R., & Reddy, M. M. (2017). Overexpression of pyruvate dehydrogenase kinase 1 in retinoblastoma: A potential therapeutic opportunity for targeting vitreous seeds and hypoxic regions. PLoS One, 12(5), e0177744.

Swerdlow, R. H., Burns, J. M., & Khan, S. M. (2014). The Alzheimer's disease mitochondrial cascade hypothesis: progress and perspectives. Biochim Biophys Acta, 1842(8), 1219-1231.

Taanman, J. W. (1999). The mitochondrial genome: structure, transcription, translation and replication. Biochim Biophys Acta, 1410(2), 103-123.

Tait, S. W., & Green, D. R. (2010). Mitochondria and cell death: outer membrane permeabilization and beyond. Nat Rev Mol Cell Biol, 11(9), 621-632.

Tamagno, E., Bardini, P., Obbili, A., Vitali, A., Borghi, R., Zaccheo, D., . . . Tabaton, M. (2002). Oxidative stress increases expression and activity of BACE in NT2 neurons. Neurobiol Dis, 10(3), 279-288.

Tamagno, E., Guglielmotto, M., Aragno, M., Borghi, R., Autelli, R., Giliberto, L., . . . Tabaton, M. (2008). Oxidative stress activates a positive feedback between the gamma- and beta-secretase cleavages of the beta-amyloid precursor protein. J Neurochem, 104(3), 683-695.

Tamagno, E., Guglielmotto, M., Bardini, P., Santoro, G., Davit, A., Di Simone, D., . . . Tabaton, M. (2003). Dehydroepiandrosterone reduces expression and activity of BACE in NT2 neurons exposed to oxidative stress. Neurobiol Dis, 14(2), 291-301.

Tamagno, E., Parola, M., Bardini, P., Piccini, A., Borghi, R., Guglielmotto, M., . . . Tabaton, M. (2005). Beta-site APP cleaving enzyme up-regulation induced by 4-hydroxynonenal is mediated by stress-activated protein kinases pathways. J Neurochem, 92(3), 628-636.

Tammariello, S. P., Quinn, M. T., & Estus, S. (2000). NADPH oxidase contributes directly to oxidative stress and apoptosis in nerve growth factor-deprived sympathetic neurons. J Neurosci, 20(1), RC53.

Thayer, S. A., Hirning, L. D., & Miller, R. J. (1987). Distribution of multiple types of Ca^{2+} channels in rat sympathetic neurons in vitro. Mol Pharmacol, 32(5), 579-586.

Tolkovsky, A. M., Walker, A. E., Murrell, R. D., & Suidan, H. S. (1990). Ca^{2+} transients are not required as signals for long-term neurite outgrowth from cultured sympathetic neurons. J Cell Biol, 110(4), 1295-1306.

Tong, Y., Zhou, W., Fung, V., Christensen, M. A., Qing, H., Sun, X., & Song, W. (2005). Oxidative stress potentiates BACE1 gene expression and Abeta generation. J Neural Transm (Vienna), 112(3), 455-469.

Vekrellis, K., McCarthy, M. J., Watson, A., Whitfield, J., Rubin, L. L., & Ham, J. (1997). Bax promotes neuronal cell death and is downregulated during the development of the nervous system. Development, 124(6), 1239-1249.

Velliquette, R. A., O'Connor, T., & Vassar, R. (2005). Energy inhibition elevates beta-secretase levels and activity and is potentially amyloidogenic in APP transgenic mice: possible early events in Alzheimer's disease pathogenesis. J Neurosci, 25(47), 10874-10883.

Viale, A., Pettazzoni, P., Lyssiotis, C. A., Ying, H., Sanchez, N., Marchesini, M., . . . Draetta, G. F. (2014). Oncogene ablation-resistant pancreatic cancer cells depend on mitochondrial function. Nature, 514(7524), 628-632.

Wallace, D. C. (2005). A mitochondrial paradigm of metabolic and degenerative diseases, aging, and cancer: a dawn for evolutionary medicine. Annu Rev Genet, 39, 359-407.

Warburg, O. (1956a). On respiratory impairment in cancer cells. Science, 124(3215), 269-270.

Warburg, O. (1956b). On the origin of cancer cells. Science, 123(3191), 309-314.

Ward, P. S., & Thompson, C. B. (2012). Metabolic reprogramming: a cancer hallmark even warburg did not anticipate. Cancer Cell, 21(3), 297-308.

Whitfield, J., Neame, S. J., Paquet, L., Bernard, O., & Ham, J. (2001). Dominant-negative c-Jun promotes neuronal survival by reducing BIM expression and inhibiting mitochondrial cytochrome c release. Neuron, 29(3), 629-643.

Wittgen, H. G., & van Kempen, L. C. (2007). Reactive oxygen species in melanoma and its therapeutic implications. Melanoma Res, 17(6), 400-409.

Wolter, K. G., Hsu, Y. T., Smith, C. L., Nechushtan, A., Xi, X. G., & Youle, R. J. (1997). Movement of Bax from the cytosol to mitochondria during apoptosis. J Cell Biol, 139(5), 1281-1292.

Wong, H. K., Fricker, M., Wyttenbach, A., Villunger, A., Michalak, E. M., Strasser, A., & Tolkovsky, A. M. (2005). Mutually exclusive subsets of BH3-only proteins are activated by the p53 and c-Jun N-terminal kinase/c-Jun signaling pathways during cortical neuron apoptosis induced by arsenite. Mol Cell Biol, 25(19), 8732-8747.

Wright, K. M., Vaughn, A. E., & Deshmukh, M. (2007). Apoptosome dependent caspase-3 activation pathway is non-redundant and necessary for apoptosis in sympathetic neurons. Cell Death Differ, 14(3), 625-633.

Wyttenbach, A., & Tolkovsky, A. M. (2006). The BH3-only protein Puma is both necessary and sufficient for neuronal apoptosis induced by DNA damage in sympathetic neurons. J Neurochem, 96(5), 1213-1226.

Xiang, H., Kinoshita, Y., Knudson, C. M., Korsmeyer, S. J., Schwartzkroin, P. A., & Morrison, R. S. (1998). Bax involvement in p53-mediated neuronal cell death. J Neurosci, 18(4), 1363-1373.

Yamaguchi, Y., & Miura, M. (2015). Programmed cell death in neurodevelopment. Dev Cell, 32(4), 478-490.

Yan, G. M., Ni, B., Weller, M., Wood, K. A., & Paul, S. M. (1994). Depolarization or glutamate receptor activation blocks apoptotic cell death of cultured cerebellar granule neurons. Brain Res, 656(1), 43-51.

Yuan, J., & Yankner, B. A. (2000). Apoptosis in the nervous system. Nature, 407(6805), 802-809.

Zaidi, N., Swinnen, J. V., & Smans, K. (2012). ATP-citrate lyase: a key player in cancer metabolism. Cancer Res, 72(15), 3709-3714.

Zhang, D. D., & Hannink, M. (2003). Distinct cysteine residues in Keap1 are required for Keap1-dependent ubiquitination of Nrf2 and for stabilization of Nrf2 by chemopreventive agents and oxidative stress. Mol Cell Biol, 23(22), 8137-8151.

Zhao, H., Kalivendi, S., Zhang, H., Joseph, J., Nithipatikom, K., Vasquez-Vivar, J., & Kalyanaraman, B. (2003). Superoxide reacts with hydroethidine but forms a fluorescent product that is distinctly different from ethidium: potential implications in intracellular fluorescence detection of superoxide. Free Radic Biol Med, 34(11), 1359-1368.

Zhuang, D., Mannava, S., Grachtchouk, V., Tang, W. H., Patil, S., Wawrzyniak, J. A., . . . Nikiforov, M. A. (2008). C-MYC overexpression is required for continuous suppression of oncogene-induced senescence in melanoma cells. Oncogene, 27(52), 6623-6634.

Zong, W. X., Rabinowitz, J. D., & White, E. (2016). Mitochondria and Cancer. Mol Cell, 61(5), 667-676.

CHAPTER 4

MEMBRANE DEPOLARIZATION PREVENTS NEURONAL APOPTOSIS BY INCREASING CELLULAR GLUTATHIONE CONCENTRATION [*]

[*] Alshamrani, A. A., Franklin, J. L.

To be submitted to Free Radical Biology and Medicine Journal

Abstract

Survival of developing sympathetic neurons is determined by the availability of nerve growth factor (NGF) at the time of innervation to their target organs. NGF-deprived sympathetic neurons in cell culture die by apoptosis within 48-72 hours after deprivation, a hallmark of which is the upregulation of multiple BH3-only pro-apoptotic proteins and a downstream Bax-dependent increase of mitochondrial-derived reactive species. Chronic depolarization induced by elevated potassium concentration $[K^+]_E$ promotes the survival of these cells and that of many other types of neurons in culture and is thought to be a model for the role of electrical activity in promoting neuronal survival during the development of the nervous system. The molecular mechanism(s) by which chronically depolarized neurons resist apoptotic death following NGF withdrawal remains elusive but appears to be mediated by a calcium influx caused by the depolarization. Here we report that elevated $[K^+]_E$ does not promote survival of NGF-deprived mouse SCG neurons in culture by suppression of upregulated BH3-only proteins but, rather, by rapidly upregulating a key antioxidant, glutathione (GSH), that prevents cytochrome *c* redistribution from mitochondria and therefore cell death.

1. Introduction

Many neurons generated during the embryogenesis of the vertebrate nervous system undergo apoptotic death before birth or soon thereafter. This process appears to be important for sculpting the developing nervous system [1,2]. A primary determinant of which neurons survive developmental apoptosis is the availability of neurotrophic factors produced by target organs or other tissues. One of the most extensively studied models for examining the cellular and molecular events underlying apoptosis during neurogenesis are sympathetic neurons derived from the superior cervical ganglia (SCG) of late embryonic or early postnatal rodents and grown in cell culture [3] . Depriving these neurons of their obligate neurotrophic factor, nerve growth factor (NGF), causes their apoptotic death within a 48-72 hour period [4-10] . Death of NGF-deprived neurons is triggered by insertion of the proapoptotic protein, Bax, into the outer mitochondrial membrane. This insertion causes release of cytochrome *c* from the mitochondrial intermembrane space into the cytoplasm where it induces formation of the apoptosome and activation of caspase 3. The caspase 3 then cleaves critical protein substrates leading to cell death [11-14].

NGF-deprived sympathetic neurons display a significant increase in the transcriptional and protein levels of multiple BH3-only proapoptotic proteins before death [15-20]. Evidence suggests that these proteins accelerate the apoptotic process in sympathetic and other neurons but are not required for death to occur [16]. Evidence also suggests that a Bax-dependent increase of mitochondrial-derived reactive oxygen species (ROS) and other reactive species (RS) downstream of the ROS are critical events in the death of these cells [21-24]. Specifically, these ROS/RS appear to be necessary for cytochrome *c* to be released from mitochondria.

In addition to neurotrophic factor-mediated block of apoptotic death during nervous system development, electrical activity also appears to be a crucial factor that determines neuronal survival. Disrupting synaptic transmission or electrical signals, either pharmacologically or mechanistically (by removing afferent input), suppresses the growth and induces apoptotic death of several types of neurons *in vitro* and *in vivo* [25-27]. While numerous studies have demonstrated how neurotrophic factors control neuronal survival during development, few efforts have been aimed toward understanding how electrical activity promotes the survival or suppresses the death of neurons at this stage of embryonic development.

Cultures of several neuronal populations, including sympathetic neurons, survive for extended periods when treated with elevated concentrations of potassium ($[K^+]_E$). Increased $[K^+]_E$ appears to promote survival by imitating the effects of naturally occurring electrical activity *in vivo* by chronically depolarizing neuronal membranes potential [28-32]. The molecular mechanism(s) by which chronically depolarized neurons resist apoptotic death following NGF withdrawal remains elusive but appears to be mediated by a calcium influx caused by the depolarization [33]. In this report we show that elevated $[K^+]_E$ does not promote survival of NGF-deprived mouse SCG neurons in culture by suppression of upregulation of BH3-only proteins but, rather, by activating antioxidant mechanisms that prevent cytochrome *c* redistribution from mitochondria.

2. Materials and methods

2.1. Chemical compounds and reagents

5-(and-6)-chloromethyl-2′, 7′-dichlorodihydrofluorescein diacetate, acetyl ester (CM-H_2DCFDA) and ThiolTracker™ Violet were purchased from Invitrogen catalog# C6827 and catalog# T10095, respectively (Carlsbad, CA). Boc-aspartyl (OMe)-fluoromethylketone (BAF) catalog# 16118 and L-buthionine-(*S, R*)-sulfoximine (BSO) catalog# 14484 were purchased from Cayman Chemical (Ann Arbor, MI). Both reagents were dissolved in dimethyl sulfoxide at concentrations that did not affect neuronal survival. Nerve growth factor 2.5S was purchased from Envigo Bioproducts Inc. catalog# B.5025 (Huntingdon, United Kingdom). Goat anti-mouse NGF-neutralizing antibody catalog# S9080 was purchased from Cedarlane Laboratories (Burlington, Canada). Type 4 collagenase catalog# LS004210 and 0.05% Trypsin-EDTA catalog# 25300054 were purchased from Worthington Biochemical (Lakewood, NJ) and Gibco (Carlsbad, CA), respectively. Heat-inactivated fetal bovine serum catalog# 10438026 and L-glutamine catalog# 25030081 were purchased from Gibco (Carlsbad, CA). Ammonium hydroxide catalog# A669-500 was purchased from Fisher Scientific (Hampton, NH). Penicillin-Streptomycin catalog# P4458, Potassium chloride solution catalog# P9327, Uridine catalog# U3003, 5-fluoro-2′-deoxyuridine catalog# 343333, L-15 Medium (Leibovitz) catalog# L5520, and Minimum Essential Medium Eagle catalog# M5650 were purchased from Sigma-Aldrich (St. Louis, MO).

2.2. Cell culture

SCG were dissected from neonatal (P_0 or P_1) wild-type C57Bl/6 mice and were subjected to enzymatic and mechanical treatments to dissociate neurons as previously described [32]. Briefly, SCG were treated for 30 min with type 4 collagenase (1mg/mL in L-15 medium) followed by a 30 min treatment with 0.05% Trypsin-EDTA at 35° C. The ganglia were then triturated, and the cell suspension filtered through a size 3-20/14 Nitex filter (Tetko Inc.) to separate debris from dissociated neurons. Cells from 0.5 ganglion were cultured on air-dried ammoniated, collagenized 24-well tissue culture plates (Costar) for cell survival assays, and on #1 glass coverslips (Electron Microscopy Sciences, catalog# 72223-01) for confocal and fluorescence microscopy experiments. For immunoblot experiments, 2.5 - 3 ganglia were plated on 35mm plastic tissue culture dishes (Falcon). All cultures were maintained in medium consisting of Eagle's minimum essential medium with Earle's salts supplemented with 10% heat-inactivated fetal bovine serum (Gibco), 100 U/ml penicillin, 100 μg/ml streptomycin, 20 μM 5-Fluoro-2′-deoxyuridine, 20 μM uridine, 1.4mM L-glutamine (Gibco), and 50 ng/ml 2.5S NGF. Cultures were maintained in the above medium at 37°C in an incubator having an atmosphere of 95% air and 5% CO_2 for 5-7 days before conducting experiments. Apoptosis was initiated by replacing this medium with the same medium lacking NGF and containing a goat anti-mouse NGF-neutralizing antibody as described [21,23,32,34]. For chronic depolarization experiments, cultures were maintained in NGF-deprived medium containing varying amounts of KCl.

2.3. Cell survival assay

For all survival assays, neurons were grown in 24 well plastic tissue culture plates and maintained in NGF-containing medium for 7 days with a refreshment of the medium every 2 days. Either cultures were then kept in this medium or had their media replaced with the same medium containing no NGF with or without added KCl in addition to various experimental treatments. At the end of treatment, all cultures were switched back to NGF-containing medium for another 5 days. They were then washed 2X with ice-cold phosphate-buffered saline (PBS) (GE Healthcare HyClone, catalog# SH30256.01) and fixed with 4% paraformaldehyde for 30 min at room temperature. After washing with PBS, cells were stained for Nissl substances using 0.1% crystal violet (Fisher Scientific, catalog# C581-25) for 30 min at room temperature to enhance visualization. Neurons from all survival experiments were counted blinded. Details of this method and how neurons were distinguished from other cells in cultures are described elsewhere [32].

2.4. Microscopy

All confocal microscopy experiments were performed using a Nikon C1 laser scanning confocal microscope (Melville, NY) mounted on a Nikon Eclipse TE 300 inverted microscope. Neurons were chosen randomly by phase-contrast microscopy using a 60X-plan oil immersion lens (numerical aperture, 1.4) and then scanned by the confocal microscope. All confocal settings including laser power, confocal pinhole size, and photomultiplier gain were maintained at constant levels during an experiment. Fluorescence microscopy was also done with a Nikon TE300 inverted microscope. The light was provided by a xenon lamp and images were acquired by a cooled CCD camera

(MicroMAX; Princeton Instruments, Trenton, NJ) controlled by MetMorph software (Molecular Devices; San Jose, CA).

2.5. RS measurement

The membrane-permeant, non-fluorescent, redox-sensitive dye CM-H_2DCFDA was used to detect intracellular levels of ROS and other RS [35,36]. This dye becomes trapped inside cells as a result of esterase-induced cleavage of its acetate groups leading to the binding of a thiol-reactive chloromethyl group to cellular thiols. The dye becomes intensely fluorescent upon oxidation. CM-H_2DCFDA is not significantly oxidized by superoxide but can serve as an indirect indicator of its production since both hydrogen peroxide (H_2O_2) and peroxynitrite lie downstream of superoxide [37]. The staining protocol of rat and mouse sympathetic neurons was extensively characterized in our previous studies [21-23]. In the current study, all cultures were incubated for 20 min at 35°C in the indicated experimental medium containing CM-H_2DCFDA (10 μM). Cells were then washed twice with L-15 medium containing the experimental treatments and left in the last wash for confocal microscopy. CM-H_2DCFDA was excited with the 488 nm line of the confocal laser and the green photomultiplier channel of the confocal microscope was used for image acquisition. All images were acquired at room temperature.

2.6. Glutathione assay

Confocal microscopy was utilized to determine the relative intracellular reduced glutathione (GSH) concentrations using ThiolTracker™ Violet, a dye that becomes intensely fluorescent upon binding to GSH [38]. Neurons were incubated in appropriate experimental medium containing 10 μM ThiolTracker™ Violet for 20 min at 35°C in a

5% CO_2 atmosphere. Cultures were then washed twice with L-15 medium containing the same experimental conditions but lacking the dye. Cultures were left in the second wash for imaging at room temperature. The dye was excited with the 408 nm line of the confocal laser and the green photomultiplier channel of the confocal microscope was used for image acquisition.

2.7. Immunoblotting

Western blotting of BH3-only proteins and the β-tubulin III were performed as described previously with a few modifications [19,22]. Briefly, neurons (from 2.5-3 ganglia) cultured on 35mm plastic tissue culture dishes were washed once with ice-cold PBS, incubated on ice for 10 min with ice-cold lysis RIPA buffer (150 mM NaCl, 1% NP-40, 0.5% sodium deoxycholate, 0.1% SDS, 50 mM Tris-HCl, 5mM EDTA pH 8.0, and protease inhibitor cocktail). The cells were then scraped off the dishes, transferred into 1.5 ml microfuge tubes, and kept on ice for another 20 min with occasional vortexing for homogenization. Cells were spun to pellet debris at 10,000 RPM for 10 min at 4^{o} C, and the supernatant was transferred to new 1.5 ml microfuge tubes. Protein concentrations were measured using RIPA buffer-compatible Pierce BCA Protein Assay Kit (Thermo Scientific, catalog# 23227). After boiling for 10 min, samples were returned to room temperature, and 15-20 µg of protein were loaded into wells of 12% Tris-Glycine precast gels (VWR, catalog# 81002-004). Gels were run for 90 min at 100V. After separation, denatured proteins were transferred onto polyvinylidene fluoride membranes (Millipore, catalog# IPVH00010) for 90 min at a constant voltage of 300 mA at 4^{o} C. Membranes were blocked in 1X Tris-buffered saline (TBS) containing 0.1% Tween 20 (TBS-T) (Fisher Scientific, catalog# BP337-500) and 5% dry milk (Lab Scientific Inc., catalog# M-0841) for 60 min at room temperature. After three washes with 1X TBS-T (5 min each), membranes were incubated overnight at 4°C with primary antibodies diluted in 2% w/v Bovine Serum Albumin (BSA) in 1X TBS-T as follows: Bim (C34C5) Rabbit mAb (1:1000 dilution; Cell Signaling, catalog# 2933), Puma (E1S7A) Rabbit mAb (Rodent Specific) (1:1000 dilution; Cell Signaling, catalog# 14570), Anti-Bmf Rabbit mAb (1:1000 dilution; Abcam, catalog# ab181148), Anti-Hrk polyclonal Ab (5µL/mL; Thermo Scientific, catalog# PA1-86773), and β-tubulin III Rabbit polyclonal Ab (1:1000 dilution; Thermo Scientific, catalog# PA1-41331). After three washes with 1X TBS-T (5 min each), membranes were incubated for 90 min at room temperature in HRP-linked Anti-rabbit IgG Antibody (Cell signaling, catalog# 7074) diluted in 2% w/v dry milk in 1X TBS-T at dilutions of 1:2000 for BH3-only proteins and 1:4000 for β-tubulin III control. The membranes were incubated for 2 min in SignalFire™ ECL Reagent (Cell Signaling, catalog# 6883) and proteins were detected using a Fluorchem HD2 chemiluminescence imaging system (Protein Simple, San Jose, CA). Blots were quantified with Image J (National Institutes of Health).

2.8. Immunocytochemistry

Immunocytochemical staining of cytochrome *c* was performed as previously described with minor optimization [21-23]. After fixing cells for 30 min at 4°C with 4% freshly made paraformaldehyde in PBS (PH 7.2) and washing three times with Tris-buffered saline (100 mm Tris-HCl, 0.9% NaCl, and pH 7.6), cells were incubated for 1 hour at room temperature in Tris-buffered saline containing 0.3% Triton X-100 and 5% BSA (blocking buffer). Cultures were then incubated overnight at 4°C in the blocking solution containing the anti-cytochrome *c* mouse monoclonal antibody (clone 6H2.B4) at a dilution 1:500 (Cell Signaling, catalog# 12963). Following three times wash with a blocking buffer, cultures were incubated for 4 hours at 4°C in the blocking solution containing an Alexa Fluor-conjugated Rabbit Anti-mouse secondary antibody (4 μg/mL). Cultures were then washed twice with Tris-buffered saline, left in this medium, and viewed by confocal microscopy.

We implemented the same criteria of scoring the cytochrome *c* redistribution inside the cells as described previously [21-23]. Briefly, neurons were scored as having retained cytochrome *c* in mitochondria when mitochondrial punctate staining was observed. Neurons showing faint, homogenous, or no staining were scored as having their mitochondrial cytochrome *c* released and rapidly subjected to cytoplasmic degradation [12,39].

2.9. Statistical analysis

Tests for normality of each dataset were performed before choosing an appropriate statistical analysis method. Based on the data distribution, statistical comparisons were made by Kruskal Wallis one-way ANOVA on ranks, followed by Dunn's multiple comparisons *post hoc test*, unless otherwise indicated. Differences were considered significant if p was < 0.05. All error bars are ± SEM. Statistical analysis and graph preparations were done with SigmaPlot 11.1 (Systat Software, Inc., San Jose, CA, USA).

3. Results

3.1. Chronic depolarization-induced survival of mouse sympathetic neurons

Sympathetic neurons derived from rat and mouse SCG undergo apoptotic death in cell culture within 48-72 hours after NGF withdrawal [5,8,10,14]. This death is blocked by chronic depolarization of membrane potential induced by exposure to culture media containing elevated $[K^+]_E$. To determine the optimal survival-promoting $[K^+]_E$ we deprived mouse sympathetic neurons of NGF 5-7 days after plating and kept them in media containing different $[K^+]_E$ for another 48 hours. Figure 3.1A, B shows the morphology and concentration-dependent enhancement of survival of NGF-deprived neurons exposed to elevated $[K^+]_E$. Similar to a previous report [14], mouse SCG neurons showed maximum survival when chronically depolarized with 40 mM K^+_E. All of the subsequent experiments in this study were conducted using this concentration.

3.2. Chronic depolarization suppressed induction of Bim_{EL} but not other BH3-only proteins

Increased levels of BH3-only proapoptotic proteins occurs in several models of apoptotic neuronal death, including that caused by depriving sympathetic neurons of NGF [15-18, 20]. We hypothesized that chronic membrane depolarization promotes survival of NGF-deprived SCG neurons by suppressing the induction of BH3-only proteins. To test this hypothesis, we utilized immunoblotting to assess the protein levels of BH3-only proteins known to be expressed in sympathetic neurons. These included the extra-long splice variant of Bim (Bim_{EL}), Puma, and Bmf [15-20, 40]. Elevated transcription of Dp5/Hrk has also been described in NGF-deprived SCG neurons [19,20, 41-43]. Neurons were deprived of NGF, deprived of NGF and chronically depolarized with 40 mM K^{+}_{E}, or maintained in NGF-containing medium from the time of plating. Different neuronal populations such as sympathetic neurons, cerebellar granule neurons, and dorsal root ganglion neurons predominantly express the Bim_{EL}, but not the other two variants Bim_{S} and Bim_{L}, after an apoptotic signal [16,17]. In accordance with previous studies, approximately 6.5-12 fold increases in the protein level of Bim_{EL} was detected in NGF-deprived neurons when compared with NGF-maintained control (Fig. 3.2A). The induction of Bim_{EL} started as early as 12 hours after NGF withdrawal and was sustained throughout the period of death. To circumvent losing cells at longer time points (24-48 hours), we prevented NGF-deprived cells from dying using the broad-spectrum caspase inhibitor boc-aspartyl (OMe)-fluoromethylketone (BAF) (50 μM). The presence or absence of the caspase inhibitor BAF did not interfere with the time, or the extent of Bim_{EL} induction in NGF-deprived neurons. NGF-deprived cells maintained in culture medium containing 40 mM K^{+}_{E} had Bim_{EL} protein levels almost identical to that of neurons maintained in an NGF-containing medium ($p > 0.05$) indicating that chronic depolarization profoundly suppressed upregulation of this protein. The BH3-only family member, Puma, was significantly induced in both NGF-deprived and chronically depolarized neurons relative to the control cells ($p < 0.05$; Fig. 3.2B). No significant changes ($p > 0.05$) were observed of Bmf protein expression (Fig. 3.2C). Dp5/Hrk protein levels were not detected in the treated sympathetic neurons (Fig 3.2D). To omit the possibility that the undetected Dp5/Hrk protein in neurons was due to a dysfunctional antibody, we treated two different prostate cancer cell lines with DMSO and

Staurosporine (SS) for 24 hours. Figure 3.2D shows that both treatments cause induction of the BH3-only proteins Bim_{EL} and Dp5/Hrk. Sympathetic neurons from mice in which Bim_{EL} has been deleted die only slightly more slowly than do wild-type neurons suggesting that Bim_{EL} merely accelerates death [17]. The expression of none of the other BH3-only proteins expressed in these cells was affected by elevated $[K^+]_E$. Therefore, because elevated $[K^+]_E$ causes long-term survival of mouse sympathetic neurons in culture [32] it seems unlikely that suppressive effect of chronic depolarization on BH3-only protein levels can explain the survival-promoting ability of elevated $[K^+]_E$..

3.3. Chronic depolarization blocked cytochrome c release from mitochondria of NGF-deprived neurons

Unlike the time-courses of rescue after NGF withdrawal by other neuroprotective agents, such as the protein synthesis inhibitor cycloheximide [5], rescue of NGF-deprived rat sympathetic neurons by chronic depolarization has an almost identical rescue time-course to that of rescue caused by readdition of NGF to culture medium [32]. To examine how similar the rescue of NGF-deprived mouse sympathetic neurons by chronic depolarization is to that of rescue by NGF readdition, we deprived mouse SCG neurons of NGF and then re-added media containing either NGF or 40 mM K^+_E at subsequent times (Fig. 3.3A). While addition of elevated $[K^+]_E$ to culture medium was not as effective as NGF readdition in stopping further death of NGF-deprived neurons, it did follow the same time-course of rescue as that of NGF readdition. The rescue time-courses were not statistically different ($p > 0.05$). These data suggest that similar antiapoptotic pathways may be stimulated by both NGF and chronic depolarization.

The release of cytochrome *c* from mitochondria is the principal means by which sympathetic neurons undergo apoptotic death following NGF deprivation [10,12,21,44]. Re-addition of NGF to the NGF-deprived sympathetic neurons rapidly blocks further cytochrome *c* release and death [14,21,23,44]. Because of the similarity in the survival time-courses of NGF and high $[K^+]_E$ rescued neurons, we examined the effects of chronic membrane depolarization on the cytochrome *c* redistribution in the NGF-deprived mouse SCG neurons. We used immunocytochemistry in conjunction with fluorescence microscopy to determine the time-course of cytochrome *c* redistribution over a 48-hour period. Figure 3.3B illustrates the two main criteria used to score cytochrome *c* compartmentalization in these neurons: 1, punctate staining indicated that cytochrome *c* was retained in mitochondria and 2, faint staining indicated that cytochrome *c* had been released from mitochondria followed by cytoplasmic degradation [10,12,21-24]. Using these criteria, in agreement with our previous studies, we found that cytochrome *c* redistribution starts as late as 18 hours post-NGF deprivation (Fig. 3.3C) [21,22]. Following NGF withdrawal, approximately 50% of neurons had released cytochrome *c* by 24 hours, and almost all neurons (93.2 ± 1.5 %) had lost mitochondrial cytochrome *c* by ~36 hours. We used the broad-spectrum caspase inhibitor, BAF, to prevent cell loss at extended time points. The presence or absence of (50µM BAF) did not alter the rate, nor the extent of cytochrome *c* redistribution in NGF-deprived neurons ($p > 0.05$) suggesting that caspase activity was not required for cytochrome *c* release. Approximately all neurons maintained in 40 mM K^+-containing medium retained cytochrome *c* in their mitochondria up to 48 hours after NGF deprivation (89.4 ± 5 %).

3.4. Chronic depolarization rapidly blocked increased RS levels in NGF-deprived sympathetic neurons

A Bax-dependent pro-oxidant state appears to serve as a pre-requisite for cytochrome *c* release from the mitochondria intermembrane space into the cytoplasm during the apoptotic death of NGF-deprived rat and mouse sympathetic neurons [21,22,24]. Re-addition of NGF to NGF-deprived rat [45] and mouse [23] sympathetic neurons rapidly suppresses the elevated mitochondria-derived RS levels and inhibits further release of cytochrome *c*. Furthermore, block of the antioxidant effect of NGF allows the cytochrome *c* release into the cytoplasm of the NGF-maintained neurons. To explore a possible antioxidant mechanism by which chronic depolarization blocked cytochrome *c* release in NGF-deprived neurons, we utilized the fluorescent redox-sensitive dye CM-H_2DCFDA. The use of this dye has been well characterized in the determination of RS and other levels in sympathetic neurons [21-24, 46,47]. Figure 3.4 A,B shows an ~10-12 fold increase in CMH_2DCFDA intensity in mouse sympathetic neurons deprived of NGF for 24-48 hours indicating dye oxidation by elevated RS levels in them. Chronically depolarized neurons showed a significant reduction (by ~ 6.3-8 fold) in RS levels when compared to NGF-deprived ones at the same time-points ($p < 0.001$). To explore how fast chronic depolarization reduced the RS levels in the NGF-deprived neurons, we deprived neurons in cell culture of NGF for 20 hours and then exposed them to a depolarizing medium (40 mM K^+_E) during the 20 min period of CM-H_2DCFDA dye loading. Figure 3.4 C shows that high $[K^+]_E$-induced chronic depolarization caused a rapid and potent suppression (~80%) of the redox dye intensity ($p < 0.05$) similar to that resulting from exposure to the membrane-permeant form of the antioxidant GSH, GSH ethyl ester. We previously demonstrated that NGF readdition to NGF-deprived mouse SCG neurons rapidly activates the GSH-antioxidant pathway [23] in them and presented evidence that this activation is important for preventing cytochrome *c* release. The suppression of cytochrome *c* release and RS by elevated $[K^+]_E$ suggested that a similar mechanism may underlie the effect of high $[K^+]_E$ on these two events.

3.5. Evidence that chronic depolarization promoted survival of NGF-deprived neurons by activating the GSH antioxidant pathway

We previously reported [21] that the protein synthesis inhibitor, cycloheximide (CHX), and the antioxidant, N-acetyl-l cysteine (L-NAC), block the increased RS, cytochrome *c* release, and apoptotic death of NGF-deprived rat sympathetic neurons by increasing cellular GSH concentration. Similar effects were observed when NGF-deprived mouse sympathetic neurons were re-exposed to NGF [23] suggesting the crucial role of glutathione redox cycling in the survival of these neurons. To test whether the GSH antioxidant pathway was crucial for the antiapoptotic effect of chronic depolarization we deprived neurons of NGF for 20 hours and then incubated them with either a NGF-containing medium or a depolarizing medium (40 mM K^+_E) for 20 min. Neurons were then stained with a GSH-sensitive dye, ThiolTracker™ Violet; [38]. Figure 3.5A shows sympathetic neurons stained with ThiolTracker™ Violet under different treatment conditions. In agreement with our previous work [23], re-addition of NGF to the NGF-deprived neurons significantly increased dye intensity indicating increased GSH (Fig. 3.5 A,B; $p < 0.05$ compared with NGF-maintained neurons from time of plating). The intracellular GSH concentration was significantly boosted when NGF-deprived neurons were acutely depolarized with elevated $[K^+]_E$ (Fig. 3.5 A,B; $p < 0.05$ by

ANOVA). These data, taken together with those in Figure 3.4, suggest that chronic membrane depolarization rapidly detoxifies RS by upregulating a key antioxidant, GSH.

To determine whether blocking this upregulation would increase inhibited RS caused by readditon of NGF or elevated $[K^+]_E$ to NGF deprived cultures, we first exposed cells for 10 hours to the GSH synthesis inhibitor L-buthionine-[S,R]-sulfoximine (BSO), an irreversible inhibitor of λ-glutamylcysteine synthetase, a key enzyme in the GSH biosynthesis pathway [48]. We previously demonstrated that this treatment significantly lowers GSH concentration in these cells [23]. The BSO pretreatment prevented both the NGF readdition and high $[K^+]_E$ addition from blocking the RS increase after NGF withdrawal consistent with both the effect of both effects being mediated by increased GSH and/or activation of the GSH redox cycling pathway (Fig. 3.5C).

To determine whether chronically depolarized neurons require increased GSH to resist apoptotic death following NGF-withdrawal, we assessed survival of NGF-maintained, NGF-deprived, and chronically depolarized neurons in the presence or absence of BSO. Treatment with BSO (200 μM) for 48 hours almost completely prevented the ability of chronic membrane depolarization to block death of NGF-deprived neurons, suggesting the importance of GSH (Fig. 3.5D). In an attempt to ascertain whether BSO treatment prevented the survival of NGF-deprived, chronically depolarized neurons by inhibiting GSH synthesis rather than non-specific toxic effects, we assessed survival of BSO-treated neurons in the presence of the membrane-permeant GSH ethyl ester (10 mM). Treatment with GSH ethyl ester completely prevented the apoptotic death of the BSO-treated, chronically depolarized neurons (Fig. 3.5 D). These data indicate that the BSO-induced death was due to a reduction in GSH concentrations rather than non-specific toxicity. The data further indicate that chronic membrane depolarization of sympathetic neurons likely requires activation of GSH antioxidant defenses to resist apoptotic death following NGF withdrawal.

Discussion

The phenomenon that elevated concentrations of potassium ($[K^+]_E$) maintain neuronal survival in the absence of neurotrophic factors has been documented since the early 1970s [49]. Evidence suggests that such high $[K^+]_E$ mediates depolarization-enhanced survival of different types of neurons, including neurotrophic factor-deprived neurons, presumably by mimicking the effects of the naturally occurring electrical activity *in vivo* [28-32]. The molecular mechanism(s) by which chronically depolarized neurons resist apoptotic death following neurotrophic factor withdrawal remains mostly unknown. We conducted a study of the effects of chronic membrane depolarization on several hallmarks of the apoptotic pathway, including the upregulation of BH3-only proapoptotic proteins and cytochrome *c* redistribution. Additionally, we explored the role of the cellular redox status of NGF-deprived mouse sympathetic neurons when chronically depolarized with elevated $[K^+]_E$.

Elevated $[K^+]_E$ suppressed the induction of proapoptotic protein Bim, but not other BH3-only proteins. Despite the induction of the proapoptotic protein Puma, immunochemical studies revealed that ~90% of chronically depolarized sympathetic neurons had retained cytochrome *c* in their mitochondria for as long as 48 hours following NGF withdrawal. These data suggest that other mechanisms by which chronic membrane depolarization promotes long-term survival of NGF-deprived sympathetic neurons may exist. We previously reported [21] that the cellular redox state regulates cytochrome *c* redistribution during the apoptotic death of NGF-deprived neurons. We performed a confocal microscopic study to compare the redox state of NGF-deprived and chronically depolarized neurons using the redox-sensitive dye CMH_2DCFDA. Maintaining neurons from the time of withdrawal in a depolarizing medium resulted in a ~6-8–fold reduction in CMH_2DCFDA intensity. Acute application of the depolarizing medium to cultures deprived of NGF for 20 hours also caused ~80% suppression of the increase in dye intensity in cells deprived of NGF.

The most likely antioxidant mechanism underlying the suppression of these RS in the NGF-maintained sympathetic neurons is the glutathione redox cycling pathway [21,23]. We used confocal microscopy in conjunction with the GSH-sensitive dye ThiolTracker™ to investigate whether chronically depolarized neurons activate this pathway to detoxify the rising RS following NGF withdrawal. Interestingly, we found that $[K^+]_E$-induced chronic depolarization rapidly increases the GSH-sensitive dye intensity. To explore the possibility that chronic depolarization prevents neuronal death via an antioxidant mechanism, we treated NGF-deprived neurons with depolarizing culture medium. BSO was included in the medium of some cultures to block GSH synthesis. As anticipated, BSO treatment prevented the ability of chronically depolarized neurons to survive NGF deprivation. Addition of a membrane-permeant form of GSH, GSH ethyl ester, restored the survival capacity of the chronically depolarized, BSO-treated neurons. We present evidence that the antioxidant activity of glutathione mediates chronic depolarization-enhanced survival of NGF-deprived mouse sympathetic neurons.

The role of BH3-only proapoptotic proteins in depolarization-induced suppression of apoptosis

De novo protein synthesis upstream of Bax translocation and release of mitochondrial cytochrome *c* is required for the apoptotic death of NGF-deprived neurons [4,21,34]. Depriving sympathetic neurons of NGF transcriptionally upregulates multiple redundant members of the BH3-only proapoptotic family proteins, including Bim, Puma, Bmf, and Dp5/Hrk [15-20,40-43]. Our study shows that maintaining NGF-deprived mouse sympathetic neurons in a depolarizing medium containing 40mM K^+ significantly suppresses the induced Bim_{EL} to a level similar to that of NGF-maintained cells. Neither of the other BH3-only family members, Bmf and Dp5/Hrk, were affected by the depolarization. Interestingly, the cellular expression of the proapoptotic protein Puma increases rather than decreases in K^+-depolarized neurons. Despite the upregulation of Puma, depolarized neurons retained cytochrome *c* in their mitochondria for extended periods following NGF withdrawal. At least in sympathetic neurons, it is likely that multiple members of the BH3-only family proteins must be simultaneously upregulated to achieve efficient activation of the intrinsic pathway of developing neurons following neurotrophic factor withdrawal. Whitfield *et al*., 2001 reported that sympathetic neurons from $Bim^{-/-}$ mice die more slowly than do wild-type neurons [17]. Similarly, deletion of Dp5 delayed but did not prevent apoptotic death of NGF-deprived sympathetic neurons [42]. In addition, cerebellar granule neurons derived from $Bim^{-/-}$, $Puma^{-/-}$ double-knockout mice displayed better resistance to apoptotic death induced by KCl deprivation than that achieved by deleting individual proteins [50]. The probability that multiple BH3-only proteins are required to execute Bax translocation to the mitochondrial outer membrane is supported by the observation that, unlike knocking out individual BH3-only proteins, Bax deletion prevented, rather than merely delayed, the NGF withdrawal-induced death of sympathetic neurons [11]. Recent studies have demonstrated that mature sympathetic neurons efficiently resist apoptotic death following NGF withdrawal by engaging different mechanisms to downregulate multiple members of the BH3-only proteins [19,51]. Chronically depolarized young sympathetic neurons likewise resist apoptotic death for extended periods following NGF withdrawal [32]. Therefore, the suppression of only one BH3-only protein does not explain how chronic depolarization promotes long-term survival.

The role of RS and glutathione redox cycling in depolarization-promoted survival of NGF-deprived mouse sympathetic neurons

Compelling evidence implicates electron leakage of the mitochondrial electron transport chain as a primary source of elevated levels of $O_2^{\cdot -}$ and other downstream RS in apoptotic sympathetic neurons [52]. As reported previously [22,24], rat-derived sympathetic neurons displayed a Bax-dependent pro-oxidant state long before any of the cells commit to death. The ability of H_2O_2 to cause rapid redistribution of cytochrome *c* from mitochondria into the cytoplasm of NGF-maintained neurons further suggests that increased RS in NGF-deprived neurons may serve as a pre-requisite for this release [21]. The significant rise in mitochondria-derived RS and the subsequent cytochrome *c* redistribution of dying neurons were rapidly blocked by NGF re-addition [23,45]. Since re-addition of both NGF and elevated $[K^+]_E$ showed nearly identical abilities to rescue dying rat [32] and mouse sympathetic neurons following NGF withdrawal, we hypothesized that high [K+]E-induced depolarization prevents the pro-oxidant state and thus cytochrome c release.

In agreement with our previous findings [21], NGF withdrawal triggers the induction of mitochondrial RS long before any cytochrome *c* redistribution occurs. Our data shows that 18 hours post-deprivation, neurons experience an ~8-fold rise in their RS levels, whereas none had released any cytochrome *c* from their mitochondria by that time. Elevated $[K^+]_E$ from the time of deprivation efficiently prevented NGF-deprived neurons from entering a pro-oxidant state for up to 48 hours post-deprivation, evidently by reducing the intensity of the redox-sensitive dye CMH_2DCFDA.

Glutathione oxidation is the central mechanism by which neurons, and most other cell types, detoxify rising RS [37,47]. We demonstrated previously that increasing the GSH concentration can decrease RS levels in NGF-deprived rat sympathetic neurons [21,23]. Here we report that acute depolarization of NGF-deprived mouse sympathetic neurons showed significant reduction in the CMH_2DCFDA dye intensities, similar to neurons treated with a cell-permeant form of GSH, suggesting the involvement of GSH redox cycling in the depolarization-prevented pro-oxidant state. Activation of glutathione redox cycling rather than reducing mitochondrial RS production may account for the rapid attenuation of the CMH_2DCFDA dye intensity by elevated $[K^+]_E$. Similar observations were reported where re-addition of NGF to cultures of NGF-deprived rat and mouse SCG sympathetic neurons rapidly suppressed only the elevated levels of H_2O_2-associated RS, as detected with dihydrorhodamine [45] and CM-H_2DCFDA [23], respectively. Confocal microscopy in conjunction with a mitochondria-targeted, $O_2^{\cdot-}$-sensitive dye, MitoSOX™ [53-55], revealed that the mitochondrial $O_2^{\cdot-}$ production did not change upon re-addition of NGF to the NGF-deprived mouse sympathetic neurons [23]. To test this possibility, we compared GSH levels in NGF-deprived mouse sympathetic neurons following acute re-exposure to NGF and depolarizing medium containing high $[K^+]_E$. The early time point (20 hours) was carefully chosen to avoid complications from loss of cells caused by apoptosis that might interfere with the readouts. In addition, measuring RS levels or GSH concentrations prior to cytochrome *c* release would eliminate any impacts of some key elements downstream of cytochrome *c* release (e.g., caspases) on the RS levels and, ostensibly, GSH concentrations [7,21-24,56,57]. Because the biochemical assays for GSH quantification requires a large number of dissected neurons, we utilized the more feasible approach of detecting relative intracellular GSH concentrations by using fluorescence microscopy in conjunction with ThiolTracker™ Violet, a sensitive dye that becomes intensely fluorescent upon binding to reduced GSH [38]. Similar to NGF, depolarization with elevated $[K^+]_E$ increases the intracellular GSH concentration of NGF-deprived neurons. To ascertain whether GSH upregulation is necessary for the depolarization-suppressed pro-oxidant state, and thus apoptotic death of the NGF-deprived neurons, we treated some cultures with the GSH biosynthesis inhibitor, BSO. We present evidence that GSH inhibition nearly abolishes the ability of elevated $[K^+]_E$ to suppress RS and maintain survival of NGF-deprived neurons. Addition of an extracellular GSH recovers the ability of $[K^+]_E$ to promote survival, even in the presence of the GSH inhibitor. These data suggest that chronic membrane depolarization prevents pro-oxidant status by rapidly upregulating a key antioxidant, GSH.

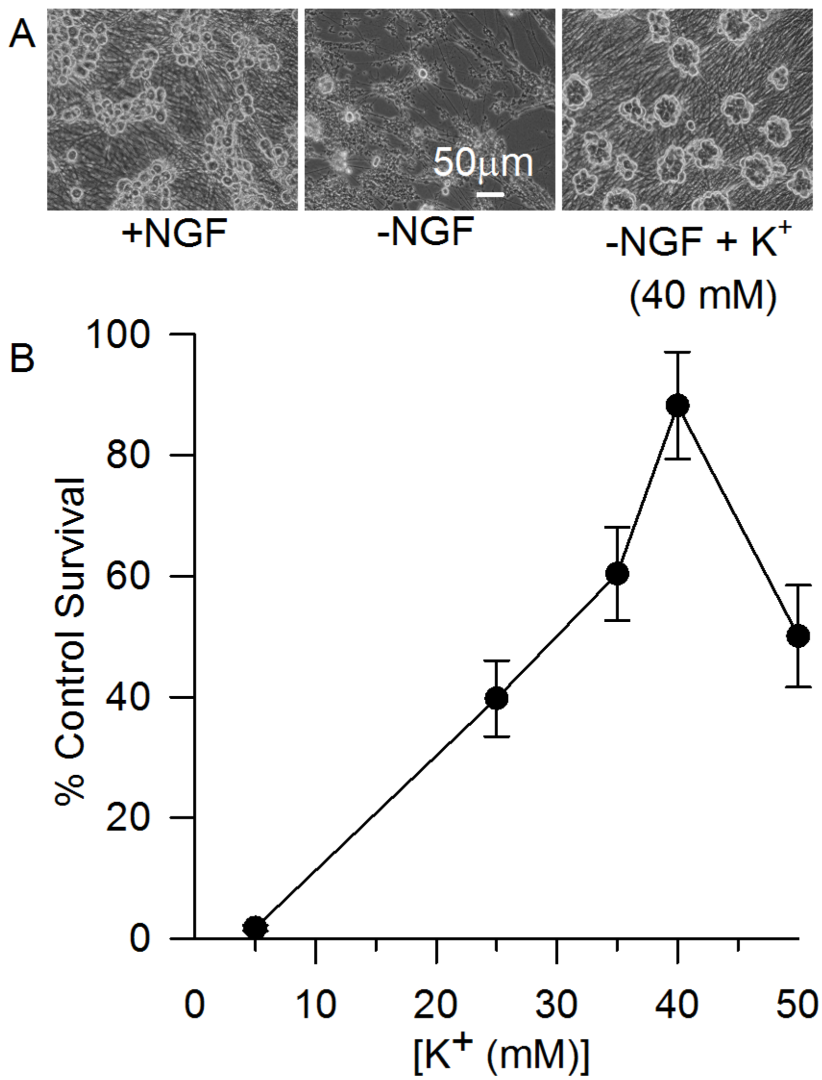

FIG. 3.1. Effects of elevated $[K^+]_E$ on the survival of NGF-deprived mouse SCG neurons. (A) Phase contrast photomicrographs showing the morphology and survival of NGF-maintained, NGF-deprived, and NGF-deprived SCG neurons exposed to the 40 mM K^+_E at 48 hours post-treatment. (B) Dose-response effect of $[K^+]_E$ on survival of NGF-deprived neurons. Cultures of mouse SCG neurons were maintained in NGF-containing medium for 7 days post-plating. On day 7, neurons were deprived of NGF and

maintained in media containing the indicated $[K^+]_E$ for the next 48 hours. All cultures were then switched back to NGF-containing medium containing 5 mM K^+ for another 5 days. Fourteen days after plating, neurons were fixed, stained with crystal violet and survival assessed by blinded counting of cells based on their morphology. Neurons showed maximal survival when chronically depolarized with medium containing 40 mM K^+_E. Neuronal survival is shown as a percentage of the average number of neurons in sibling cultures maintained for 14 days after plating in NGF-containing media (N = 8-11 cultures from three separate platings for each $[K^+]_E$).

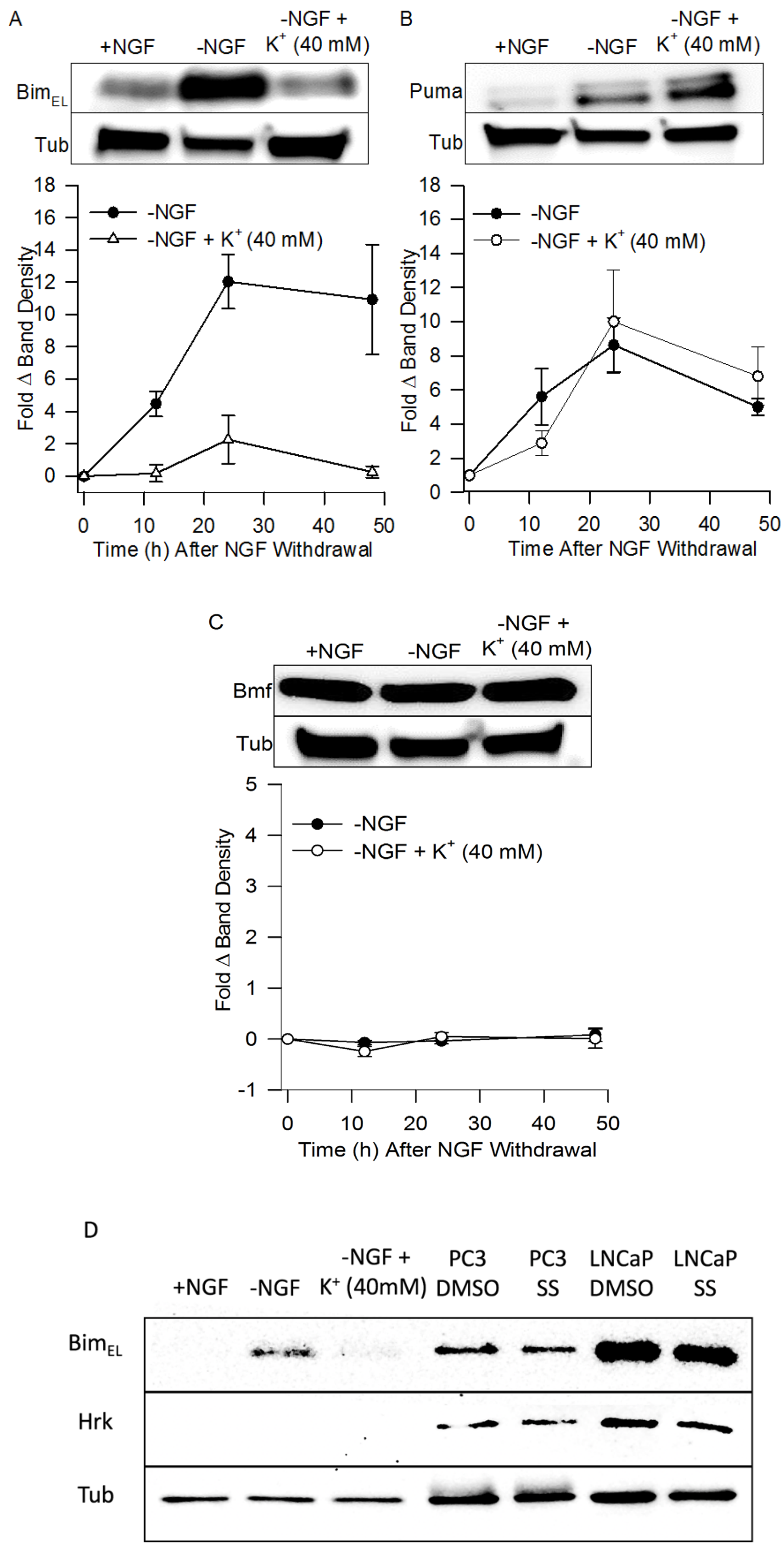
A
+NGF
-NGF
-NGF + K+ (40 mM)
BimEL
Tub
-NGF
-NGF + K+ (40 mM)
Fold Δ Band Density
Time (h) After NGF Withdrawal
B
+NGF
-NGF
-NGF + K+ (40 mM)
Puma
Tub
-NGF
-NGF + K+ (40 mM)
Fold Δ Band Density
Time After NGF Withdrawal
C
+NGF
-NGF
-NGF + K+ (40 mM)
Bmf
Tub
-NGF
-NGF + K+ (40 mM)
Fold Δ Band Density
Time (h) After NGF Withdrawal
D
+NGF
-NGF
-NGF + K+ (40mM)
PC3 DMSO
PC3 SS
LNCaP DMSO
LNCaP SS
BimEL
Hrk
Tub

FIG. 3.2. Elevated $[K^+]_E$ suppressed the induction of Bim_{EL} but not other BH3-only proteins in NGF-deprived mouse SCG neurons. P_0-P_1 neurons from 2.5 - 3 ganglia were maintained in NGF-containing medium for 7 days. On day 7, neurons were either left untreated (+NGF) or deprived of NGF in the absence (-NGF) or the presence of 40 mM K^+_E-containing medium. To prevent the death of neurons, only cells deprived of NGF (-NGF) for more extended periods (24-48 hours) were maintained in a culture medium containing the broad-spectrum caspase inhibitor BAF (50 μM) at the time of NGF withdrawal. Relative protein levels of Bim_{EL}, Puma, Bmf, and Hrk were determined by Western blotting. (A-D) Immunoblots and graphs showing Bim_{EL}, Puma, Bmf, and Hrk levels at different time-points after NGF withdrawal. The loading control is β-tubulin III. Among the BH-3 only proapoptotic proteins tested, only Bim_{EL} was significantly suppressed in NGF-deprived neurons when chronically depolarized by 40 mM K^+_E for 12, 24, and 48 hours, $p < 0.05$ by ANOVA. Chronically depolarized neurons showed an increase rather than a decrease in the BH3-only protein Puma levels, $p < 0.01$ for the 12, 24,48 hours treatments by ANOVA. No changes were observed, Bmf, nor the endogenous levels were detected, Hrk, proteins between the different treatments at the indicated times, $p > 0.05$ by ANOVA. All proteins were normalized first to the amount of control β- tubulin III found in the same cultures and then to the sibling cultures maintained in NGF-containing medium (+NGF) since the time of plating (N = 3-4 from three separate platings).

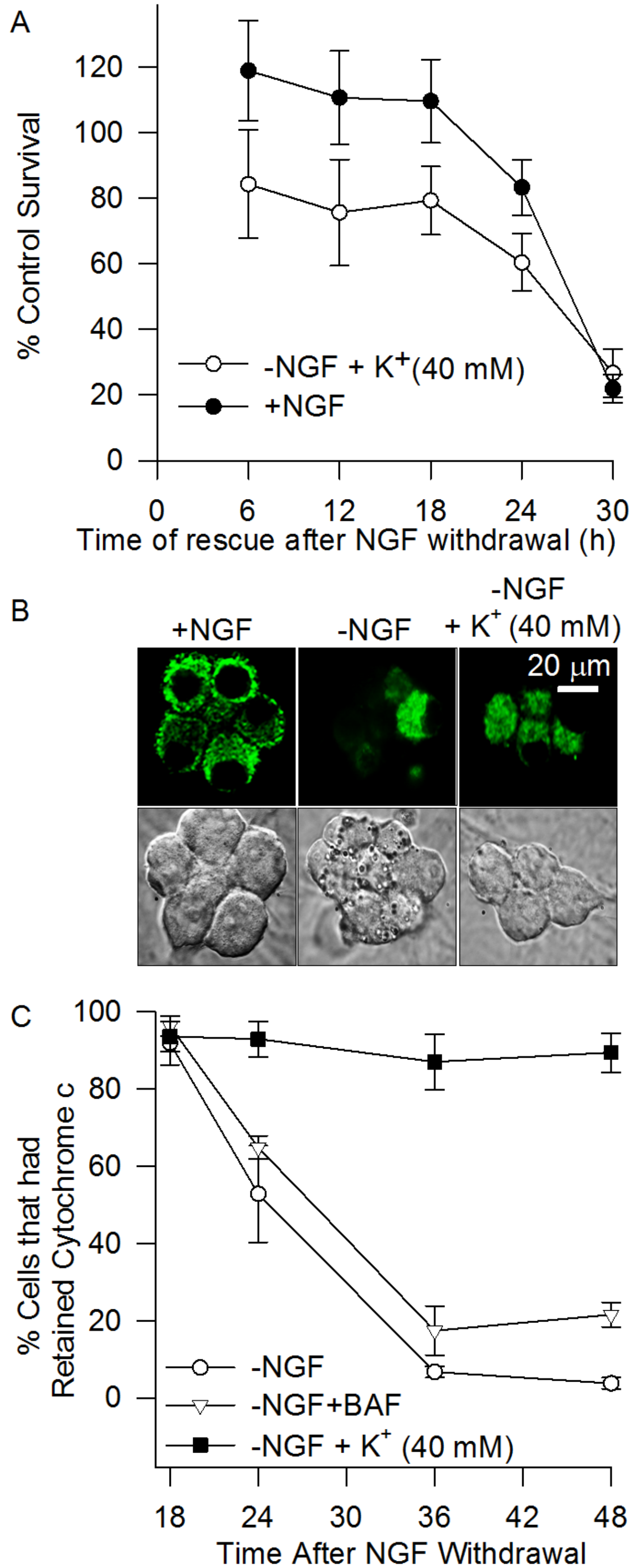
A
% Control Survival
120
100
80
60
40
20
0
-NGF + K+(40 mM)
+NGF
0
6
12
18
24
30
Time of rescue after NGF withdrawal (h)
B
+NGF
-NGF
-NGF
+ K+ (40 mM)
20 μm
C
% Cells that had Retained Cytochrome c
100
80
60
40
20
0
-NGF
-NGF+BAF
-NGF + K+ (40 mM)
18
24
30
36
42
48
Time After NGF Withdrawal

FIG. 3.3. Time-courses of SCG neuronal rescue and cytochrome *c* release by NGF and elevated $[K^+]_E$. (A) High $[K^+_E]$-induced depolarization of plasma membrane rescued mouse SCG neurons over the same time course as NGF. Statistical analysis showed no differences between the time-courses of two conditions ($p > 0.05$ by ANOVA). Neurons were deprived of NGF 7 days after plating. 40 mM K^+_E-containing or NGF-containing media were added to the culture medium at the indicated times after withdrawal and maintained for 48 hours after the last time point. All cultures were then switched back to NGF-containing medium for another 5 days. Neuronal survival was assessed one week after the last rescue time point. Survival is shown as a percentage of the average number of neurons maintained from the beginning in an NGF-containing medium (N = 8-11 cultures from three separate platings). (B) Fluorescent micrographs (top panels) illustrating the criteria used to score cytochrome *c* redistribution by immunocytochemistry. The bottom panels show differential interference contrast images of the same neurons. P_0-P_1 neurons were maintained in an NGF-containing medium for 7 days. On day 7, neurons were either kept in NGF-containing medium (left), deprived of NGF in the presence of broad-spectrum caspase inhibitor BAF (50 μM) at the time of NGF withdrawal (middle), or chronically depolarized with 40 mM K^+_E for 36 hours (right). The cultures were then fixed, immunostained for cytochrome *c*, and observed with a 60X-plan oil immersion lens. The punctate staining indicates that cytochrome *c* was retained in mitochondria, whereas faint staining indicates cytoplasmic degradation of cytochrome *c* after it has been released from mitochondria [21,22]. Unlike NGF-deprived

neurons, cells maintained in NGF- containing medium or chronically depolarized with 40 mM K^+ retained cytochrome *c* in mitochondria. (C) Time courses of cytochrome *c* loss in NGF-deprived and chronically depolarized neurons. Seven days after plating, neurons were either kept in NGF-containing medium, deprived of NGF in the absence or presence of 50 μM BAF at the time of NGF withdrawal, or chronically depolarized with 40 mM K^+_E for 18, 24, 36, and 48 hours. The cultures were then fixed and immunostained for cytochrome *c* at the indicated times. Neurons were scored as having punctate (no cytochrome *c* release) or faint staining (released cytochrome *c*) (N = 24 neurons from 3 separate platings for each time point). Chronic depolarization of NGF-deprived neurons suppressed cytochrome *c* release as long as 48 hours post-deprivation. Chronic depolarization-induced suppression of cytochrome *c* release was statistically different from the other conditions ($p < 0.05$ by ANOVA at 24, 36, and 48 hours).

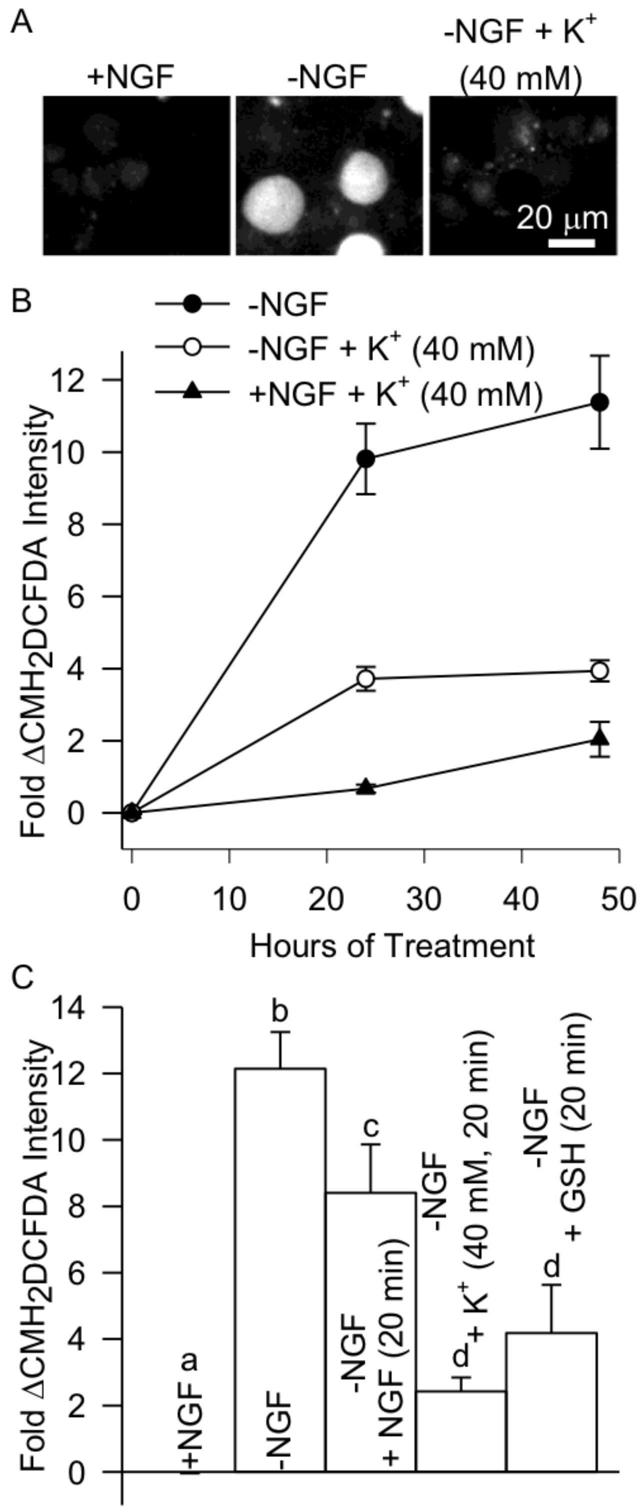
A
+NGF
-NGF
-NGF + K+ (40 mM)
20 μm
B
-NGF
-NGF + K+ (40 mM)
+NGF + K+ (40 mM)
Fold ΔCMH2DCFDA Intensity
0
2
4
6
8
10
12
0
10
20
30
40
50
Hours of Treatment
C
Fold ΔCMH2DCFDA Intensity
0
2
4
6
8
10
12
14
+NGF
a
-NGF
b
-NGF + NGF (20 min)
c
-NGF + K+ (40 mM, 20 min)
d
-NGF + GSH (20 min)
d

FIG. 3.4. K^+-induced depolarization of mouse SCG neurons inhibited elevated levels of RS caused by NGF deprivation. (A) Confocal micrographs of neurons receiving the indicated treatments from the time of NGF deprivation and then incubated with the redox-sensitive dye CM-H_2DCFDA (10 μM, 20 min). The elevated CM-H_2DCFDA intensity in NGF-deprived neurons was suppressed by high $[K^+]_E$. (B) Time-courses of RS production after NGF withdrawal as measured by CM-H_2DCFDA fluorescence. Depolarization with elevated $[K^+]_E$ significantly suppressed RS production ($p < 0.001$ by ANOVA; N = 84-305 neurons from three separate platings). (C) Acute incubation with high $[K^+]_E$-containing medium for 20 min significantly inhibited CM-H_2DCFDA oxidation as did re-addition of NGF for the same period ($p < 0.001$ by ANOVA). The membrane-permeant antioxidant GSH ethyl ester also potently suppressed RS levels (N = 74-368 neurons from three separate platings). CM-H_2DCFDA dye intensities were normalized to the average intensities of sibling cultures maintained in NGF from the time of plating.

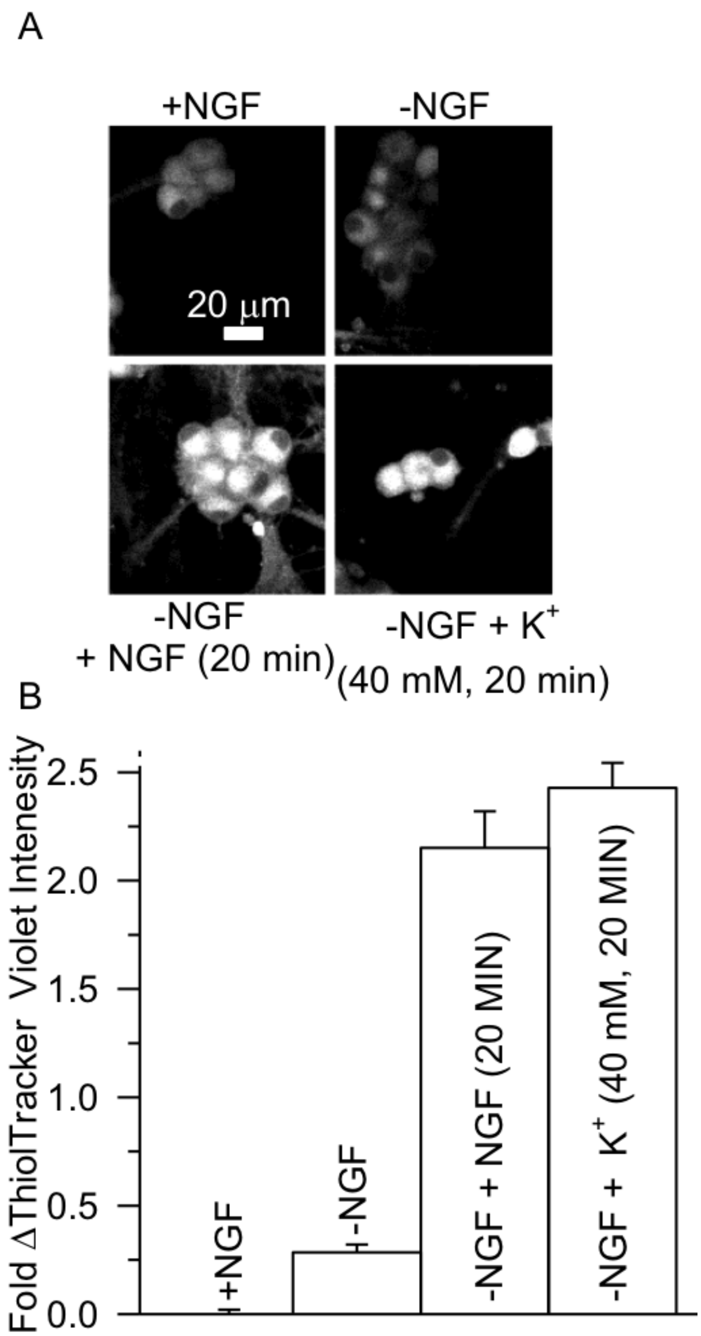
A
+NGF
-NGF
20 µm
-NGF
+ NGF (20 min)
-NGF + K+
(40 mM, 20 min)
B
Fold ΔThiolTracker Violet Intenesity
2.5
2.0
1.5
1.0
0.5
0.0
+NGF
-NGF
-NGF + NGF (20 MIN)
-NGF + K+ (40 mM, 20 MIN)

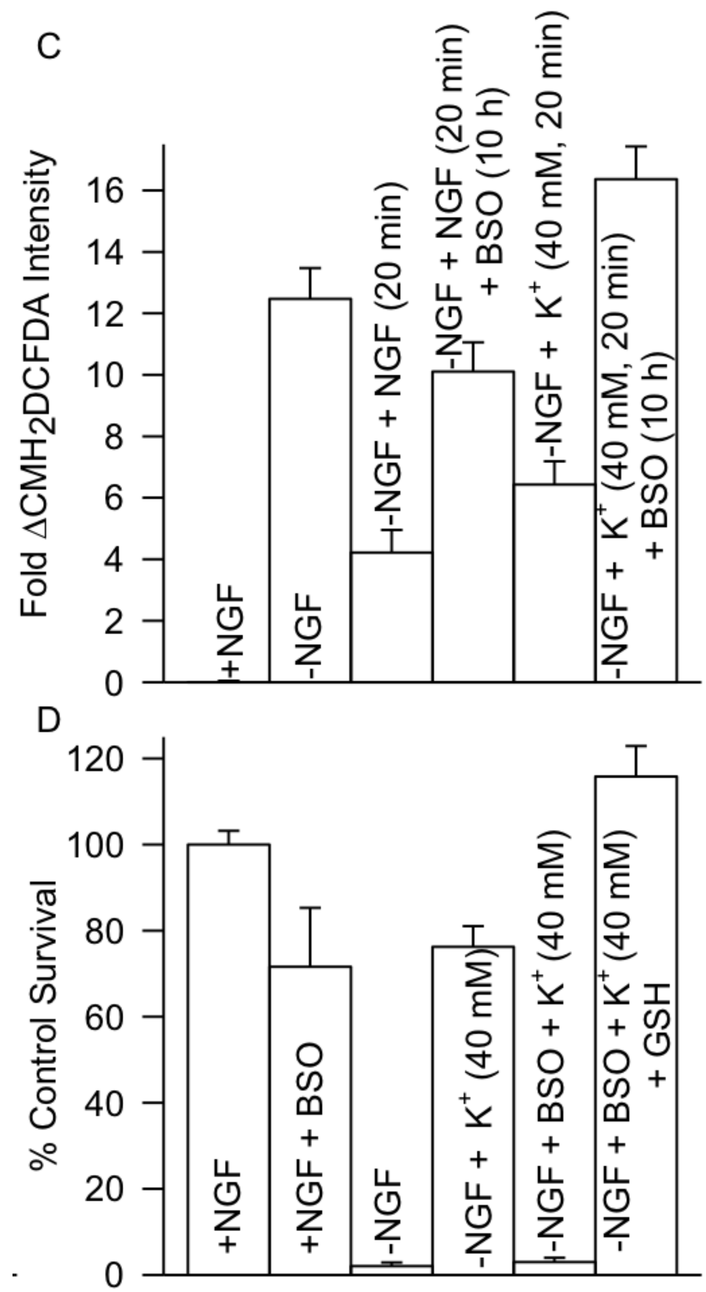

FIG. 3.5. An increase of GSH induced by elevated $[K^+]_E$ was required for block of apoptotic death of NGF-deprived neurons. (A) Fluorescence micrographs of sympathetic neurons receiving the indicated treatments and then loaded with the GSH-

sensitive dye, ThiolTracker™ Violet. (B) Quantification of the ThiolTracker™ Violet intensities in sympathetic neurons exposed to the indicated treatments. NGF withdrawal (20 hours) slightly increased the basal GSH levels (dye intensity) by ~ 0.5 ± 0.01-fold. Acute re-exposure of cells to either NGF or 40 mM $[K^+]_E$ (20 min) resulted in significantly stronger fluorescence signals indicating increase GSH levels ($p < 0.05$ by ANOVA; N =193-334 neurons from three separate platings). Dye intensities are shown as fold change from values of neurons maintained in NGF-containing media from the time of plating. (C) The inhibitor of GSH synthesis BSO blocked the ability of both NGF and elevated $[K^+]_E$ to acutely suppress increased RS (CM-H_2DCFDA intensity) caused by NGF withdrawal. Cultures were exposed to BSO (200 μM) for 10 hours to allow time for GSH depletion. (D) The ability of high $[K^+]_E$ to prevent death of NGF-deprived neurons was abolished by including BSO (200 μM) in the culture medium (N = 8-11 cultures from three separate platings). Treatment with membrane-permeant GSH ethyl ester (10 mM), prevented death of BSO-treated, chronically depolarized neurons (p < 0.001; by ANOVA; N = 9-14 cultures from three separate platings). All cultures were maintained for 48 hours in the indicated conditions from the time of NGF withdrawal. They were then switched to NGF-containing medium for five days for the survival assay (see methods). Survival is shown as a percentage of the average number of neurons in sibling cultures maintained in NGF-containing medium from the time of plating.

REFERENCES

[1] R.W. Oppenheim, Cell death during development of the nervous system. Annu. Rev. Neurosci. 14 (1991) 453-501.

[2] J. Yuan, B.A.Yankner, Apoptosis in the nervous system. Nature 407 (2000) 802-809.

[3] M. Kristiansen, J. Ham, Programmed cell death during neuronal development: the sympathetic neuron model. Cell Death Differ. 21 (2014) 1025-1035.

[4] D.P. Martin, R.E. Schmidt, P.S. DiStefano, O.H. Lowry, J.G. Carter, E.M. Johnson Jr., Inhibitors of protein synthesis and RNA synthesis prevent neuronal death caused by nerve growth factor deprivation. J. Cell Biol. 106 (1988) 829-844.

[5] T.L. Deckwerth, E.M. Johnson Jr., Temporal analysis of events associated with programmed cell death (apoptosis) of sympathetic neurons deprived of nerve growth factor. J. Cell. Biol. 123 (1993). 1207-1222.

[6] S.N. Edwards, A.M. Tolkovsky, Characterization of apoptosis in cultured rat sympathetic neurons after nerve growth factor withdrawal. J. Cell Biol. 124 (1994) 537-546.

[7] M. Deshmukh, J. Vasilakos, T.L. Deckwerth, P.A. Lampe, B.D. Shivers, E.M. Johnson Jr., Genetic and metabolic status of NGF-deprived sympathetic neurons saved by an inhibitor of ICE family proteases. J. Cell Biol. 135 (1996) 1341-1354.

[8] M. Deshmukh, E.M. Johnson Jr., Programmed cell death in neurons: focus on the pathway of nerve growth factor deprivation-induced death of sympathetic neurons. Mol. Pharmacol. 51 (1997) 897-906.

[9] M.J. McCarthy, L.L. Rubin, K.L. Philpott, Involvement of caspases in sympathetic neuron apoptosis. J. Cell Sci. 110 (1997) 2165-2173.

[10] M. Deshmukh, E.M. Johnson Jr., Evidence of a novel event during neuronal death: development of competence-to-die in response to cytoplasmic cytochrome c. Neuron 21 (1998) 695-705.

[11] T.L. Deckwerth, J.L. Elliott, C.M. Knudson, E.M. Johnson Jr., W.D. Snider, S.J. Korsmeyer, BAX is required for neuronal death after trophic factor deprivation and during development. Neuron, 17 (1996) 401-411.

[12] S.J. Neame, L.L. Rubin, K.L. Philpott, Blocking cytochrome c activity within intact neurons inhibits apoptosis. J. Cell Biol. 142 (1998) 1583-1593.

[13] F.A. White, C.R. Keller-Peck,C.M. Knudson, S.J. Korsmeyer, W.D. Snider, Widespread elimination of naturally occurring neuronal death in Bax-deficient mice. J. Neurosci. 18 (1998) 1428-1439.

[14] G.V. Putcha, M. Deshmukh, E.M. Johnson Jr., BAX translocation is a critical event in neuronal apoptosis: regulation by neuroprotectants, BCL-2, and caspases. J. Neurosci. 19 (1999) 7476-7485.

[15] C.A. Harris, E.M. Johnson Jr., BH3-only Bcl-2 family members are coordinately regulated by the JNK pathway and require Bax to induce apoptosis in neurons. J. Biol. Chem. 276 (2001) 37754-37760.

[16] G.V. Putcha, K.L. Moulder, J.P. Golden, P. Bouillet, J.A. Adams, A. Strasser, E.M. Johnson Jr., Induction of BIM, a proapoptotic BH3-only BCL-2 family member, is critical for neuronal apoptosis. Neuron 29 (2001) 615-628.

[17] J. Whitfield, S.J. Neame, L. Paquet, O. Bernard, J. Ham, Dominant-negative c-Jun promotes neuronal survival by reducing BIM expression and inhibiting mitochondrial cytochrome c release. Neuron 29 (2001) 629-643.

[18] C.G. Besirli, E.F. Wagner, E.M. Johnson Jr., The limited role of NH2-terminal c-Jun phosphorylation in neuronal apoptosis: identification of the nuclear pore complex as a potential target of the JNK pathway. J. Cell. Biol. 170 (2005) 401-411.

[19] A.J. Kole, V. Swahari, S.M. Hammond, M. Deshmukh, miR-29b is activated during neuronal maturation and targets BH3-only genes to restrict apoptosis. Genes Dev. 25 (2011) 125-130.

[20] M. Kristiansen, F.Menghi, R. Hughes, M. Hubank, J. Ham, Global analysis of gene expression in NGF-deprived sympathetic neurons identifies molecular pathways associated with cell death. B.M.C. Genomics 12 (2011) 551.

[21] R.A. Kirkland, J.L. Franklin, Evidence for redox regulation of cytochrome C release during programmed neuronal death: antioxidant effects of protein synthesis and caspase inhibition. J. Neurosci. 21(2001) 1949-1963.

[22] R.A. Kirkland, J.A.Windelborn, J.M. Kasprzak, J.L. Franklin, A Bax-induced pro-oxidant state is critical for cytochrome c release during programmed neuronal death. J. Neurosci. 22 (2002) 6480-6490.

[23] R.A. Kirkland, G.M. Saavedra, J.L. Franklin, Rapid activation of antioxidant defenses by nerve growth factor suppresses reactive oxygen species during neuronal apoptosis: evidence for a role in cytochrome c redistribution. J. Neurosci. 27 (2007) 11315-11326.

[24] R.A. Kirkland, G.M. Saavedra, B.S. Cummings, J.L. Franklin, Bax regulates production of superoxide in both apoptotic and nonapoptotic neurons: role of caspases. J. Neurosci. 30 (2010) 16114-16127.

[25] S. Mennerick, C.F. Zorumski, Neural activity and survival in the developing nervous system. Mol. Neurobiol. 22 (2000) 41-54.

[26] Y. Liu, R.M. Grumbles,C.K. Thomas, Electrical stimulation of embryonic neurons for 1 hour improves axon regeneration and the number of reinnervated muscles that function. J. Neuropathol Exp. Neurol. 72 (2013) 697-707.

[27] O. Blanquie, W. Kilb, A. Sinning, H.J. Luhmann, Homeostatic interplay between electrical activity and neuronal apoptosis in the developing neocortex. Neuroscience 358 (2017) 190-200.

[28] A. Chalazonitis, G.D. Fischbach, Elevated potassium induces morphological differentiation of dorsal root ganglionic neurons in dissociated cell culture. Dev. Biol. 78 (1980) 173-183.

[29] R. Nishi, D.K. Berg, Effects of high K+ concentrations on the growth and development of ciliary ganglion neurons in cell culture. Dev. Biol. 87 (1981) 301-307.

[30] A.M. Tolkovsky, A.E. Walker, R.D. Murrell, H.S. Suidan, Ca^{2+} transients are not required as signals for long-term neurite outgrowth from cultured sympathetic neurons. J. Cell Biol. 110 (1990) 1295-1306.

[31] J.L. Franklin, D.J. Fickbohm, A.L. Willard, Long-term regulation of neuronal calcium currents by prolonged changes of membrane potential. J. Neurosci. 12 (1992) 1726-1735.

[32] J.L. Franklin, C. Sanz-Rodriguez, A. Juhasz, T.L. Deckwerth, E.M. Johnson Jr., Chronic depolarization prevents programmed death of sympathetic neurons in vitro but does not support growth: requirement for Ca^{2+} influx but not Trk activation. J. Neurosci. 15(1995) 643-664.

[33] J.L. Franklin, E.M. Johnson Jr., Suppression of programmed neuronal death by sustained elevation of cytoplasmic calcium. Trends Neurosci. 15 (1992) 501-508.

[34] J.L. Franklin, E.M. Johnson Jr., Control of neuronal size homeostasis by trophic factor-mediated coupling of protein degradation to protein synthesis. J. Cell Biol. 142 (1998) 1313-1324.

[35] J.A. Royall, H. Ischiropoulos, Evaluation of 2',7'-dichlorofluorescin and dihydrorhodamine 123 as fluorescent probes for intracellular H_2O_2 in cultured endothelial cells. Arch. Biochem. Biophys. 302 (1993) 348-355.

[36] M.J. McManus, M. Murphy, J.L. Franklin, The mitochondria-targeted antioxidant, MitoQ, prevents loss of spatial memory retention and early neuropathology in a transgenic mouse model of Alzheimer's disease. J. Neurosci. 31(2011) 15703-15715.

[37] B. Halliwell, J.M. Gutteridge. Free radicals in biology and medicine. Oxford University Press USA (2015).

[38] B.S. Mandavilli, M.S. Janes, Detection of intracellular glutathione using ThiolTracker violet stain and fluorescence microscopy. Curr. Protoc. Cytom., Chapter 9, (2010) Unit 9 35. 39V.

[39] Gama, V. Swahari, J. Schafer, A.J. Kole, A. Evans, Y. Huang, A. Cliffe, B. Golitz, N. Sciaky, X. Pei, Y. Xiong, M. Deshmukh, The E3 ligase PARC mediates the

degradation of cytosolic cytochrome c to promote survival in neurons and cancer cells. Sci. Signal 7 (2014) ra67.

[40] R. Akhter, S. Saleem, A. Saha, S.C. Biswas, The pro-apoptotic protein Bmf co-operates with Bim and Puma in neuron death induced by beta-amyloid or NGF deprivation. Mol Cell Neurosci. 88 (2018) 249-257.

[41] L. Coultas, S. Terzano, T. Thomas, A. Voss, K. Reid, E.G. Stanley, A. Strasser, Hrk/DP5 contributes to the apoptosis of select neuronal populations but is dispensable for haematopoietic cell apoptosis. J Cell Sci. 120 (2007) 2044-2052.

[42] K. Imaizumi, M. Tsuda, Y. Imai, A. Wanaka, T. Takagi, M. Tohyama, Molecular cloning of a novel polypeptide, DP5, induced during programmed neuronal death. J Biol Chem. 272 (1997) 18842-18848.

[43] E. Towers, J. Gilley, R. Randall, R. Hughes, M. Kristiansen, J. Ham, The proapoptotic dp5 gene is a direct target of the MLK-JNK-c-Jun pathway in sympathetic neurons. Nucleic Acids Res. 37 (2009) 3044-3060.

[44] I. Martinou, S. Desagher, R. Eskes, B. Antonsson, E. Andre, S. Fakan, J.C. Martinou, The release of cytochrome c from mitochondria during apoptosis of NGF-deprived sympathetic neurons is a reversible event. J. Cell Biol. 144 (1999) 883-889.

[45] L.L. Dugan, D.J. Creedon, E.M. Johnson Jr., D.M. Holtzman, Rapid suppression of free radical formation by nerve growth factor involves the mitogen-activated protein kinase pathway. Proc. Natl. Acad. Sci. U. S. A. 94 (1997) 4086-4091.

[46] L.J. Greenlund, T.L., Deckwerth, E.M. Johnson Jr., Superoxide dismutase delays neuronal apoptosis: a role for reactive oxygen species in programmed neuronal death. Neuron 14 (1995) 303-315.

[47] R.A.Kirkland, J.L. Franklin, Bax, reactive oxygen, and cytochrome c release in neuronal apoptosis. Antioxid Redox Signal 5 (2003) 589-596.

[48] O.W. Griffith, A. Meister, Potent and specific inhibition of glutathione synthesis by buthionine sulfoximine (S-n-butyl homocysteine sulfoximine). J. Biol. Chem. 254 (1979) 7558-7560.

[49] B.S. Scott, B. S., K. C. Fisher. Potassium concentration and number of neurons in cultures of dissociated ganglia." Exp Neurol 27, no. 1 (1970) 16-22.

[50] D. Ren, H. C. Tu, H. Kim, G. X. Wang, G. R. Bean, O. Takeuchi, J. R. Jeffers, G.P. Zambetti, J. J-D. Hsieh, and E. H-Y. Cheng, Bid, bim, and puma are essential for activation of the bax- and bak-dependent cell death program." Science 330, no. 6009 (2010) 1390-3.

[51] R.P. Annis, V. Swahari, A. Nakamura, A. X. Xie, S. M. Hammond, M. Deshmukh, Mature neurons dynamically restrict apoptosis via redundant premitochondrial brakes. FEBS J 283, no. 24 (2016) 4569-82.

[52] J.L. Franklin, Redox regulation of the intrinsic pathway in neuronal apoptosis. Antioxid Redox Signal 14, no. 8 (2011) 1437-48.

[53] H. Zhao, S. Kalivendi, H. Zhang, J. Joseph, K. Nithipatikom, J. Vasquez-Vivar, B. Kalyanaraman. Superoxide reacts with hydroethidine but forms a fluorescent product that is distinctly different from ethidium: potential implications in

intracellular fluorescence detection of superoxide. Free Radic Biol Med 34, no. 11 (2003) 1359-68.

[54] H. Zhao, J. Joseph, H. M. Fales, E. A. Sokoloski, R. L. Levine, J. Vasquez-Vivar, B. Kalyanaraman. Detection and characterization of the product of hydroethidine and intracellular superoxide by hplc and limitations of fluorescence." Proc Natl Acad Sci U S A 102, no. 16 (2005) 5727-32.

[55] K.M. Robinson, M. S. Janes, M. Pehar, J. S. Monette, M. F. Ross, T. M. Hagen, M. P. Murphy, J. S. Beckman. Selective fluorescent imaging of superoxide in vivo using ethidium-based probes. Proc Natl Acad Sci U S A 103, no. 41 (2006) 15038-43.

[56] M. Deshmukh, K. Kuida, E.M. Jr., Johnson, Caspase inhibition extends the commitment to neuronal death beyond cytochrome c release to the point of mitochondrial depolarization. J Cell Biol, 150 (2000) 131-143.

[57] R.A. Kirkland, R.M. Adibhatla, J.F. Hatcher, J.L. Franklin, Loss of cardiolipin and mitochondria during programmed neuronal death: evidence of a role for lipid peroxidation and autophagy. Neuroscience, 115 (2002) 587-602.

Chapter 5

SUMMARY AND CONCLUDING REMARKS

The principal goal of this dissertation is to investigate, using different *in vitro* models, how the mitochondria-controlled redox status determines cellular fate. Whether with cancer cells or normal cells, mitochondria executes several critical cellular functions, including bioenergetics homeostasis, intracellular Ca^{2+} buffering, lipid and steroid biosynthesis, production and clearance of reactive species (RS), and control of different forms of programmed cell death, apoptosis in particular (Miller, 2013; Nunnari & Suomalainen, 2012). The association of several pathologies—including neurodegenerative disorders and many types of cancers (Wallace, 2005), as well as some forms of physiological neuronal apoptosis (Franklin, 2011)—with cells' pro-oxidant status inspired the work presented here.

The work presented here argues for the appreciation of mitochondria as the center of cellular vitality. The results from this study strengthen the ever-growing association of mitochondria-derived RS with apoptotic death. To our knowledge, the work presented in the first part of this dissertation is among the first to demonstrate targeting mitochondria as a potential approach to treat melanoma tumors with wild-type BRAF. In addition, the work demonstrated in the second part of this dissertation is the first to specifically address the mechanism by which chronically depolarized sympathetic neurons resist apoptotic death following NGF withdrawal.

Mitochondrial Redox Signaling and Cellular Bioenergetics

Recent advances in cancer research have implicated mitochondria-derived RS among the mechanisms by which many cancers, including melanomas, resist targeted therapeutics (Wittgen & van Kempen, 2007). Cancer cells can presumably tolerate excessive RS production by the continuous activation of scavenging enzymes, e.g., glutathione (GSH) (Gorrini, Harris, & Mak, 2013). Such an abnormal persistent pro-oxidant state promotes several aspects that drive tumor progression and therapeutic resistance, including induction of genomic instability (Vafa et al., 2002), activation of inflammatory responses (Naik & Dixit, 2011), stabilization of the hypoxia-inducible factors (Gao et al., 2007), and, most notably, metabolic reprogramming (Anastasiou et al., 2011; Gao et al., 2009). Mounting evidence indicates that several tumors promote survival under harsh conditions by redirecting their metabolic machinery to maintain a favorable above-normal threshold of RS (Panieri & Santoro, 2016). Therapeutic manipulations aimed at disrupting the crosstalk between RS homeostasis and multiple metabolic pathways might serve as a promising anticancer treatment approach.

As mentioned in Chapters 1 and 2, the heterogeneity of the melanoma tumor microenvironment makes it an ideal model for investigating newer treatment approaches to effectively inducing their death. Mounting evidence suggests that melanoma cells may vacillate between utilizing either glycolysis or mitochondrial oxidative phosphorylation, depending on the environmental conditions (Theodosakis, Micevic, Kelly, & Bosenberg, 2014). Oncogenic-activating mutation in BRAF has also been linked with such bioenergetic switching (Haq, Fisher, & Widlund, 2014). This evidence further suggests that melanomas expressing wild-type BRAF versus mutant BRAF proteins would respond differently to compounds that target different metabolic pathways.

Our findings demonstrate that micromolar concentrations of the mitochondria-targeted cation, MitoQ, induce death in several melanoma cell lines, surpassing multiple conventional and investigational therapeutics. Melanoma cell lines expressing wild-type BRAF, which are dependent upon oxidative phosphorylation (Vazquez et al., 2013), showed higher sensitivity to MitoQ-induced mitochondrial dysfunction. Intriguingly, inhibition of lactate dehydrogenase-A through the small-molecule FX-11 further sensitized melanoma cells of different genetic backgrounds to MitoQ-mediated cell death. It is likely that such a combination created a pro-oxidant status beyond what these tumors are able to tolerate, as evidence suggests that excessive oxidative stress can result from mitochondrial dysfunction (Jezek, Cooper, & Strich, 2018) or lactate dehydrogenase-A inhibition (Le et al., 2010). The work presented in this dissertation suggests that targeting different metabolic pathways is far more effective than conventional therapeutics, especially in melanoma cells with wild-type BRAF, for which a clear strategy for targeted therapy is lacking.

Several open questions need to be addressed in future investigations. For example, to what extent can the genetic background of different melanoma cells (mutant vs. wild-type BRAF) affect the intracellular RS levels? How do different metabolic pathways (cytosolic glycolysis vs. oxidative phosphorylation) contribute to the RS production in melanoma cells? Would the dual disruption of major metabolic pathways induce cell death by creating an uncontrollable pro-oxidant state? How would this combination therapy perform *in vivo*, since cellular respiration and the tumor microenvironment are entirely different?

Mitochondria Orchestrate the Death and Survival of Developing Sympathetic Neurons

Over the last 70 years, countless studies have been conducted to decipher the purpose and the mechanisms of physiological neuronal death during the embryonic development of the nervous system. Overwhelming evidence indicates that the availability of the appropriate neurotrophic factor at the time at which neurons innervate their target organs is the central means that determines which neurons survive this apocalyptic event (Oppenheim, 1991). Several *in vitro* models have been developed to examine the cellular and molecular events underlying apoptosis during neurogenesis. Among these models is that involving NGF-deprived sympathetic neurons derived from the superior cervical ganglia (SCG) of late embryonic or early postnatal rodents (Kristiansen & Ham, 2014). These models have allowed the identification of multiple key proteins and signaling pathways that drive the apoptotic death of developmental neurons and could also help identify new targets contributing to the development of neurodegenerative diseases. As demonstrated in detail in Chapter 3, mitochondria can be viewed as the master regulators that coordinate and connect these signaling networks.

In addition to the neurotrophic factor-mediated survival of different neuronal populations during nervous system development, considerable evidence suggests electrical activity as another crucial factor that determines such a fate (Blanquie, Kilb, Sinning, & Luhmann, 2017; Liu, Grumbles, & Thomas, 2013; Mennerick & Zorumski, 2000). While numerous studies have investigated the molecular mechanisms by which neurotrophic factors maintain neuronal survival during development, few efforts have been aimed toward understanding how electrical activity promotes the survival or suppresses the death of neurons at this stage of embryonic development. The effects of electrical activity *in vivo* can be recapitulated *in vitro* by maintaining neurotrophic factor-deprived neurons in a medium with elevated potassium concentration ($[K^+]$). Electrophysiological *in vitro* studies have revealed that membranes of different types of neurons remain depolarized as long as they are exposed to elevated extracellular ($[K^+]_E$) (Table 2 in Chapter 3). To our knowledge, the increased influx of Ca^{2+} through L-type voltage-dependent Ca^{2+} channels and the subsequent steady-state rise in the intracellular Ca^{2+} ($[Ca^{2+}]_i$) is the only reported mechanism by which chronic membrane depolarization promotes survival of NGF-deprived SCG neurons (Collins & Lile, 1989; Franklin, Sanz-Rodriguez, Juhasz, Deckwerth, & Johnson, 1995; Koike & Tanaka, 1991). However, the involvement of Ca^{2+} in a countless number of intracellular pathways (Brini, Cali, Ottolini, & Carafoli, 2014) makes it more difficult to outline the correlation between $[Ca^{2+}]_i$ and survival in chronically depolarized cells. Therefore, we sought to investigate more specifically the molecular mechanism(s) by which chronically depolarized sympathetic neurons resist apoptotic death following NGF withdrawal.

The induction of the Bcl-2 family of pro-apoptotic proteins, cytochrome *c* redistribution, caspase activation, and mitochondria-mediated cellular pro-oxidant status are among the well-documented events occur during neuronal death following NGF withdrawal (see Chapter 3 for details). It was of great interest to determine how these major pathways that execute the death of the NGF-deprived mouse sympathetic neurons respond to elevated $[K^+]_E$. The finding that chronically depolarized neurons blocked cytochrome *c* redistribution from the inner mitochondrial membrane (IMM) to the cytoplasm strongly suggests that whatever causes that action lies upstream of cytochrome *c* release. As discussed in Chapter 3, cytochrome *c* mainly exits the mitochondrial intermembrane space after the activation and the mitochondrial translocation of the pro-apoptotic protein, Bax. Activated Bax oligomerizes, inserts itself into, and permeabilizes the outer mitochondrial membrane, creating exit routes for the unbound cytochrome *c* (Kirkland & Franklin, 2003; Pena-Blanco & Garcia-Saez, 2018; Zhang, Zheng, Nussinov, & Ma, 2017). Induction of multiple members of the BH3-only pro-apoptotic proteins upstream of Bax activation appears to play a role in the apoptotic death of NGF-deprived neurons (Besirli et al., 2005; Harris & Johnson, 2001; Kole et al. , 2011; Kristiansen et al., 2011; Putcha et al., 2001; Whitfield et al., 2001). Our data show that high $[K^+]_E$ suppressed the induction of only one member, Bim_{EL}. Previous studies have shown that suppression of multiple members of the BH3-only pro-apoptotic proteins is required to achieve complete resistance to death following neurotrophic factor withdrawal (Annis et al., 2016; Imaizumi et al., 2004; Kole et al., 2011; Ren et al., 2010; Whitfield et al., 2001). Hence, we concluded that other unexplored pathways upstream of cytochrome *c* might exist through which $[K^+]_E$-induced chronic depolarization promotes the survival of sympathetic neurons in the absence of NGF.

Mitochondria-mediated pro-oxidant status seems to be an essential instructive step that initiates cytochrome *c* redistribution and subsequent death of the NGF-deprived neurons (Franklin, 2011). In agreement with the previous studies, our study here shows that NGF deprivation induces a pro-oxidant state that preceded cytochrome *c* release.

$[K^+]_E$-induced chronic depolarization almost abolished the increased RS levels and thus apoptotic death triggered by NGF withdrawal. How chronic membrane depolarization prevents cytochrome *c* release remains an open question. Evidence suggests that prior to cytochrome *c* liberation from the IMM, cytochrome *c* must dissociate first from cardiolipin (CL), a mitochondria-specific phospholipid at the outer leaflet of the IMM, a step enabled by CL peroxidation (Orrenius & Zhivotovsky, 2005; Ott, Robertson, Gogvadze, Zhivotovsky, & Orrenius, 2002; Shidoji, Hayashi, Komura, Ohishi, & Yagi, 1999). Previous studies have shown that Bax-mediated production of ROS causes CL peroxidation and subsequent cytochrome *c* release in different models of apoptotic death, including in rat sympathetic neurons deprived of NGF (Jiang et al., 2008; Kirkland, Adibhatla, Hatcher, & Franklin, 2002). It is conceivable that elevated $[K^+]_E$ prevents CL peroxidation and thus blocked cytochrome *c* release. Moreover, Nie *et al*. demonstrated that H_2O_2 treatment caused Bax oligomerization and activation, evidently by oxidizing the conserved cysteine 62 residue (Nie et al., 2008). This result further suggests that chronic depolarization blocks Bax translocation and thus cytochrome *c* release by preventing cellular oxidative stress rather than by merely downregulating the BH3-only proteins.

Previous reports from different laboratories, including ours, suggest that the vast majority of RS in dying sympathetic neurons following NGF removal are produced when electrons leak from the mitochondrial electron-transport chain (Dugan, Creedon, Johnson, & Holtzman, 1997; Kirkland & Franklin, 2001; Kirkland, Windelborn, Kasprzak, & Franklin, 2002). The reduced intensities of the redox-sensitive dye CM-H_2DCFDA following chronic depolarization indicate that elevated $[K^+]_E$ either suppresses mitochondrial RS production or activates antioxidant defenses. Similar to the previously reported effects of NGF (Kirkland, Saavedra, & Franklin, 2007), chronic depolarization rapidly prevents the pro-oxidant state and thus apoptotic death of NGF-deprived sympathetic neurons by upregulating a key antioxidant, GSH. Even though the effects of elevated $[K^+]_E$ on mitochondrial RS production were not assessed in this study, the similarities between the re-exposure of deprived neurons to NGF, GSH ethyl ester, or high $[K^+]_E$ strongly suggest that activating the RS detoxifying machinery is the mechanism by which chronically depolarized sympathetic neurons resist death following NGF removal. It has yet to be determined how chronic membrane depolarization causes upregulation of the antioxidant GSH in sympathetic neurons.

Several possible mechanisms exist by which chronic membrane depolarization could cause increased GSH levels to promote neuronal survival following NGF removal. First, GSH synthesis primarily depends on the availability of the sulfur amino acid precursor, cysteine. Following the influx of extracellular cysteine to the cellular cytoplasm, the incorporation of cysteine into either proteins or GSH largely depends on cellular demands (growth vs. survival) (Lu, 2009). Several laboratories, including ours, have presented evidence that the protein synthesis inhibitor, cycloheximide (CHX), and the antioxidant, N-acetyl-L cysteine (L-NAC), block increased RS bursts, cytochrome *c* release and apoptotic death of different types of neurons, including NGF-deprived sympathetic neurons, by increasing cellular GSH concentration (Ferrari, Yan, & Greene, 1995; Kirkland & Franklin, 2001; Ratan, Murphy, & Baraban, 1994). The availability of cysteine residues, either directly by L-NAC or indirectly by CHX-mediated shunting of cysteine from incorporation into protein to GSH synthesis, is evidently one way by which these surviving neurons upregulate GSH. Cultures of sympathetic neurons maintained in a depolarizing medium show decreased growth and lower total protein concentrations compared to NGF-maintained neurons (Franklin et al., 1995). These studies indicate that the elevated $[K^+]_E$ could have promoted neuronal survival at the expense of protein synthesis and cellular growth by shunting more cysteine residues from protein synthesis to GSH synthesis.

The second possible mechanism is that elevated $[K^+]_E$ maintains an adequate mitochondrial pool of GSH to detoxify the increased RS following NGF deprivation. Zimmermann *et al*. presented evidence that, in cerebellar granule cells (CGC), such a pool of GSH is maintained when the pro-survival protein Bcl-2 binds and transports GSH to the mitochondria. They also showed that BH3 mimetics and the BH3-only protein, Bim_L, displace GSH by binding with the BH3 groove of Bcl-2, causing mitochondrial oxidative stress and subsequent death (Zimmermann et al., 2007). Since CG neurons also require high $[K^+]_E$ for survival, the elevated $[K^+]_E$-mediated chronic depolarization might exert similar antioxidant effects in NGF-deprived sympathetic neurons through suppressing the pro-apoptotic protein Bim_{EL}, thereby preventing the displacement of GSH from Bcl-2, which maintain adequate mitochondrial GSH levels to detoxify increased RS.

Finally, it is possible that elevated $[K^+]_E$ increases GSH concentrations via a Ca^{2+}-dependent nuclear translocation and activation of the nuclear factor erythroid2-related factor, Nrf2. The rate of GSH synthesis is primarily controlled by the activity of γ-glutamylcysteine synthetase (also known as glutamate-cysteine ligase, GCL), and by the availability of cysteine/cystine (Bender, Reichelt, & Norenberg, 2000; Dringen, Pfeiffer,

& Hamprecht, 1999; Griffith & Mulcahy, 1999). Nrf2 transcriptionally regulates the expression of several key enzymes of GSH synthesis, including the catalytic and modulatory subunits of GCL, in addition to the antiporter system x_c^-, which facilitates cellular uptake of the amino acid cystine, the oxidized form of cysteine (Kensler, Wakabayashi, & Biswal, 2007; Lewerenz et al., 2013). Under normal conditions, Nrf2-dependent transcription is repressed by the Kelch-like ECH-associated protein 1 (Keap1) through rapid proteasomal degradation. In response to different stressors, Keap1-mediated Nrf2 ubiquitination and subsequent degradation are repressed, leading to the stabilization and nuclear translocation of Nrf2, where it induces antioxidant response element (ARE)-dependent gene expression to re-establish cellular redox homeostasis (Kensler et al., 2007). One of the recently identified upstream activators of Nrf2 is the central regulator of cell survival, AMP-activated protein kinase (AMPK). Upstream kinases can activate AMPK by phosphorylating the Thr^{172} residue on the α subunit. The Ca^{2+}/calmodulin-dependent protein kinase kinase (CaMKKβ) is a C^{2+}-sensitive kinase that rapidly phosphorylates and activates AMPK (Hawley et al., 2005; Hurley et al., 2005). Interestingly, $[K^+]_E$-induced depolarization in rat cerebrocortical slices phosphorylates and activates AMPK, an effect blocked by CaMKK inhibitor STO-609 and siRNAs against the β isoform (Hawley et al., 2005). A recent report demonstrated that AMPK directly phosphorylates Nrf2 at the Ser^{550} residue, promoting its nuclear translocation and accumulation (Joo et al., 2016). These pieces of evidence collectively suggest that chronic depolarization might upregulate GSH by activating the CaMKKβ → AMPK → Nrf2 pathway, which is triggered by the depolarization-induced rise of cytosolic Ca^{2+} in sympathetic neurons.

REFERENCES

Anastasiou, D., Poulogiannis, G., Asara, J. M., Boxer, M. B., Jiang, J. K., Shen, M., . . . Cantley, L. C. (2011). Inhibition of pyruvate kinase M2 by reactive oxygen species contributes to cellular antioxidant responses. *Science, 334*(6060), 1278-1283.

Annis, R. P., Swahari, V., Nakamura, A., Xie, A. X., Hammond, S. M., & Deshmukh, M. (2016). Mature neurons dynamically restrict apoptosis via redundant premitochondrial brakes. *FEBS J, 283*(24), 4569-4582.

Bender, A. S., Reichelt, W., & Norenberg, M. D. (2000). Characterization of cystine uptake in cultured astrocytes. *Neurochem Int, 37*(2-3), 269-276.

Besirli, C. G., Wagner, E. F., & Johnson, E. M., Jr. (2005). The limited role of NH2-terminal c-Jun phosphorylation in neuronal apoptosis: identification of the nuclear pore complex as a potential target of the JNK pathway. *J Cell Biol, 170*(3), 401-411.

Blanquie, O., Kilb, W., Sinning, A., & Luhmann, H. J. (2017). Homeostatic interplay between electrical activity and neuronal apoptosis in the developing neocortex. *Neuroscience, 358*, 190-200.

Brini, M., Cali, T., Ottolini, D., & Carafoli, E. (2014). Neuronal calcium signaling: function and dysfunction. *Cell Mol Life Sci, 71*(15), 2787-2814.

Collins, F., & Lile, J. D. (1989). The role of dihydropyridine-sensitive voltage-gated calcium channels in potassium-mediated neuronal survival. *Brain Res, 502*(1), 99-108.

Dringen, R., Pfeiffer, B., & Hamprecht, B. (1999). Synthesis of the antioxidant glutathione in neurons: supply by astrocytes of CysGly as precursor for neuronal glutathione. *J Neurosci, 19*(2), 562-569.

Dugan, L. L., Creedon, D. J., Johnson, E. M., Jr., & Holtzman, D. M. (1997). Rapid suppression of free radical formation by nerve growth factor involves the mitogen-activated protein kinase pathway. *Proc Natl Acad Sci U S A, 94*(8), 4086-4091.

Ferrari, G., Yan, C. Y., & Greene, L. A. (1995). N-acetylcysteine (D- and L-stereoisomers) prevents apoptotic death of neuronal cells. *J Neurosci, 15*(4), 2857-2866.

Franklin, J. L. (2011). Redox regulation of the intrinsic pathway in neuronal apoptosis. *Antioxid Redox Signal, 14*(8), 1437-1448.

Franklin, J. L., Sanz-Rodriguez, C., Juhasz, A., Deckwerth, T. L., & Johnson, E. M., Jr. (1995). Chronic depolarization prevents programmed death of sympathetic neurons in vitro but does not support growth: requirement for Ca^{2+} influx but not Trk activation. *J Neurosci, 15*(1 Pt 2), 643-664.

Gao, P., Tchernyshyov, I., Chang, T. C., Lee, Y. S., Kita, K., Ochi, T., . . . Dang, C. V. (2009). c-Myc suppression of miR-23a/b enhances mitochondrial glutaminase expression and glutamine metabolism. *Nature, 458*(7239), 762-765.

Gao, P., Zhang, H., Dinavahi, R., Li, F., Xiang, Y., Raman, V., . . . Dang, C. V. (2007). HIF-dependent antitumorigenic effect of antioxidants in vivo. *Cancer Cell, 12*(3), 230-238.

Gorrini, C., Harris, I. S., & Mak, T. W. (2013). Modulation of oxidative stress as an anticancer strategy. *Nat Rev Drug Discov, 12*(12), 931-947.

Griffith, O. W., & Mulcahy, R. T. (1999). The enzymes of glutathione synthesis: gamma-glutamylcysteine synthetase. *Adv Enzymol Relat Areas Mol Biol, 73*, 209-267, xii.

Haq, R., Fisher, D. E., & Widlund, H. R. (2014). Molecular pathways: BRAF induces bioenergetic adaptation by attenuating oxidative phosphorylation. *Clin Cancer Res, 20*(9), 2257-2263.

Harris, C. A., & Johnson, E. M., Jr. (2001). BH3-only Bcl-2 family members are coordinately regulated by the JNK pathway and require Bax to induce apoptosis in neurons. *J Biol Chem, 276*(41), 37754-37760.

Hawley, S. A., Pan, D. A., Mustard, K. J., Ross, L., Bain, J., Edelman, A. M., . . . Hardie, D. G. (2005). Calmodulin-dependent protein kinase kinase-beta is an alternative upstream kinase for AMP-activated protein kinase. *Cell Metab, 2*(1), 9-19.

Hurley, R. L., Anderson, K. A., Franzone, J. M., Kemp, B. E., Means, A. R., & Witters, L. A. (2005). The Ca^{2+}/calmodulin-dependent protein kinase kinases are AMP-activated protein kinase kinases. *J Biol Chem, 280*(32), 29060-29066.

Imaizumi, K., Benito, A., Kiryu-Seo, S., Gonzalez, V., Inohara, N., Lieberman, A. P., . . . Nunez, G. (2004). Critical role for DP5/Harakiri, a Bcl-2 homology domain 3-only Bcl-2 family member, in axotomy-induced neuronal cell death. *J Neurosci, 24*(15), 3721-3725.

Jezek, J., Cooper, K. F., & Strich, R. (2018). Reactive Oxygen Species and Mitochondrial Dynamics: The Yin and Yang of Mitochondrial Dysfunction and Cancer Progression. *Antioxidants (Basel), 7*(1).

Jiang, J., Huang, Z., Zhao, Q., Feng, W., Belikova, N. A., & Kagan, V. E. (2008). Interplay between bax, reactive oxygen species production, and cardiolipin oxidation during apoptosis. *Biochem Biophys Res Commun, 368*(1), 145-150.

Joo, M. S., Kim, W. D., Lee, K. Y., Kim, J. H., Koo, J. H., & Kim, S. G. (2016). AMPK Facilitates Nuclear Accumulation of Nrf2 by Phosphorylating at Serine 550. *Mol Cell Biol, 36*(14), 1931-1942.

Kensler, T. W., Wakabayashi, N., & Biswal, S. (2007). Cell survival responses to environmental stresses via the Keap1-Nrf2-ARE pathway. *Annu Rev Pharmacol Toxicol, 47*, 89-116.

Kirkland, R. A., Adibhatla, R. M., Hatcher, J. F., & Franklin, J. L. (2002). Loss of cardiolipin and mitochondria during programmed neuronal death: evidence of a role for lipid peroxidation and autophagy. *Neuroscience, 115*(2), 587-602.

Kirkland, R. A., & Franklin, J. L. (2001). Evidence for redox regulation of cytochrome C release during programmed neuronal death: antioxidant effects of protein synthesis and caspase inhibition. *J Neurosci, 21*(6), 1949-1963.

Kirkland, R. A., & Franklin, J. L. (2003). Bax, reactive oxygen, and cytochrome c release in neuronal apoptosis. *Antioxid Redox Signal, 5*(5), 589-596.

Kirkland, R. A., Saavedra, G. M., & Franklin, J. L. (2007). Rapid activation of antioxidant defenses by nerve growth factor suppresses reactive oxygen species during neuronal apoptosis: evidence for a role in cytochrome c redistribution. *J Neurosci, 27*(42), 11315-11326.

Kirkland, R. A., Windelborn, J. A., Kasprzak, J. M., & Franklin, J. L. (2002). A Bax-induced pro-oxidant state is critical for cytochrome c release during programmed neuronal death. *J Neurosci, 22*(15), 6480-6490.

Koike, T., & Tanaka, S. (1991). Evidence that nerve growth factor dependence of sympathetic neurons for survival in vitro may be determined by levels of cytoplasmic free Ca^{2+}. *Proc Natl Acad Sci U S A, 88*(9), 3892-3896.

Kole, A. J., Swahari, V., Hammond, S. M., & Deshmukh, M. (2011). miR-29b is activated during neuronal maturation and targets BH3-only genes to restrict apoptosis. *Genes Dev, 25*(2), 125-130.

Kristiansen, M., & Ham, J. (2014). Programmed cell death during neuronal development: the sympathetic neuron model. *Cell Death Differ, 21*(7), 1025-1035.

Kristiansen, M., Menghi, F., Hughes, R., Hubank, M., & Ham, J. (2011). Global analysis of gene expression in NGF-deprived sympathetic neurons identifies molecular pathways associated with cell death. *BMC Genomics, 12*, 551.

Le, A., Cooper, C. R., Gouw, A. M., Dinavahi, R., Maitra, A., Deck, L. M., . . . Dang, C. V. (2010). Inhibition of lactate dehydrogenase A induces oxidative stress and inhibits tumor progression. *Proc Natl Acad Sci U S A, 107*(5), 2037-2042.

Lewerenz, J., Hewett, S. J., Huang, Y., Lambros, M., Gout, P. W., Kalivas, P. W., . . . Maher, P. (2013). The cystine/glutamate antiporter system x(c)(-) in health and disease: from molecular mechanisms to novel therapeutic opportunities. *Antioxid Redox Signal, 18*(5), 522-555.

Liu, Y., Grumbles, R. M., & Thomas, C. K. (2013). Electrical stimulation of embryonic neurons for 1 hour improves axon regeneration and the number of reinnervated muscles that function. *J Neuropathol Exp Neurol, 72*(7), 697-707.

Lu, S. C. (2009). Regulation of glutathione synthesis. *Mol Aspects Med, 30*(1-2), 42-59.

Mennerick, S., & Zorumski, C. F. (2000). Neural activity and survival in the developing nervous system. *Mol Neurobiol, 22*(1-3), 41-54. doi:10.1385/MN:22:1-3:041

Miller, W. L. (2013). Steroid hormone synthesis in mitochondria. *Mol Cell Endocrinol, 379*(1-2), 62-73.

Naik, E., & Dixit, V. M. (2011). Mitochondrial reactive oxygen species drive proinflammatory cytokine production. *J Exp Med, 208*(3), 417-420.

Nie, C., Tian, C., Zhao, L., Petit, P. X., Mehrpour, M., & Chen, Q. (2008). Cysteine 62 of Bax is critical for its conformational activation and its proapoptotic activity in response to H2O2-induced apoptosis. *J Biol Chem, 283*(22), 15359-15369.

Nunnari, J., & Suomalainen, A. (2012). Mitochondria: in sickness and in health. *Cell, 148*(6), 1145-1159.

Oppenheim, R. W. (1991). Cell death during development of the nervous system. *Annu Rev Neurosci, 14*, 453-501.

Orrenius, S., & Zhivotovsky, B. (2005). Cardiolipin oxidation sets cytochrome c free. *Nat Chem Biol, 1*(4), 188-189.

Ott, M., Robertson, J. D., Gogvadze, V., Zhivotovsky, B., & Orrenius, S. (2002). Cytochrome c release from mitochondria proceeds by a two-step process. *Proc Natl Acad Sci U S A, 99*(3), 1259-1263.

Panieri, E., & Santoro, M. M. (2016). ROS homeostasis and metabolism: a dangerous liason in cancer cells. *Cell Death Dis, 7*(6), e2253.

Pena-Blanco, A., & Garcia-Saez, A. J. (2018). Bax, Bak and beyond - mitochondrial performance in apoptosis. *FEBS J, 285*(3), 416-431.

Putcha, G. V., Moulder, K. L., Golden, J. P., Bouillet, P., Adams, J. A., Strasser, A., & Johnson, E. M. (2001). Induction of BIM, a proapoptotic BH3-only BCL-2 family member, is critical for neuronal apoptosis. *Neuron, 29*(3), 615-628.

Ratan, R. R., Murphy, T. H., & Baraban, J. M. (1994). Macromolecular synthesis inhibitors prevent oxidative stress-induced apoptosis in embryonic cortical neurons by shunting cysteine from protein synthesis to glutathione. *J Neurosci, 14*(7), 4385-4392.

Ren, D., Tu, H. C., Kim, H., Wang, G. X., Bean, G. R., Takeuchi, O., . . . Cheng, E. H. (2010). BID, BIM, and PUMA are essential for activation of the BAX- and BAK-dependent cell death program. *Science, 330*(6009), 1390-1393.

Shidoji, Y., Hayashi, K., Komura, S., Ohishi, N., & Yagi, K. (1999). Loss of molecular interaction between cytochrome c and cardiolipin due to lipid peroxidation. *Biochem Biophys Res Commun, 264*(2), 343-347.

Theodosakis, N., Micevic, G., Kelly, D. P., & Bosenberg, M. (2014). Mitochondrial function in melanoma. *Arch Biochem Biophys, 563*, 56-59.

Vafa, O., Wade, M., Kern, S., Beeche, M., Pandita, T. K., Hampton, G. M., & Wahl, G. M. (2002). c-Myc can induce DNA damage, increase reactive oxygen species, and mitigate p53 function: a mechanism for oncogene-induced genetic instability. *Mol Cell, 9*(5), 1031-1044.

Vazquez, F., Lim, J. H., Chim, H., Bhalla, K., Girnun, G., Pierce, K., . . . Puigserver, P. (2013). PGC1alpha expression defines a subset of human melanoma tumors with increased mitochondrial capacity and resistance to oxidative stress. *Cancer Cell, 23*(3), 287-301.

Wallace, D. C. (2005). A mitochondrial paradigm of metabolic and degenerative diseases, aging, and cancer: a dawn for evolutionary medicine. *Annu Rev Genet, 39*, 359-407.

Whitfield, J., Neame, S. J., Paquet, L., Bernard, O., & Ham, J. (2001). Dominant-negative c-Jun promotes neuronal survival by reducing BIM expression and inhibiting mitochondrial cytochrome c release. *Neuron, 29*(3), 629-643.

Wittgen, H. G., & van Kempen, L. C. (2007). Reactive oxygen species in melanoma and its therapeutic implications. *Melanoma Res, 17*(6), 400-409.

Zhang, M., Zheng, J., Nussinov, R., & Ma, B. (2017). Release of Cytochrome C from Bax Pores at the Mitochondrial Membrane. *Sci Rep, 7*(1), 2635.

Zimmermann, A. K., Loucks, F. A., Schroeder, E. K., Bouchard, R. J., Tyler, K. L., & Linseman, D. A. (2007). Glutathione binding to the Bcl-2 homology-3 domain groove: a molecular basis for Bcl-2 antioxidant function at mitochondria. *J Biol Chem, 282*(40), 29296-29304.